DISSERTATIONES
TECHNOLOGIAE
UNIVERSITATIS
TARTUENSIS
86

SIIM LAANESOO

Novel high-performance biomass-based polymers

DISSERTATIONES TECHNOLOGIAE UNIVERSITATIS TARTUENSIS
86

DISSERTATIONES TECHNOLOGIAE UNIVERSITATIS TARTUENSIS
86

SIIM LAANESOO

Novel high-performance biomass-based polymers

UNIVERSITY OF TARTU
Press
1632

Institute of Technology, Faculty of Science and Technology, University of Tartu, Estonia

The dissertation was accepted for the commencement of the degree of Doctor of Philosophy in Engineering of Bioactive Compounds on 15.08.2024, by the Joint Council of the Doctoral Program of Engineering and Technology of the University of Tartu.

Supervisors: Lauri Vares, PhD
Associate Professor of Organic Chemistry
Institute of Technology, Faculty of Science and Technology
University of Tartu, Estonia

Patric Jannasch, PhD
Visiting Professor,
Institute of Technology, Faculty of Science and Technology,
University of Tartu, Estonia,
Professor of Polymer Technology,
Department of Chemistry, Faculty of Science,
Lund University, Sweden

Reviewer: Uno Mäeorg, PhD
Associate Professor of Bioorganic Chemistry
Institute of Chemistry, Faculty of Bioorganic Chemistry
University of Tartu, Estonia

Opponent: Peter Olsén, PhD
Assistant Professor in Synthetic Chemistry from Forest Resources towards Functional and Sustainable Materials,
Laboratory of Organic Electronics,
Linköpings University, Sweden

Commencement: Auditorium 121, Nooruse 1, Tartu, Estonia, at 13.15 on September 27th, 2024

Publication of this thesis is granted by the Institute of Technology, Faculty of Science and Technology, University of Tartu.

ISSN 2228-0855 (print)
ISBN 978-9916-27-635-8 (print)
ISSN 2806-2620 (pdf)
ISBN 978-9916-27-636-5 (pdf)

University of Tartu Press
www.tyk.ee

ABSTRACT

The excessive consumption of petrochemicals for energy and materials has caused a significant adverse impact on the environment. Using widely non-renewable fossil-based resources is not sustainable and requires replacement in many fields. Plastics belong to the most common petroleum-based products that are manufactured on a very large scale.

Isosorbide is considered as one of the potential biobased compounds that could offer alternatives to fossil-based polymer building blocks. It is a rigid bicyclic diol which is commercially produced from glucose and has found use mostly in medicine and cosmetics. In the present thesis, isosorbide monomethacrylates were investigated as monofunctional polymer building blocks, where residual hydroxyl groups were functionalized with different saturated aliphatic fatty acids or aromatic lignin-related carboxylic acid esters. The monomers were polymerized by conventional free-radical polymerization, and the structural influence of different functionalities on the polymer characteristics was systematically studied.

A second approach involved the preparation and investigation of thiol-acrylate copolymers, which were derived from biobased building blocks such as citric acid, glycerol and trimethylolpropane. Moreover, the hydrolytic degradation of corresponding thiol-acrylate polymers was demonstrated to open the path for chemical recycling of the copolymers.

In summary, this thesis focuses on the preparation and investigation of novel high-performance biobased polymers that may provide alternatives to non-renewable fossil-based thermoplastics, and at least partially alleviate the environmental problems caused by today's plastics.

TABLE OF CONTENTS

LIST OF ORIGINAL PUBLICATIONS

This thesis is based on the following publications. The articles are referred in the text by Roman numerals I–III.

I. **Laanesoo, S**.; Bonjour, O.; Parve, J.; Parve, O.; Matt, L.; Vares, L.; Jannasch, P. Poly(Alkanoyl Isosorbide Methacrylate)s: From Amorphous to Semicrystalline and Liquid Crystalline Biobased Materials. *Biomacromolecules*. **2021**, 22 (2), 640–648. https://doi.org/10.1021/acs.biomac.0c01474.

II. **Laanesoo, S**.; Bonjour, O.; Sedrik, R.; Tammsalu, I.; Jannasch, P.; Vares, L. Combining isosorbide and lignin-related benzoic acids for high-T_g polymethacrylates. *Eur. Polym. J*. **2024**, 202, 112595–112595. https://doi.org/10.1016/j.eurpolymj.2023.112595.

III. Sedrik, R.; Bonjour, O.; **Laanesoo, S**.; Liblikas, I.; Pehk, T.; Jannasch, P.; Vares, L. Chemically Recyclable Poly(β-Thioether Ester)s Based on Rigid Spirocyclic Ketal Diols Derived from Citric Acid. *Biomacromolecules*. **2022**, 23 (2), 2685–2696. https://doi.org/10.1021/acs.biomac.2c00452.

Publications not included in the thesis:

Bonjour, O.; Nederstedt, H.; Arcos-Hernandez, M. V.; **Laanesoo, S**.; Vares, L.; Jannasch, P.; Lignin-Inspired Polymers with High Glass Transition Temperature and Solvent Resistance from 4-Hydroxybenzonitrile, Vanillonitrile, and Syringonitrile Methacrylates. *ACS Sustainable Chem. Eng*. **2021**. 9 (50), 16874–16880. doi.org/10.1021/acssuschemeng.1c07048

Author contributions:

Paper I: Contributed to the monomer synthesis. Performed all the polymerizations. Chemical characterization of monomers and polymers. Participated in the preparation of the first draft of the manuscript. Preparation of supporting information.

Paper II: Performed all the experimental work, except rheology and thermal analyses. Chemical characterization of monomers and polymers. Made the first draft of the manuscript and actively participated in the preparation of manuscript. Preparation of supporting information.

Paper III: Performed half of the experimental work. Characterization of half of the monomers and polymers. Participated in the preparation of supporting information.

ABBREVIATIONS

ABS	acrylonitrile butadiene styrene
ACN	acetonitrile
AIBN	azobis(isobutyronitrile)
AIMA	alkanoyl isosorbide methacrylate
BuOH	butanol
$Đ$	polydispersity index (M_w/M_n)
DBU	1,8-diazabicyclo[5.4.0]undec-7-en
DMI	dimethyl isosorbide
DMF	dimethyl formamide
DMPA	2,2-dimethoxy-2-phenylacetophenone
DMSO	dimethyl sulfoxide
DSC	differential scanning calorimetry
EtOAc	ethyl acetate
Et_2O	diethyl ether
GHG	greenhouse gas
GVL	γ-valerolactone
ΔH_m	melt enthalpy
HRMS (ESI)	high-resolution mass spectroscopy, where ionization is performed by electron spray ionization
HQ	hydroquinone
HQMME	4-methoxyquinone
5-**IMA**	isosorbide-5-methacrylate
2-**IMA**	isosorbide-2-methacrylate
MeOH	methanol
M_n	number average molecular mass
mol%	mole percent
MTBE	methyl tert-butyl ether
M_w	weight average molecular mass
NMR	nuclear magnetic resonance spectroscopy
PAIMA	poly(alkanoyl isosorbide-5-methacrylate)
PE	polyethylene
PEG	poly(ethylene glycol) (PEO with $M_n < 20$ kg/mol)
PEO	poly(ethylene oxide) ($M_n > 20$ kg/mol)
PET	poly(ethylene terephthalate)
Ph	phenyl
PLA	poly(lactic acid)
PMMA	poly(methyl methacrylate)
PP	polypropylene
PS	polystyrene
PVC	poly(vinyl chloride)
RID	refractive index detector
r-(**P**)**AIMA**	5-alkanoyl-isosorbide-2-(poly)methacrylates

RT	room temperature
SEC	size-exclusion chromatography
$T_{d,95\%}$	decomposition temperature at a 5% mass loss
T_g	glass-transition temperature
T_i	isotropization temperature
T_m	melting temperature
TMP	trimethylolpropane
w%	weight percentage
XRD	X-ray diffraction spectroscopy

INTRODUCTION

Plastics play a crucial role in our everyday life. Most essential goods and commercial products are manufactured, or at least packaged, using plastics. Plastics are produced by polymerizing monomers and adding different additives, if required, which help to enhance corresponding material characteristics.[1] This makes plastics ultimately very versatile materials, that can be obtained with the desired softness, durability, and stability. Today, there are numerous conventional and high-performance plastic materials that are suitable for casual everyday applications, or very harsh and demanding conditions.

However, plastics production has been growing extensively from 1950 to 2018 from 1.5 to 358 Mt, respectively, and is predicted to triple by 2060.[2–3] The rising plastics production has caused serious environmental problems, e.g., plastic pollution both in land and marine ecosystems, CO_2 emissions, excessive usage of non-renewable fossil resources, microplastics in food.[4–6]

To improve this situation, a lot stricter rules for single-use plastic should be considered to lessen a plastic consumption and thus avoid possible adverse effects to the environment. There are many ways to optimize the plastic exploitation and possible solutions should be discussed separately for each product category. For instance, the current situation may be improved by selling some of products, e.g., primary everyday food products (e.g., milk, bread), directly in reusable containers. Packaging requirements should be discussed depending on the specific product to lessen the amount of packaging material used. Many products could be placed into more economical packaging or sold without packaging. People should be encouraged to think carefully about what they need and save the environment by not buying non-essential products.

In contrast, there are a few efforts that can be made from a chemist's perspective. First, many conventional fossil-based plastics can be replaced with renewable biobased counterparts. Exploitation of biobased resources can potentially reduce CO_2 emissions because they are derived mostly from plants, which absorb CO_2 during photosynthesis.[7] However, the development of biobased plastics is still challenging. Polymer chemists are actively seeking valuable biobased polymer building blocks to prepare high-performance materials, because many of the biobased plastics are either too soft for many applications, or too expensive to manufacture in industrial scales due to complicated intermediate production steps.[8,9] In addition, the research involves the development of feasible and cost-effective industrial routes to biobased plastics.[10]

Second, the new plastics should be designed to be recyclable in order to reduce plastic waste in the environment and to be reusable as a source of chemicals for the production of new plastics. Currently, only 9% of the plastics are recycled globally, while 22% are mismanaged, 49% are landfilled and 19% are incinerated.[11] These numbers are surely convincing that the recycling and utilization of plastics continuously need continuously new feasible solutions. For example, chemical recycling is a potentially useful method for polymers that have chemically labile functionalities in the structure, which helps to degrade the

polymer back to monomers or to valuable chemicals.[12] On the other hand, as polymers consist of different chemical entities, research is required to identify specific chemical degradation pathways for a given plastic material.

The focus of the present thesis is on the investigation of novel biobased thermoplastic polymers that have competitive thermal properties compared to other commercially available biobased plastics (such as, e.g., PLA), and which could potentially provide a replacement to fossil-based plastics. For this purpose, isosorbide was investigated as a renewable polymer building block. Isosorbide is a commercially available rigid bicyclic diol manufactured from starch.[13] The first approach was to use isosorbide to prepare monofunctional methacrylate monomers, where the residual hydroxyl group was derivatized with various linear saturated fatty-acid or lignin-related carboxyl acid esters. The monomers were polymerized by conventional free-radical polymerization and the influence of the side groups on polymer characteristics was systematically investigated. The main goal was to find new biobased alternatives to fossil-based engineering plastics such as PMMA, PS and to achieve competitive polymer properties.

The second approach involved the synthesis and characterization of rigid thiol-acrylate copolymers from biobased building blocks, e.g., citric acid, glycerol and trimethylolpropane.[14–16] As a last part, biobased copolymers of isosorbide dilevulinate and dihydrazides were investigated to seek new alternative plastics.

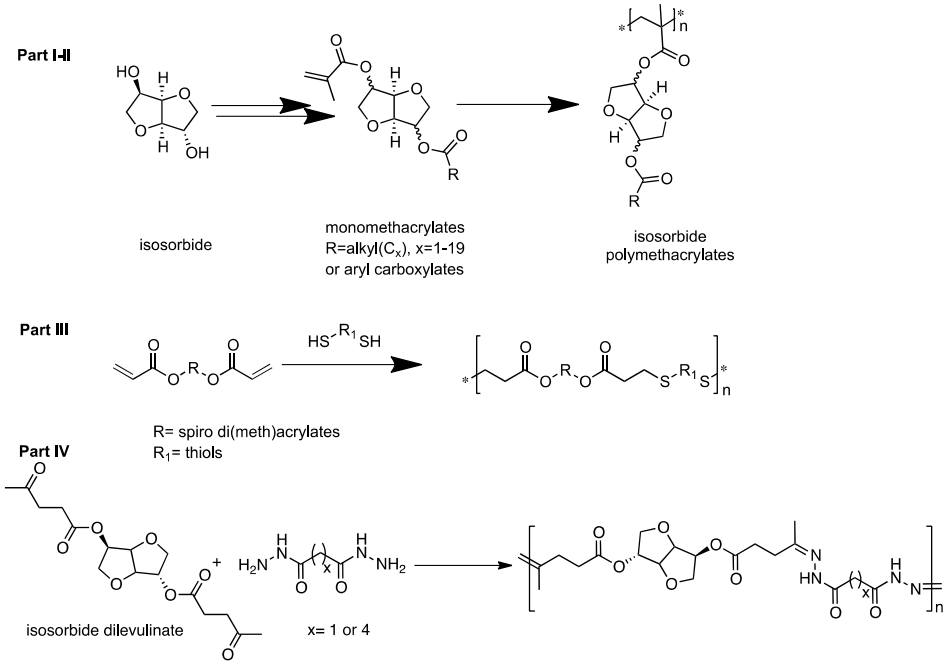

Scheme 1. Outline of the present thesis. **Part I–II** – preparation and investigation of isosorbide polymethacrylates. **Part III** – preparation and investigation of thiol-acrylate polymers. **Part IV** – investigation of copolymers of isosorbide dilevulinate copolymers with and dihydrazides.

1. LITERATURE OVERVIEW

1.1 About plastics

Since the 20th century, industrial development and the explosive growth of the human population initiated the start of the plastic industry.[17] Plastics are polymeric materials consisting of monomers chemically attached to form long chains. There are plenty of additives that can be added to enhance the final properties of polymeric materials. Common additives are plasticizers to obtain the proper softness, stabilizers to protect from weather and extreme temperatures, flame-retardants, pigments, odor scavengers, etc.[18] The most common plastics (PP, PE, PVC) are manufactured from fossil-based resources. They are cheap and readily available due to cost-efficient production process and low price of fossil raw materials.[19] Plastics have vast spectrum of characteristics and are therefore used in many different applications and can be manufactured according to specific material requirements.

In general, plastics are characterized by many different parameters, which determine their applicability in different applications. Firstly, plastics are divided into two main types – thermoplastics and thermosets. Thermoplastics are linear or branched polymers that can be either soft or hard, depending on temperature. In contrast, a thermoset has crosslinked (network) polymer that cannot be softened by heating until it starts to decompose. Secondly, polymers can be described by their different thermal characteristics, such as glass-transition temperature (T_g), melting point (T_m), and decomposition temperature (T_d). The glass-transition temperature indicates the temperature when rigid and glassy polymer chains become mobile, and the polymer starts to soften. The melting point is characteristic to semicrystalline polymers, in which polymer chains are partially or fully crystalline. The crystallinity disappears above melting point.[20]

1.2 Plastic recycling

Since the plastics have become widespread materials, a large amount of plastic waste needs to be managed to mitigate plastic pollution. Plastics are, in general, landfilled, incinerated, recycled, or simply mismanaged.[21,22] However, landfilling, incineration and mismanagement can cause serious environmental issues. This includes general pollution of both marine and land ecosystems, depletion of valuable land resources, greenhouse gas contribution from incineration, etc.[23] Hence, plastic management methods employed today are insufficient and more efficient solutions are thus needed.

More sustainable plastic management methods include reuse and recycling, which includes reusing plastic materials mostly in three main ways. First, used plastics, e.g., plastic containers, are directly reused after cleaning. Second, old plastics are reprocessed to similar or lower value products. Third, plastics are

chemically recycled. In chemical recycling, the polymers are converted back into monomers or other valuable chemicals for further (re)processing.[24] Although these methods may sound simple and sustainable, there are different issues involved. For example, many plastic products consist of multiple types of polymers and should be recycled separately as they have different physical and chemical properties.[25] Thermoset polymers are particularly difficult to recycle, as they are not melt processable.[26] Moreover, an industrial-scale plastic management is often hindered due to mixed and dirty plastic wastes.[27]

In summary, each plastic requires a specific approach. Plastics that are not considered recyclable should preferably be incinerated to prevent land or marine pollution. However, some of plastics can emit toxic gases during incineration, such as dioxins, hydrochloric acid and sulfur dioxide.[28]

From a chemist's perspective, if primary and secondary plastic recycling techniques are not applicable, the alternative approach could be to degrade and recycle the polymers back to monomers or valuable chemicals (e.g., solvents).[29] However, a suitable chemical degradation pathway is not available for all the plastics and depends on the polymer structure. Preferably, the polymers should be designed to be recyclable, or to at least have functional groups that can be easily cleaved. For instance, ester groups can be hydrolyzed under acidic or basic conditions, or by using enzymatic catalysis.[30]

1.3 Biobased plastics

Biobased plastics are materials, that are fully or partially derived from renewable carbon resources.[31] The most manufactured biobased plastics are PLA and different starch blends.[32] However, the biobased plastic market remains marginal. Around 2.1 Mt (less than 1% of the plastic market) of plastics were manufactured from biomass in 2018.[31] However, there are several driving forces towards the production of biobased plastics. First, biomass is renewable.[31] Second, biobased plastics may reduce CO_2 emissions, because CO_2 is absorbed during the photosynthesis, which would partially compensate the emitted CO_2 after possible incineration.[33,34] On the other hand, fossil-based plastics contribute to overall CO_2 emissions, because there is no CO_2 absorbing process during its lifecycle and CO_2 will be emitted during the possible incineration or decomposition (Figure 1).

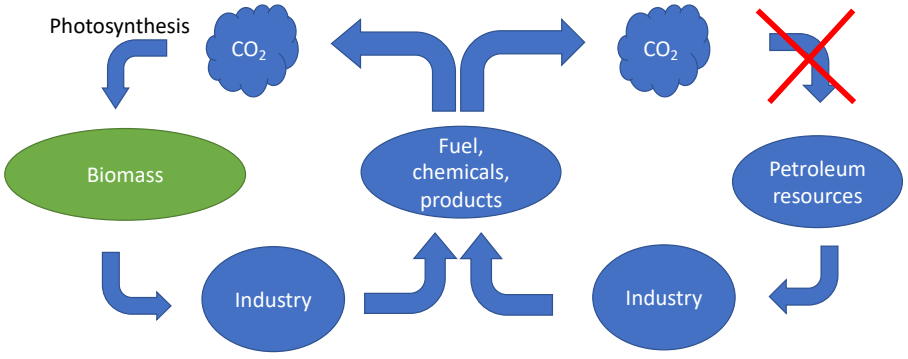

Figure 1. A simplified carbon cycle for biobased and petroleum-based resources.

However, the development of biobased plastics remains challenging. The main issues are the higher production costs and difficulties to achieve high-performance materials.[35,36] Higher cost is caused by several reasons. Firstly, some of the bio-based polymers have complex manufacturing procedure by having more inter-mediate production steps.[37] Secondly, common commercial biobased plastics have poor thermal properties for more demanding applications (e.g., PLA has $T_g = 55$ °C).[38,39] Because of the previously mentioned problems, the current research in the biobased polymer field focuses to a high degree on materials with high thermal stability, scalable and viable production routes.[40]

1.4 Isosorbide as a sustainable building block

Isosorbide (**1,4:3,6-Dianhydro-*D*-glucitol**) is a valuable non-toxic, structurally rigid, glucose-derived bicyclic diol.[41,42] The interest in this compound has rapidly increased over the last decades due to its biobased origin and versatile uses. Isosorbide is manufactured from biomass by a multistep synthesis.[43] In the first step, glucose is derived preferably from starch or cellulose by depolymerization. The route from cellulose is more complex due to its poor solubility.[44] Although an efficient (65% yield) one-pot synthesis from cellulose to isosorbide has been proposed, but it is not favored due to the use of mineral acids and complicated waste treatment.[45,46] After obtaining glucose, a sorbitol is synthesized by hydro-genation. The final isosorbide product is obtained by twofold dehydration (Scheme 2).[43] Much effort has been put into the optimization of the isosorbide synthesis, which may help to boost its use and lower the production costs.[47–49]

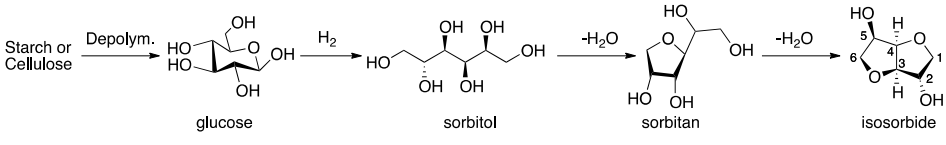

Scheme 2. Isosorbide production from biomass.

1.4.1 Properties

Isosorbide appears as a white crystalline solid at room temperature and is very hygroscopic.[50] It has a melting point around 61–64 °C and is thermally stable up to 270 °C.[51] It is soluble in water and in common organic solvents, such as ethanol, chloroform, dioxane, and EtOAc.[52,53] Isosorbide consists of two fused furane rings in a 120° angle, which gives a V-shaped molecule backbone.[54] There are four chiral centers, which arise from tertiary center carbons and hydroxyl groups. Isosorbide has two diastereomers – isomannide (both-OH groups in *endo* configuration) and isoidide (both-OH in *exo* configuration, Figure 2).[55] Moreover, the stereoisomeric configuration determines the reactivity of the hydroxyl groups.[43] For isomannide and isoidide, both hydroxyl groups are chemically equivalent. Isosorbide has two hydroxyl groups that are chemically non-equivalent – the *endo* hydroxyl group has hydrogen bonding with oxygen from the neighboring furane ring, while the *exo* hydroxyl group does not.

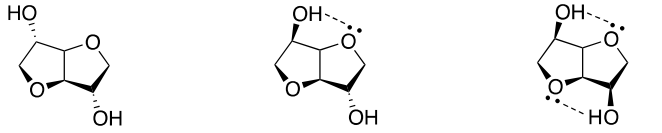

Figure 2. Structures of three stereoisomers of dianhydrohexitols.

Isosorbide is the cheapest and the commercially most available stereoisomer (production of 20 kT in 2017), while isomannide and isoidide are much less frequent. Isomannide is obtained from *D*-mannitol and is more expensive due to lower abundance.[41] Isoidide is the most expensive stereoisomer because *L*-idose is rarely found from natural sources, and there is a lack of feasible synthetic pathways to isoidide.[56] In summary, isosorbide is the only diastereomer under extensive investigation. The other diastereomers still remain too expensive for large-scale production and further developments.

1.4.2 Applications of isosorbide and its derivates

Isosorbide has been investigated as a starting material for several pharmaceuticals and other useful compounds and as a polymer building block.[57] Isosorbide nitrates (Figure 3) are well-known drugs for the treatment of heart angina, and help to prevent heart failure and improve blood supply.[58] Dimethyl isosorbide (DMI) has been investigated as a replacement for more toxic solvents such as DMSO and DMF.[57,59] DMI is also used in cosmetics and pharmaceutical applications.[59] Isosorbide diesters are used in plasticizers and household chemicals such as detergents.[57,60,61]

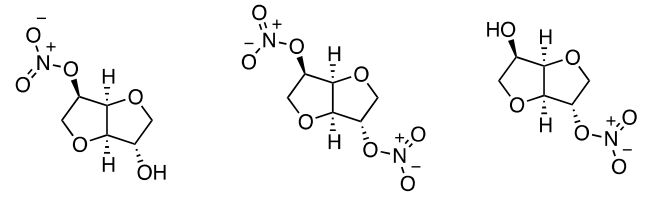

Figure 3. Structures of isosorbide nitrates.

1.4.3 The regioselective synthesis of isosorbide monomethacrylates

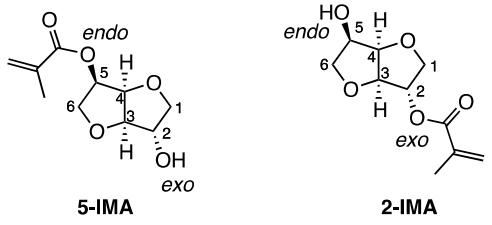

Figure 4. Isosorbide monomethacrylate regioisomers

Isosorbide has been investigated as a difunctional monomer or as a mixture of regioisomers of monofunctional monomer for years.[62–65] Recently, a regio-selective method was developed in our group to obtain both clean regioisomers of isosorbide monomethacrylate (Figure 4).[66] The regioselective modification is possible due to the chemically non-equivalent hydroxyl groups. The *endo* hydroxyl group has hydrogen bonding with an oxygen in the furane ring, while *exo* has no hydrogen bonding. Moreover, intramolecular hydrogen bonding makes the endo hydroxyl group a stronger nucleophile and more reactive. Regioselective synthesis is performed by using Lipozyme RM IM catalyzed esterification, which is highly regioselective towards the *endo* hydroxyl group. This development opens a path to use isosorbide as a single regioisomer in a polymer side chain. The remaining hydroxyl group of the monomer can be functionalized with a wide variety of side groups to obtain polymers with very different characteristics.

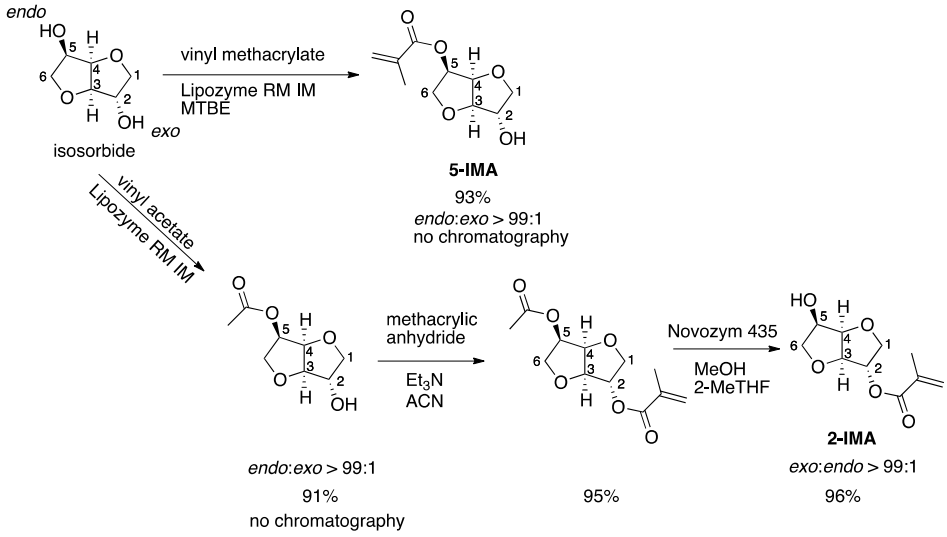

Scheme 3. Synthesis of both isosorbide monomethacrylate regioisomers

During the regioselective esterification (Scheme 3), the *endo* hydroxyl group was acylated with methacrylic group from the vinyl methacrylate to afford isosorbide-5-monomethacrylate (5-**IMA)** as a single detectable regioisomer (*endo*:*exo* > 99:1). Furthermore, the product was isolated with high yield (93%) without using chromatographic purifications.

Another regioisomer, isosorbide-2-methacrylate (2-**IMA**), was prepared using three step procedure as lipases are mainly selective towards the 5-position of isosorbide. First, the *endo* hydroxyl was protected by an easily removable ester (e.g., acetate) using Lipozyme RM IM. Similar to 5-**IMA**, the isosorbide-5-acetate was obtained with high yield (91%) without using chromatographic purification. After that, the methacrylic group was introduced to the *exo* position by using methacrylic anhydride. To obtain the final product (**2-IMA**), acetate in the *endo* position was regioselectively removed by Novozym 435.[66]

1.4.4 Isosorbide-containing monomers and polymers

In addition to isosorbide-based compounds, a lot of effort has also been put into the development of isosorbide-containing polymers. Isosorbide has certain advantages that have increased the interest towards polymers. This includes most notably the V-shaped rigid and chiral structure, which is rare among biobased building blocks. Thus, isosorbide has been studied in many types of polymers – polyesters, polycarbonates, polyethers, polyurethanes, poly(meth)acrylates, and isosorbide thiol-acrylate polymers.[62–64,67–69]

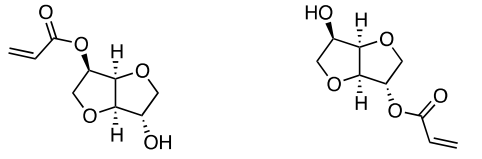

Figure 5. Regioisomers of isosorbide monoacrylates.

Nonque et al. have reported the synthesis of isosorbide monoacrylates (Figure 5) and their polymerization by conventional free-radical polymerization.[62] The monomers were prepared as mixtures of the two isosorbide monoacrylate regioisomers. They discovered that the polymerization of monoacrylates is highly dependent on the solvent. The polymer prepared from the mixture of the two isosorbide regioisomeric acrylates showed relatively high T_g values, reaching up to 112 °C. The authors found that polymerization in DMSO provided higher M_n values (75.1–78.6 kg/mol) compared to polymerizations in DMF (25.9 kg/mol). The corresponding polyacrylate polymer was converted into a thermoset material by curing the remaining hydroxyl groups with succinic anhydride at 190 °C. As a result, the thermoset was not soluble in any solvent and had somewhat higher T_g (116 °C).

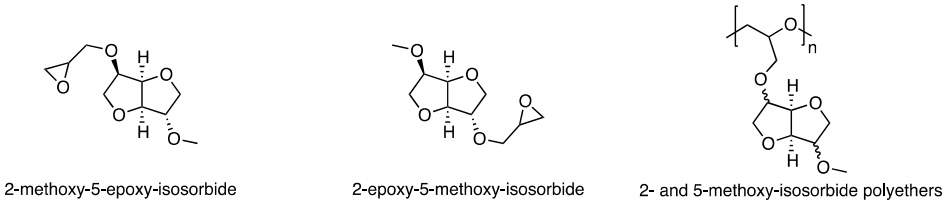

Figure 6. Structures of isosorbide epoxy monomers and their polymer structure

A method for preparing single regioisomers of methoxyisosorbide polyether has also been reported.[69] Regioisomers of epoxy-methoxy isosorbide monomers (Figure 6) were polymerized separately by anionic polymerization to obtain isosorbide polyethers. The resultant polymers showed high thermal stability under N_2, while a slight polymer decomposition started above 300 °C. However, the main mass-loss was observed above 390 °C. Glass transitions were around 10–15 °C, which is significantly higher compared to common polyethers, such as poly(ethylene oxide) at –66 °C and poly(propylene oxide) at –75 °C.[70]

Isosorbide has also been employed in an enzymatic transesterification copolymerization to obtain isosorbide polyesters with different diester fragments, such as succinate, adipate, suberate, sebacate, dodecaonate, etc.[65] These copolymerizations were performed using Novozym 435 (immobilized lipase B from *Candida arctica*) catalysis, which has shown excellent activity, considering that isosorbide is a somewhat hindered diol. Water was removed by azeotropic distillation with toluene, benzene and cyclohexane using Dean-Stark apparatus. The copolyesters were obtained with M_n-s up to 47 kg/mol but the value varied a

lot depending on the diester fragment. Moreover, the structure of diester fragment determined the T_g of the final product and T_g drops when the ester fragment became longer. The T_g-s of the succinate and dodecanoate copolyesters were 56 and –7 °C, respectively.[63]

1.5 Lignin

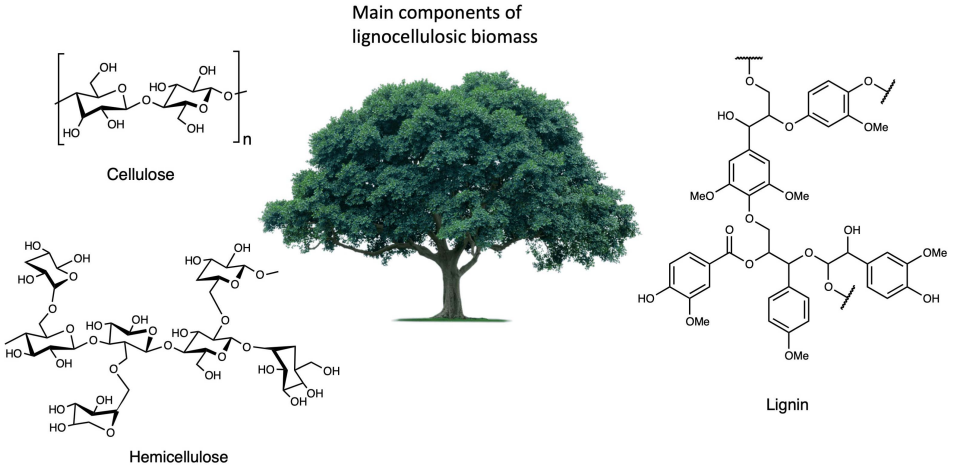

Figure 7. Main components of lignocellulosic biomass.

Lignin is one of the main components of lignocellulosic biomass, along with cellulose and hemicellulose (Figure 7).[71] Hence, lignin is the most abundant natural source of aromatic compounds.[72] Around 18–35% of the wood by weight consists of lignin depending on its origin (hard- or softwood).[73] Lignin has no specific structure and consist of a highly variable crosslinked structure of three main aromatic fragments: *p*-hydroxyphenyl, guaiacyl and syringyl (Figure 8), which are combined into the complex aromatic network.[74]

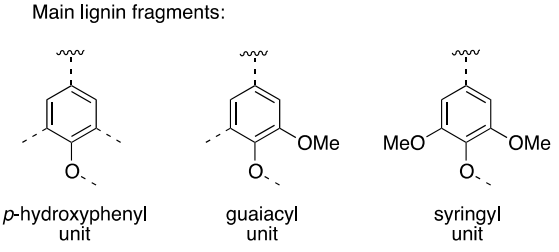

Figure 8. Structures of three main lignin fragments.

Around 50 Mt of lignin is produced annually as a byproduct of the pulp- and paper industry, and is mainly used as a low-value fuel.[75] However, the lignin valorization has been under the spotlight for the past 20 years as the lignin-

derived aromatics could potentially replace the fossil-based resources. Regarding the plastic industry, only a few strategies exist to convert waste lignin into plastic materials.

1.5.1 Lignin-related polymeric materials

First, lignin can be used in blends or composites with different commercial polymers.[76] Using crude lignin as a source of polymeric materials is challenging because lignin has a highly varying chemical composition of subunits and solubility issues.[77] Moreover, the high chemical variation also affects the material properties, which makes it difficult to obtain materials with reproducible characteristics. Lignin properties can be roughly established by the choice of lignin source (hard- or softwood) and the lignin processing technologies.[78] The softwood lignin has higher T_g (138–160 °C) than hardwood lignin (110–130 °C).[79] In addition, there are several lignin chemical separation techniques, such as extraction by Kraft, soda, organosolv or acid hydrolysis, that may influence lignin properties. For example, T_g of the processed lignin can range from 91 to 174 °C, respectively, for organosolv and Kraft lignin.[80]

The common examples incorporating lignin in plastics are polyurethane and PLA composites.[77,81] Lignin is used in polyurethane composites as a replacement for fossil-based polyols. Moreover, impressive tensile strength (41.6 MPa) was reached with a lignin content up to 47% by mass. These materials can be used as coatings which require hardness and solvent resistance.[82] Another example involves PLA, which is currently one of the most manufactured biobased polymers, but suffers from low ductility and thermal stability.[83] Parajo et al. showed a significant improvement in ductility of PLA butyl-esterified pine lignin blends compared to the neat PLA.[84]

In another approach, the lignin has been studied as a biobased source of aromatic polymer building blocks. Depolymerizing lignin into pure aromatic compounds from lignin is highly challenging due to its poor solubility and variable chemical composition.[85] Thus, the only commerially produced building block from lignin is vanillin from the guaiacyl unit (20 kT annually).[86] In summary, the high interest towards lignin valorization has motivated studies of depolymerization and isolation methods to obtain different chemicals, which may reach markets soon.

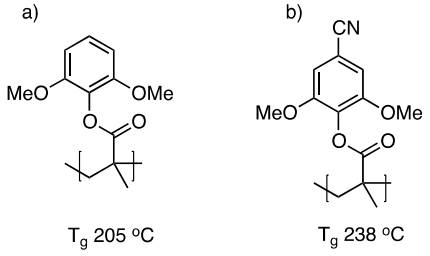

Figure 9. Lignin-based polymethacrylates prepared in studies by a) Epps et al. and b) Jannasch et al.

Lignin-based aromatic building blocks have been investigated in various polymers. Successful polymerizations of lignin-based methacrylates have recently been reported (Figure 9). Epps et al. have demonstrated *o*-, *p*- substituted lignin-based benzoyl polymethacrylates that achieved impressive T_g (205 °C).[87] Furthermore, Jannasch et al. have reported the polymerization of lignin-based poly(*p*-cyanobenzoylmethacrylate)s using a strongly polar and rigid cyano group to increase the T_g even further. As a result, very high T_g (238 °C) was achieved for poly(*p*-cyano-*o*-dimethoxybenzoylmethacrylate).[88]

1.6 Polymerization methods

1.6.1 Radical polymerization

Radical polymerization is one of the most widely employed polymerization methods in industry, comprising approximately 40–55% of all polymerizations.[89] Radical polymerizations are typically initiated by thermal initiators, which decompose homolytically into active radicals under certain conditions, most commonly by UV-light or elevated temperatures (Scheme 4). Common radical initiators are azo- or peroxy-compounds that readily undergo homolysis of specific unstable chemical bonds, for example, in AIBN and DMPA.[90]

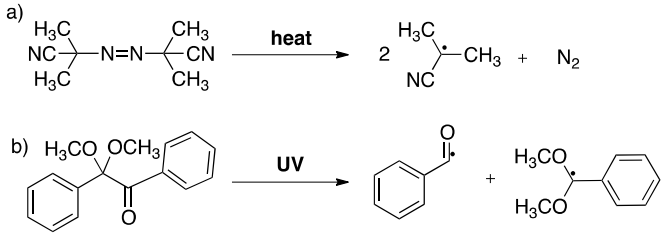

Scheme 4. Homolysis of radical initiator. a) AIBN homolysis at elevated temperatures; b) DMPA photolysis under UV light.

The radicals can initiate polymerization of different unsaturated functionalities such as (meth)acrylates, styrene, vinyl, chloroprene, acrylonitrile and ethylene.[91] In general, the mechanism of radical polymerization is divided into three main steps: initiation, propagation and termination (Scheme 5).[92]

During the initiator cleavage under certain conditions, one molecule forms two radicals. These radicals will react with specific unsaturated monomer fragments and initiate chain-growth radical polymerization. Eventually, the reactive radicals may terminate in two different ways: by a combination of two long-chain radicals into one polymer chain, or by disproportionation, where two polymer radicals form two separate polymer chains .[92]

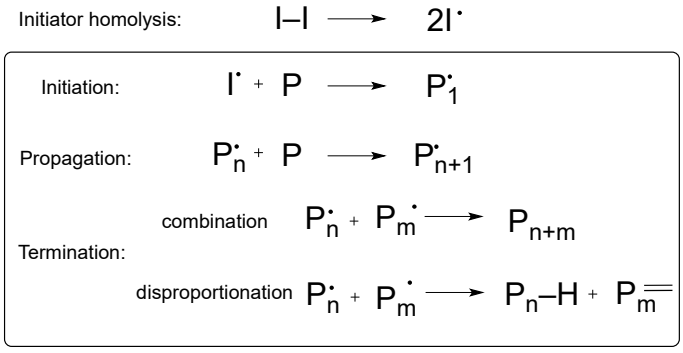

Scheme 5. A general mechanism for radical polymerization

In addition to free-radical polymerization, there are several controlled radical polymerization methods. The most known methods are RAFT[93] (reversible addition-fragmentation chain transfer), NMP[94] (nnitroxide-mediated polymerization) and ATRP[95] (atom transfer radical polymerization). The main advantages of these methods are the narrower MW distribution and more controlled polymer composition.[96,97]

1.6.2 Thiol-acrylate polymerization

Thiol-acrylate polymerization is a method to copolymerize thiols and acrylates by forming C–S bonds. The method is analogous to the extensively investigated thiol-ene polymerization.[98] The polymerization can be performed using basic or radical catalysis (Scheme 6). The chemical pathway involves Michael addition, where a (deprotonated) dithiol reacts with a diacrylate, forming polymeric chains via new C–S bond. The deprotonation is typically carried out by mild organic N-bases, such as DBU, Et_3N, etc.[99] The polymerization can also be performed via a radical pathway, where initiated sulfur radicals reacts with acrylate groups. The photoinitiated thiol-acrylate has been studied with different mixtures of diacrylates, dithiols, and monoacrylates, obtaining linear or cross-linked materials depending on specific monomers or monomer ratios used.[100]

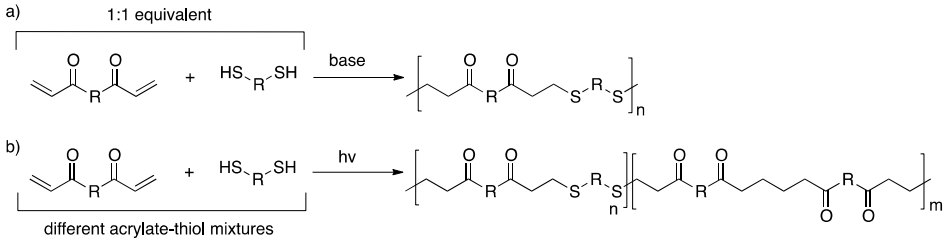

Scheme 6. Thiol-acrylate polymerization by a) base-catalyzed Michael addition; b) photo-induced polymerization.

Thiol-acrylate copolymers have been so far prepared mainly by UV-curing, by using different thiol:acrylate equivalents or trifunctional acrylates to obtain crosslinked network. Crosslinking polymers is a good strategy to improve thermal properties compared to linear polymers. The linear thiol-acrylate polymers tend to exhibit low T_g-s, most likely due to flexibility of a polymer backbone and dithiol structure. Long et al. have studied linear isosorbide-based thiol-acrylate polymers, which showed T_g-s from –14 to 15 °C depending on the dithiol structure. These polymers were studied for bio-medical applications due to their low toxicity.[101]

1.7 Polymer characterization techniques used in the current thesis

1.7.1 Differential scanning calorimetry (DSC)

Differential scanning calorimetry is a method to determine the heat flow required to increase or decrease the sample temperature as a function of temperature. In that way, important polymer transitions can be determined and quantified.

For amorphous polymers, the glass transitions can be studied. The T_g indicates the temperature where polymer chains become mobile and the material starts to soften during heating. The T_g is an important characteristic determining the thermal range for use and processing of the polymer. In addition, the solid or liquid crystallinity of polymers can be observed by DSC, determining melting and isotropization temperatures.[102]

1.7.2 Thermogravimetric analysis (TGA)

Thermogravimetric analysis is a method used to determine the thermal stability of polymers, and thereby their suitable temperature range for using. In this method, the sample weight is continuously measured, while increasing the temperature. At some point, the sample weight starts to decrease, and the decomposition temperature can be determined at a specific mass loss.[103]

1.7.3 Dynamic mechanical analysis (DMA)

Dynamic mechanical analysis is method to determine polymer viscoelastic properties. The analysis is typically performed by applying a sinusoidal stress with a certain frequency at increasing temperature. The resulting modulus (stiffness) of the material is thus measured as a function of temperature, frequency, or time. As a result, the analysis gives an overview about polymer mechanical properties.[104]

1.7.4 Size-exclusion chromatography (SEC)

Size-exclusion chromatography is a method to determine polymer molecular weight and its polydispersity. The method is based on chromatography, where porous stationary phase is used to separate polymer molecules with different lengths and sizes. After that, the amount of different molecular weight fractions is determined by a detector system comparing sample and reference peaks. This technique allows to evaluate polymer characteristics depending on molecular weight. It is important to obtain polymers with a sufficiently high molecular weight to obtain materials with high mechanical strength.[105]

2. AIMS OF THE STUDY

The main goal of the thesis was to develop and study novel biobased thermoplastic polymers that may offer alternatives to conventional fossil-based polymers, such as, e.g., PMMA, PS and thiol-enes, in various fields. To that end, isosorbide-based polymethacrylates and thiol-acrylate copolymers from biobased building blocks were prepared and investigated. In addition, copolymerizations of isosorbide dilevulinate and dihydrazides were studied and evaluated. The thesis is divided into four parts:

1) Preparation and characterization of isosorbide monomethacrylate monomers and polymers substituted with linear saturated fatty-acid side chains. The influence of different regioisomers and side chain length on the polymer characteristics was studied.

2) Preparation and characterization of isosorbide-5-methacrylate monomers and polymers substituted with different lignin-related aromatic building blocks. The most suitable reaction media for the polymerizations were determined and the influence of different aromatic substituents on polymer characteristics was studied.

3) Preparation of spiro-di(meth)acrylate monomers. Thiol-(meth)acrylate copolymerizations were performed via Michael addition reactions. The structure-property relationship of the polymers was determined. The hydrolytic degradation for polymers was demonstrated.

4) This part discusses some unpublised results on the preparation and investigation of isosorbide dilevulinate hydrazone copolymers.

3. RESULTS AND DISCUSSION

3.1 Isosorbide polymethacrylates with linear alkanoyl side chains (Paper I)

This paper focuses on isosorbide monomethacrylates synthesized from the pure regioisomers 5-**IMA** and 2-**IMA**. The disubstituted monomers were obtained by the enzymatic or chemical acylation of linear pendant saturated fatty acids to the residual hydroxyl groups of the corresponding regioisomer of **IMA**. The acylated linear pendant side chains had chain lengths from acetate (C2) to eicosoanate (C20). Alkanoyl isosorbide methacrylate (**AIMA*x***) monomers were polymerized by free-radical polymerization under the same conditions to obtain **PAIMA*x*** polymers, where ***x*** indicates the number of carbons in the pendant alkanoyl substituent. The polymers were systematically investigated by SEC, NMR, DSC and TGA. Polymer structures, thermal properties, and the influence of regiochemistry were evaluated.

3.1.1 Preparation of alkanoyl isosorbide monomethacrylate (AIMA*x*) monomers

The monomers were synthesized by using regioselectively pure (>99%) 5-**IMA** and 2-**IMA**, obtained by the regioselective esterification using Lipozyme RM IM catalysis. Subsequently, the vacant hydroxyl group was acylated with different alkanoyl groups by using enzyme Novozym 435 catalysis (method **A**) or conventional chemical acylation with corresponding alkanoyl chlorides in ACN (method **B**) or DCM (method **B1**). As a result, **AIMA*x*** monomers were obtained with moderate to high yields (47–98%) (Scheme 7). The reaction yields were not optimized and the choice of acyl donor depended on the availability.

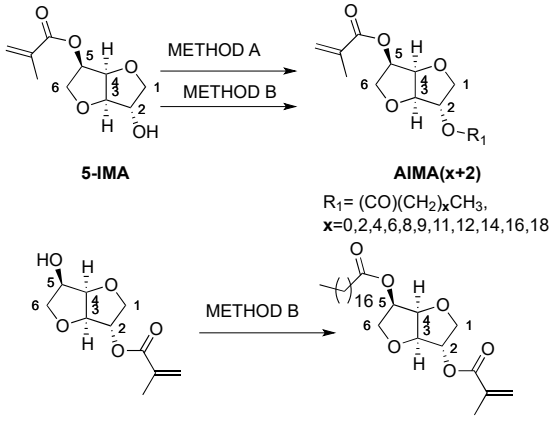

MONOMER		Isolated yield (%)
AIMA2	R = $OCCH_3$	98 (A)
AIMA4	R = $OC(CH_2)_2CH_3$	98 (A), 95 (B)
AIMA6	R = $OC(CH_2)_4CH_3$	92 (B)
AIMA8	R = $OC(CH_2)_6CH_3$	93 (B)
AIMA10	R = $OC(CH_2)_8CH_3$	87 (A)
AIMA11	R = $OC(CH_2)_9CH_3$	67 (B1)
AIMA13	R = $OC(CH_2)_{11}CH_3$	47 (B1)
AIMA14	R = $OC(CH_2)_{12}CH_3$	82 (A)
AIMA16	R = $OC(CH_2)_{14}CH_3$	79 (A), 77 (B1)
AIMA18	R = $OC(CH_2)_{16}CH_3$	57 (B1)
AIMA20	R = $OC(CH_2)_{18}CH_3$	71 (B1)

Scheme 7. Preparation of **AIMA** and *r*-**AIMA18** monomers by Novozym 435 catalysis (method **A**) or by chemical acylation in ACN (method **B**) or DCM (method **B1**).

3.1.2 Polymerization of isosorbide monomethacrylates with linear pendant fatty acid alkanoyl side chains

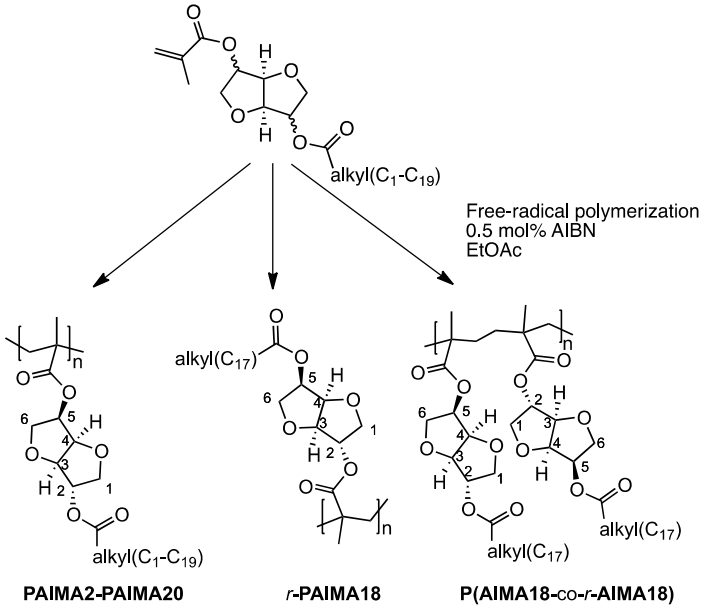

POLYMER	Conv.(%)
PAIMA2	85
PAIMA4	84
PAIMA6	63
PAIMA8	76
PAIMA10	56
PAIMA11	79
PAIMA13	81
PAIMA14	82
PAIMA16	82
PAIMA18	75
***r*-PAIMA18**	58
P[PAIMA18-*co*-*r*-PAIMA18]	81
PAIMA20	46

Scheme 8. Polymerization of isosorbide polymethacrylates **PAIMA2-PAIMA20**; ***r*-PAIMA18; P(AIMA18-**co**-*r*-AIMA18).**

After the monomer synthesis, 5-**IMA** derived monomers (Scheme 8): **AIMA2-AIMA20** and 2-**IMA** derived *r*-**AIMA18** and two **AIMA18** and *r*-**AIMA18** regioisomers in 1:1 molar ratio were polymerized by the conventional free-radical polymerization in EtOAc solution (0.1 g/mL) using AIBN (0.5 mol%) as a radical source. Before to the reaction, the monomer solution in a pressure tube was sparged with argon gas, typically for 30–60 minutes and then placed into the pre-heated oven at 63 °C for 24 hours.

After the reaction, the monomer conversion was determined from ^{1}H NMR data by comparing non-overlapping broad polymer signal with an unreacted double bond signal of the monomer at 6.15–6.17 ppm. Next, the crude mixture was precipitated in MeOH or Et_2O. Polymers were obtained with good-to-relatively high molecular weights M_n = 32–81 kg/mol and $Đ$ = 1.8–3.0 (Table 1). The molecular weight variation could be explained with the influence of several factors. First, elongation of the alkanoyl tail changes the monomer polarity and thereby solubility in a polymerization solvent. Second, some of the prepared monomers had a large amount of inhibitor dissolved in a solution, which was in some cases problematic to remove properly (especially HQMME), and a minor amount of inhibitor could be left in the monomer solution. The same problem could also affect the polymer conversions, which were relatively high (up to 85%, entry 2) but in some cases significantly lower than others (especially for **PAIMA6, PAIMA10** and *r*-**PAIMA18**; entries 4, 6 and 13).

Table 1. The results of **AIMA*x*** polymerizations.

entry	sample	conv. (%)[a]	M_n (kg/mol)[b]	$Đ$ (M_w/M_n)[b]	$T_{d,95\%}$ (°C)[c]	T_g (°C)[d]	T_m (°C)[d]	T_i (°C)[d]
1	**PAIMA0**[e (66)]	96	n.a	n.a	238	167	–	–
2	**PAIMA2**	85	32	3.0	208	107	–	–
3	**PAIMA4**	84	60	1.8	190	80	–	–
4	**PAIMA6**	63	56	2.1	188	57	–	–
5	**PAIMA8**	76	38	2.2	199	46	–	–
6	**PAIMA10**	56	47	2.1	201	52	–	–
7	**PAIMA11**	79	56	2.3	209	56	–	–
8	**PAIMA12**[e (66)]	87	43	2.7	226	54	–	–
9	**PAIMA13**	81	32	2.2	228	–	–	75
10	**PAIMA14**	82	61	2.2	233	–	–4	82
11	**PAIMA16**	82	58	2.1	231	76	19	92
12	**PAIMA18**	75	62	2.6	254	79	32	97
13	***r*-PAIMA18**	58	49	2.1	251	–	30	–
14	**P(AIMA18-*co*-*r*-AIMA18)**	75	81	2.1	247	–	41	69
15	**PAIMA20**	81	46	2.6	259	74	55	94

[a]Determined by NMR from a crude mixture. [b]Measured by SEC, using THF as eluent and PEG/PEO calibration standards for MW determination. [c]Measured by TGA under N_2 at 5% mass loss. [d]Determined by DSC. [e]Brought in for a wider comparison from another publication.[66]

3.1.3 Inhibitor removal

The samples contained inhibitors (HQ and HQMME), which were problematic to remove. HQ is more polar than HQMME and easier to remove by eluting through the short silica or basic aluminium oxide flash column. However, some samples contained HQMME, which tends to move at the same speed in a flash column as a target monomer. Another solution was to remove inhibitors by converting them into Na-salts by washing the monomer solution with 1% NaOH aqueous solution. This method was suitable only for **AIMA2**–**AIMA10**. Monomers with longer alkanoyl tails precipitated out shortly after adding 1% NaOH solution. Most likely, the alkanoyl tails were hydrolyzed off from the isosorbide unit and the remaining **AIMA0** partially polymerized instantly. The presence of **PAIMA0** was assumed by the fact that **PAIMA0** was not soluble in common solvents such as EtOAc or DCM.[66]

3.1.4 Solubility of PAIMA polymers

PAIMAs were immersed in different solvents to evaluate solubility properties. Solubility tests were performed in polar hydrogen-bonding solvents such as MeOH, n-BuOH and H_2O; in ethereal solvents (THF, Et_2O); in polar non-hydrogen bonding solvents DMSO, EtOAc and ACN; and in mid polar $CHCl_3$ or

relatively less polar toluene. None of the polymers were soluble in hydrogen-bonding polar solvents. Thus, MeOH was chosen as a precipitation media because it could separate polymers from monomer traces after polymerization. Interestingly, polymers were not soluble in Et_2O but were fully soluble in THF, which was also used as an eluent for these polymers in SEC. Mid polar EtOAc and $CHCl_3$ or less polar toluene could dissolve all the polymers. Also, **PAIMA16**–**PAIMA20** dissolved rapidly in toluene whereas the polymers with shorter alkanoyl tails did not. The complete solubility data for the polymers and monomers are presented in Supporting Information of Paper I.

3.1.5 Thermal properties of PAIMA polymers

PAIMAs were investigated by DSC and TGA to assess their thermal properties (DSC curves in Figure 10). Polymer **PAIMA0** and **PAIMA12**, having T_g, 167 and 54 °C, respectively, were brought in for comparison from a previous study. **PAIMA2** showed lower T_g in the current study compared to our previous results (107 vs 129 °C).[66] This is most likely caused by different MW-s of polymers. As expected, the T_g-s of the samples decreased from **PAIMA2** to **PAIMA8** by elongation of the linear alkanoyl tail. Hence, the T_g drops from 107 to 46 °C for **PAIMA2** and **PAIMA8**, respectively. **PAIMA8** has slightly lower T_g than expected, most likely due to a somewhat lower MW compared to the others in the series. After **PAIMA6**, the T_g seems to stabilize around 50–60 °C until **PAIMA12** (Table 1).

PAIMA2 and **PAIMA4** were additionally investigated by DMA to evaluate their mechanical properties. As a result, it was found that **PAIMA2** and **PAIMA4** had high mechanical stiffness until T_g, where storage modulus went below 1 GPa (graphs are presented in Paper I).

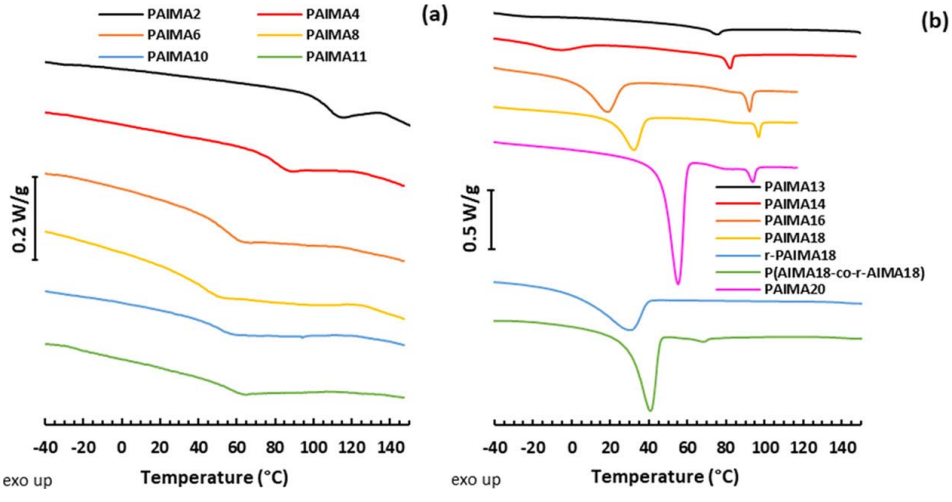

Figure 10. DSC graphs for a) amorphous **AIMA2**–**AIMA11** b) semicrystalline **AIMA13**-**AIMA20**, *r*-**PAIMA18**, **P**(**AIMA18**-*co*-*r*-**AIMA18**)

After the alkanoyl tail length increased beyond 13 carbons, DSC showed melting transitions as the **PAIMA** polymers became semicrystalline. **PAIMA14** showed melting point at –4 °C, which started rise by the elongation of the alkanoyl tail, reaching 55 °C for **PAIMA20**. Similarly, the ΔH_m increased from 5.5 to 53 J/g, indicating increasing crystallinity. After further heating, **PAIMA14**–**PAIMA20** samples also showed isotropization transitions, which indicated the presence of a liquid crystal mesophase (most likely nematic liquid crystal phase). Unfortunately, we could not confirm liquid crystallinity with XRD analysis, which could be due to small crystallization energies. ΔH_i reached up to 2.7 J/g for **PAIMA16**, while ΔH_m was more than 10-fold higher, reaching up to 44 J/g for 1:1 copolymer **P**(**AIMA18**-*co*-*r*-**AIMA18**). Next, **PAIMA20** was studied under cross-polarized light in a heated microscope to observe material textures at different temperatures (Figure 11). Initially, **PAIMA20** has a semicrystalline spherulitic texture, which disappears after further heating beyond the T_m. Instead, the material show a fine grainy texture, indicating the presence of the liquid crystal mesophase. After further heating beyond T_i, the grainy texture disappears, indicating no crystallinity in the melt state.

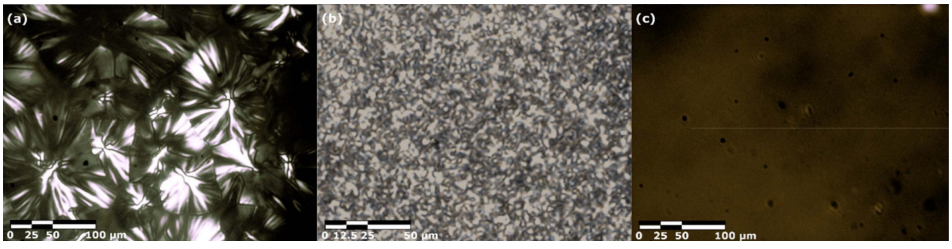

Figure 11. **PAIMA20** under the cross-polarized optical microscope at different temperatures. a) semicrystalline spherulitic texture at 22.5 °C; b) grainy liquid crystal mesophase at 52.2 °C; c) isotropic polymer melt at 113 °C.

Next, *r*-**PAIMA18** was synthesized to assess the influence of the regioisomeric configuration of isosorbide unit. As a result, regiosiomeric *r*-**PAIMA18** showed a melting transition similarly to **PAIMA18** at 30 °C, but no isotropization transition, which indicated the absence of liquid crystal mesophase. In the same manner, 1:1 copolymer of [**P**(**AIMA18**-*co*-*r*-**AIMA18**)] were investigated. This copolymer showed T_m at 41 °C and a very small isotropization transition at 69 °C (ΔH_i was only 0.5 J/g). The minor ΔH_i can be caused by the **AIMA18** monomer residues in the polymer sample. However, it is evident that the formation of liquid crystal mesophase in **PAIMA** polymers depends on the regiochemistry of the isosorbide unit.

The thermal stability of the corresponding polymers was determined by TGA measurements, where samples were heated under N_2 atmosphere to determine the $T_{d,95\%}$. **PAIMA** polymers have $T_{d,95\%}$ ranging from 188–259 °C. Non-substituted **PAIMA0** has $T_{d,95\%}$ 238 °C[66], after alkanoyl tail substitution, it decreases to 190 and 188 °C respectively for **PAIMA4** and **PAIMA6**. After **PAIMA6**, $T_{d,95\%}$ rises

almost linearly to 259 °C for **PAIMA20**, most likely due to heat-sensitive isosorbide unit dilution by the pendant alkanoyl tails.

3.2 Isosorbide 5-polymethacrylates with lignin-related aromatic substituents (Paper II)

In this paper, different 5-**IMA** derived monomers were synthesized by chemical acylation using various lignin-related aromatic substituents attached to the *exo* hydroxyl group of isosorbide. Some of the aromatic substituents (especially vanillic acid derivates) can be derived directly from lignin.[106,107] The monomers were polymerized by free-radical polymerization and the optimized polymerization conditions were determined. Next, all monomers were polymerized under the same conditions to obtain comparable data (Scheme 9). All polymers were systematically studied by SEC, NMR, DSC and TGA. The main goal was to investigate the influence of aromatic substituents on isosorbide 5-polymethacrylates and compare the results with previous linear fatty acid substituted isosorbide polymethacrylates (**PAIMA**s).

3.2.1 Monomer synthesis

Before the monomer preparation, the corresponding acyl chlorides from aromatic acids were synthesized (see procedure 4.1.2 General procedure for chlorination of carboxylic acids). After that, 5-**IMA** di(tri)esters were synthesized by chemical acylation using DCM or 2-MeTHF as a solvent (for detailed experimental data, see ESI in Paper II). The monomers were named according to their chemical composition in the *endo* side chain of isosorbide: **M** refers to monomer; **B** refers to benzoate fragment; numbers 3–5 refer to the positions of the methoxy group in a benzoate; **C*x*** refers to the length of alkanoate ester at vanillate fragment, **CN** refers to *p*-cyanobenzoate.

In most reactions, DCM was used as a solvent because it provided high monomer yields (76–98%). As a greener alternative, 2-MeTHF was tested as a solvent in a monomer **MB** synthesis. However, in this case, the conversion stopped at 75% and the product was isolated in 68% yield. The lower yield was most likely caused by the resultant triethylammonium salt, which blocked the stirring of the reaction mixture.

The monomers **MB**, **M4**, **MC18** and **MCN** were solids, while **M34**, **M345**, **MC2** and **MC6** were transparent viscous liquids. Solid monomers **MB**, **M4** and **MCN** can be purified by crystallization after the reaction using a 5% EtOAc solution in a petroleum ether as a crystallization medium. Products were isolated up to 90% yield by crystallization. This was a bit lower compared to the reactions with chromatographic purification (yield up to 98%) but should be preferred as a

more sustainable method. Also, it is noteworthy that for a successful crystallization, the stoichiometry of alcohol and acyl chloride during the reaction must be kept close to 1:1.

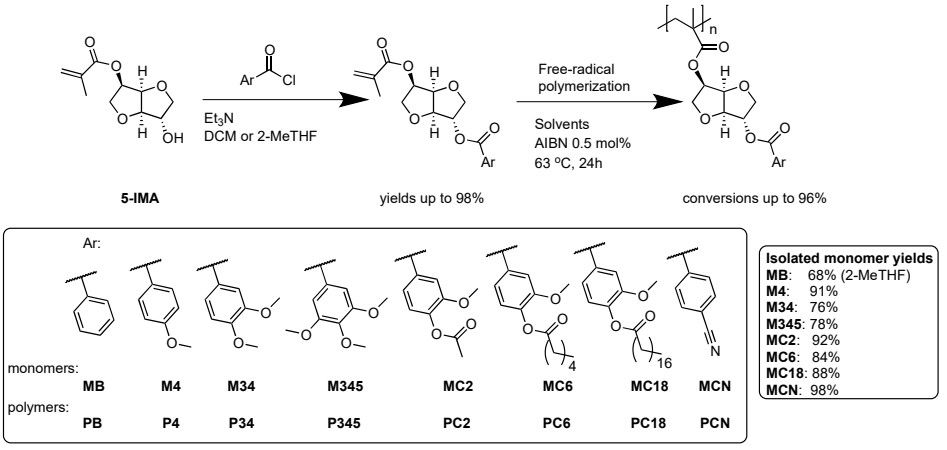

Scheme 9. **Chemical acylation**: 1–1.5 eq. corresponding acyl chloride, 1.2–1.7 eq. Et_3N, solvent: DCM or 2-MeTHF, 16 h at room temperature. **Polymerization**: 0.5 mol% AIBN, degassing by Ar gas, 63 °C, 24 h, precipitation in MeOH.

As aromatic units we chose vanillic acid derivates substituted with acetate, caproate and stearate; *p*-cyanobenzoate was chosen to study the influence of the highly polar cyano group; and (methoxy)benzoates were investigated to assess the impact of methoxy groups in *p*- and *o*-positions on polymer thermal characteristics.

3.2.2 Polymerizations

The monomers were polymerized by conventional free-radical polymerization using 0.5 mol% AIBN at 63 °C for 24 hours. Prior to the polymerizations in a larger gram scale, polymerizations were tested in smaller amounts (100–150 mg) in different solvents (EtOAc, GVL, toluene, DMSO, $CHCl_3$, and 2-MeTHF) to find the most suitable one. The polymers were named using the same principles as for the monomers, except using **P** instead of **M**, which refers to a polymer.

Initial polymerizations (Table 2) were performed in a small scale (100–150 mg of monomer) to find the most suitable polymerization solvent. EtOAc was firstly selected as a solvent, since it showed relatively good results in Paper I (M_n = 32–81 kg/mol).[108] However, in the present work, EtOAc caused solubility issues during the polymerizations. Polymers were obtained with M_n-s up to 28 kg/mol (entries 3,12), but the polymers precipitated during the polymerizations, which most likely hindered the further polymer chain growth. However, the precipitated polymers were soluble in some other solvents, for example in DCM.

Table 2. Selected polymerizations in a smaller scale performed in various solvents.

entry	sample	solvent	M_n (kg/mol)[a]	$Đ$ (M_w/M_n)	conversion (%)[b]
1	**PB**	DMSO	52	6.2	90
2	**PB**	GVL	18	4.4	85
3	**P4**	EtOAc	28	1.4	n.d.
4	**P4**	DMSO	61	3.4	94
5	**P4**	Toluene	14	3.7	n.d.
6	**P34**	EtOAc	17	1.7	n.d
7	**P34**	Toluene	15	2.2	n.d.
8	**P34**	Chloroform	8	1.8	61
9	**P345**	DMSO	65	2.1	80
10	**P345**	EtOAc	27	1.9	n.d.
11	**P345**	GVL	28	3.2	85
12	**PC2**	EtOAc	28	1.9	66
13	**PC2**	GVL	12	3.1	82
14	**PC2**	2-MeTHF	6	2.5	n.d.
15	**PC6**	DMSO	38	2.7	86

Standard conditions: the monomer solution was heated for 24 hours at 63 °C using 0.5 mol% AIBN as a radical source. [a]Measured in SEC, using THF as eluent and PEO/PEG standards. [b]Conversion determined by NMR.

Next, polymerizations were tested in greener solvents like GVL and 2-MeTHF. GVL gave M_n up to 28 kg/mol (entry 11), but unfortunately this result was not reproducible. 2-MeTHF performed poorly, affording polymers with M_n up to only 6 kg/mol (entry 14), or without any monomer conversion, which discouraged further trials with 2-MeTHF.

After that, chloroform was selected due to its excellent solubility properties for the monomers and polymers. Unfortunately, chloroform showed very poor results in the polymerizations, affording polymers with low M_n (only up to 8 kg/mol) or without any monomer conversion at all.

Next, toluene was tested as an example of a low-polarity solvent. Paper I showed that toluene dissolves polymers with longer alkanoyl tails (C16–C20) very rapidly. Despite the excellent solubility properties, toluene performed poorly in the current polymerizations (M_n-s up to 15 kg/mol; entry 7).

Eventually, DMSO was evaluated as a polymerization solvent and polymers with significantly higher molecular weights (M_n 38–65 kg/mol, Table 2, entries 1, 4, 9, 15) were obtained. Also, the monomer conversions in DMSO were higher compared to **PAIMA**-s polymerized in EtOAc in Paper I. Moreover, the polymers (except **PB** and **PC18**) did not precipitate during the polymerizations as observed in EtOAc. Consequently, DMSO was selected for the larger gram scale polymerizations.

Table 3. Polymerizations performed in DMSO on a larger gram scale.

entry	sample	M_n (kg/mol)[a]	$Đ$ (M_w/M_n)	conv. (%)[b]	isol.yield (%)[c]	T_g (°C)[d]	$T_{d,95\%}$ (°C)[e]
1	**PB**[f]	62	4.8	94	71	122	218
2	**P4**	90	2.5	93	75	124	225
3	**P34**	51	2.9	90	71	132	268
4	**P345**	87	2.5	93	74	107	249
5	**PC2**	38	3.4	94	72	103	255
6	**PC6**	44	3.7	88	49	80	263
7	**PCN**	80	3.7	94	90	168	268

Standard conditions: 24 hours at 63 °C using AIBN as a radical source. [a]Measured in SEC, using THF as eluent. MW was determined using PEO/PEG standards. [b]Conversion determined by NMR. [c]Isolated yield determined by mass after the polymer was collected and dried. [d]T_g was measured by DSC. [e]$T_{d,\ 95\%}$ was determined by TGA at a 5% mass loss under N_2. [f]Decreased monomer concentration (0.068 g/mL).

The results of the larger (gram) scale polymerizations in DMSO are presented in Table 3. The M_n range of obtained polymers varied from 38 to 90 kg/mol. The vanillic acid derived polymers **PC2** and **PC6** (entries 5–6) had notably smaller molecular weights than the average in the series, which can be caused by the structural differences (i.e., an additional carbonyl group). The polydispersity $Đ$ varied between 2.5–4.8, being especially broad for polymer **PB** ($Đ$= 4.8, entry 1). The high conversions (>90%) may explain the increased polydispersity. Potier et al. have reported that polydispersity of polymer prepared in DMSO may increase rapidly (up to 10) once the monomer conversion exceeds 90%.[109] The conversions ranged from 88 to 94%, which is higher than observed for AIMAs polymerizations in EtOAc in Paper I (up to 87%). The isolated yields of polymers were 49–90%, but most products were isolated in 70–74% yield. Most likely, the isolated product yield depended on the material properties, e.g., stickiness or packaging, which may influence the material isolation procedure.

In addition, the monomer concentration was decreased from 0.1 to 0.048 g/mL for **PB** (entry 1) in a polymerization mixture because at higher concentrations it tended to form insoluble gel-like product during the reaction.

3.2.3 Polymer PC18 synthesis

Polymerization of monomer **MC18** was investigated separately in more detail due to reproducibility issues after the preliminary successful experiment (Table 4, entry 1). The main issue was that in most cases **MC18** (similarly to **MB)** tended to form an insoluble gel-like product during the polymerization. To overcome this issue, the polymerization of **MC18** was carried out under different conditions to find the conditions where the monomer is reproducibly polymerizable. Thus,

different solvents (and solvent ratios), monomer and radical initiator concentrations were explored. Mixtures of DMSO with DCM or $CHCl_3$ were tested to improve the solubility but maintain the effect of DMSO which generally resulted in higher MW polymers. The results of the **MC18** polymerizations are presented in Table 4.

Table 4. MC18 polymerizations with AIBN in various solvent mixtures

entry	monomer conc. (g/ml)	solvent A	solvent B	solvent ratio (A:B)	M_n (kg/mol)[a]	$Đ$ (M_w/M_n)
1	0.1	DMSO	DCM	9:1	145.0	3.09
2	0.076	DMSO	DCM	9:1	insoluble product	
3	0.1	DMSO	DCM	9:1	insoluble product	
4	0.1	DMSO	toluene	1:3	insoluble product	
5[b]	0.1	DMSO	toluene	1:2	no conversion	
6	0.1	DMSO	toluene	1:1	50.1	2.96
7	0.067	toluene	–	–	no conversion	
8	0.1	toluene	–	–	13.5	1.55
9	0.1	chloroform	–	–	no conversion	
10	0.06	DMSO	chloroform	6:1	insoluble product	
11	0.038	DMSO	chloroform	3:1	insoluble product	
12	0.1	DMSO	chloroform	1:1	insoluble product	

AIBN was used as a radical source (typically 0.5 mol%, if not stated otherwise). Polymerizations were performed within 24 hours at 63 °C. [a]Measured by SEC, using THF as eluent and PEO/PEG standards for mass determination. [b]AIBN concentration was increased to 1 mol%.

The first strategy was to dilute the polymerization mixture. Dilution did not show any beneficial results. In DMSO, dilution from 0.1 to 0.076 g/mL (entries 1–3) also resulted in an insoluble product after polymerization. Use of pure toluene showed a low MW (M_n= 13.5 kg/mol) and did not show any monomer conversion after dilution (entries 7–8). The second strategy was to use mixtures of these solvents. DMSO and chloroform mixtures (similarly to the DMSO and DCM) gave insoluble products in all the monomer concentrations tested (entries 10–12). In summary, there were only two successful polymerizations (entries 1, 6), which unfortunately were not repeatable. The possible explanation for this phenomenon could be that polymers gained too high molecular weights (common in DMSO) and bulky monomer structures, which could not dissolve afterward in polymerization solvent.

3.2.4 Polymer thermal characterization

The thermal stability of the polymers was determined under the N_2 atmosphere by TGA. The polymers showed a 5% mass loss between 218–288 °C. The polymer thermal transitions were determined by DSC (Figure 12–13). As expected, all the polymers (except **PC18**) were amorphous materials with a single glass transition. Detailed TGA data are presented in Paper II.

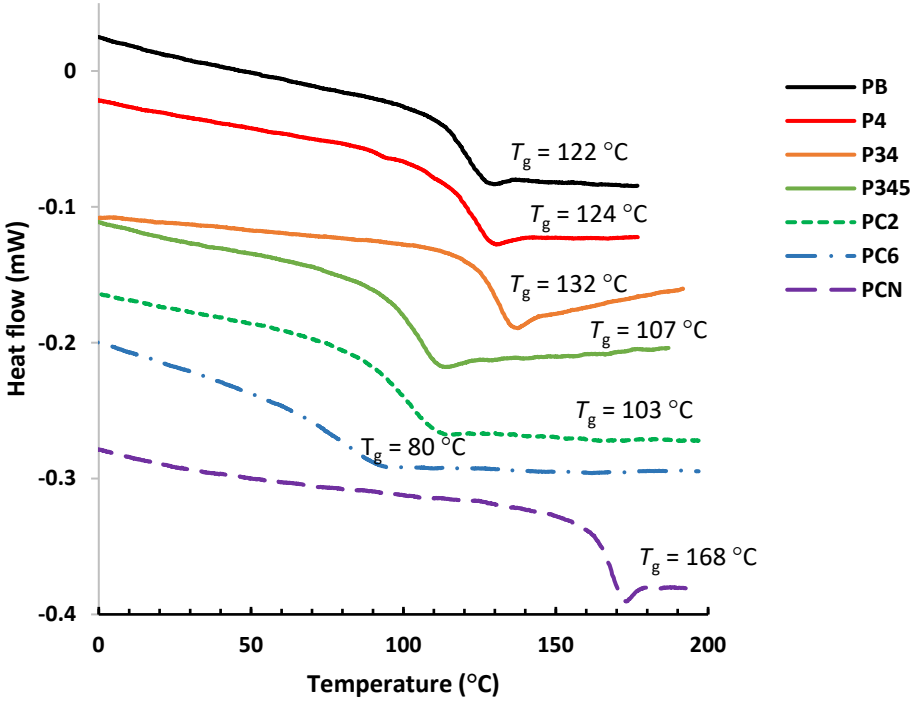

Figure 12. DSC graph for amorphous 5-**IMA** polymer samples with aromatic side groups.

The polymers were divided into three main groups based on their structural similarities. The first group consists of the benzoate polymers: unsubstituted **PB** and methoxy-substituted polymers **P4**, **P34** and **P345**, where the influence of methoxy substitutions were investigated in a row.

PB and **P4** have similar T_g values, 122 and 124 °C, respectively. The T_g of **PB** may be higher due to lower M_n compared to **P4**, M_n = 62 and 90 kg/mol, respectively (Table 3, entries 1–2).

After the second methoxy substitution to aromatic ring (**P34**), T_g rises from 124 to 132 °C (entries 2–3), respectively from **P4** to **P34**, despite **P34** had lower M_n. The higher T_g of **P34** can be caused by additional methoxy substitution, which most likely increases the rotational barrier of the aromatic ring.

After the third methoxy substitution (**P345**), T_g drops significantly from 132 to 107 °C (entries 3–4). Possibly, the T_g decreases after *m*-positions of the aromatic ring are substituted with methoxy groups. The same phenomenon was described by Epps et al. for poly(dimethoxyphenyl methacrylate)s, where they reported that after the *m*- and *p*-positions of the aromatic ring were substituted

with methoxy groups, the T_g likely dropped due to increased rotational freedom, which is caused by distorted arrangement of aromatic rings.[110]

The second group consists of polymer **PCN**, which is compared with unsubstituted **PB** and *p*-substituted methoxybenzoate **P4**. Polymer **PCN** bears strongly polar *p*-cyano groups in the aromatic rings and this can be expected to increase the T_g.[111] Indeed, **PCN** reached the highest determined T_g= 168 °C among the isosorbide monomethacrylate polymers (Table 3, entry 7).

However, the melt processability of **PCN** can be limited as the decomposition starts slowly at 210–220 °C and reaches $T_{d,95\%}$ at 268 °C. Furthermore, the influence of the isosorbide unit on the T_g can be roughly estimated by the comparison with analogous *p*-cyanobenzoyl polymethacrylate, which has T_g at 150 °C and $T_{d,95\%}$ at 302 °C.[111] Thus, the rigid isosorbide unit increases T_g, but concurrently reduces the thermal stability as isosorbide is one of the thermally sensitive fragments in the polymer.

As the third group of polymers consists of three vanillic acid esters, i.e., acetate **PC2**, caproate **PC6** and stearate **PC18**. The main goal was to determine the effect of linear alkanoyl tail on polymer thermal properties and compare them with analogous **PAIMA2**, **PAIMA6** and **PAIMA18** from Paper I. However, polymers **PC2** and **PC6** are amorphous polymers and, as expected, a longer alkanoyl tail acts as an internal plasticizer and reduces T_g from 103 to 80 °C, respectively (Table 3, entries 5,6). Similarly, in Paper I, isosorbide-2-acetate-5-polymethacrylate (**PAIMA2**) and isosorbide-2-caproate-5-polymethacrylate (**PAIMA6**) showed a T_g decrease from 107 to 57 °C.

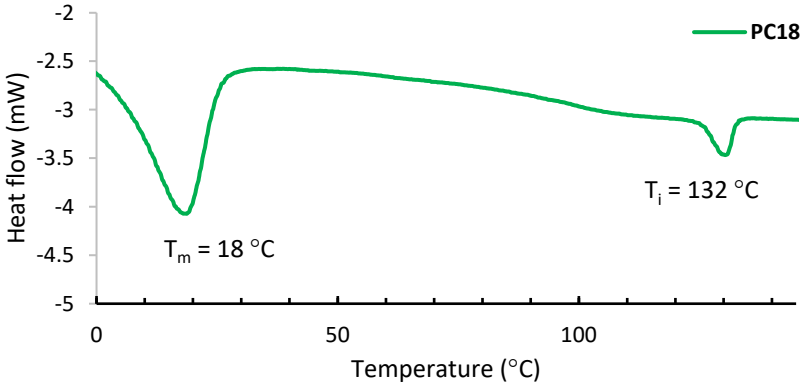

Figure 13. DSC graph for semicrystalline **PC18**.

PC18 (Figure 13) was also investigated to evaluate the influence of vanillic acid fragment compared to the isosorbide-2-stearate-5-polymethacrylate **PAIMA18** (from Paper I). As expected, **PC18** showed semicrystallinity by DSC similarly to **PAIMA18** by having melting and isotropization transitions. Compared to the non-aromatic analog, **PC18** showed a notably wider temperature range of liquid crystal mesophase, from 18 to 132 °C, while **PAIMA18** showed from 32 to 97 °C. Furthermore, **PC18** showed a slightly higher thermal stability by TGA, respectively 288 and 259 °C for **PC18** and **PAIMA18**.

3.3 Thiol-(meth)acrylate copolymers (Paper III)

This paper focused on novel thiol-(meth)acrylate polymers. Rigid primary diol monomers, derived from biobased citric acid, glycerol and TMP building blocks, were converted into di(meth)acrylates and copolymerized via the Michael addition reaction using various commercial dithiols. The obtained polymers were characterized by NMR spectroscopy and SEC, and the thermal properties were determined by DSC and TGA. In addition, the hydrolytic degradation of polymers was demonstrated.

3.3.1 Monomer preparation

The monomers were prepared by the two-step synthesis involving ketalization of diketones **B** (*cis*-bicyclo[3.3.0]octane-3,7-dione) and **T** ([4.3.3]propellane-8,11-dione) (Scheme 10). Afterward, the terminal hydroxyl groups were esterified using (meth)acryloyl chlorides to obtain di(meth)acrylate monomers. In the first step, **B** and **T** were ketalized with **g** (glycerol) and **t** (TMP). The ketalization was performed under *p*-toluenesulfone acid monohydrate catalysis (0.01–0.05 eq). The resultant water from the reaction was removed during the refluxing by the Dean-Stark apparatus. Toluene was used as a solvent for the ketalization with **t**, whereas for the ketalization with highly polar **g**, a DMF/cyclohexane 1:12.5 mixture was used. After the reaction, the crude mixture was concentrated and purified by silica-flash chromatography (eluent: 3–5% MeOH in DCM).

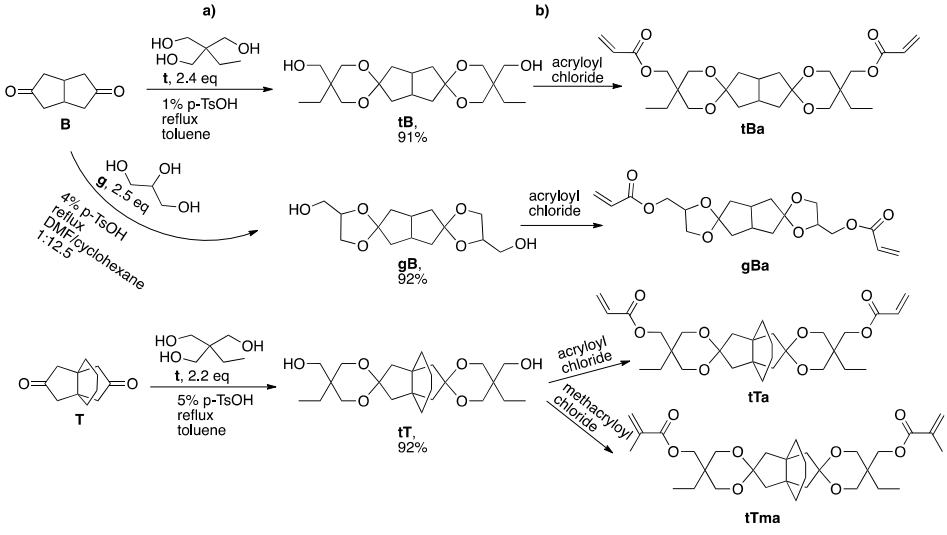

Scheme 10. Synthesis of spiro monomers. **a**) the ketalization: TMP (2.2–2.4 eq.) or glycerol (2.5 eq) toluene or cyclohexane: DMF (1:12.5), 0.01–0.05 eq. *p*-TsOH•H_2O, reflux. **b**) (meth)acryloyl chloride, Et_3N, DCM or 2-MeTHF, RT.

Three spirodiols: **tB**, **gB** and **tT** were obtained as final products. The spirodiols and monomers were named by the following principles: **t** and **g** correspond to TMP and glycerol, respectively; **B** and **T** correspond to bicyclic or tricyclic diketones, respectively; **a** and **ma** correspond to acrylate and methacrylate terminal groups, respectively.

Spirodiol **gB** was obtained as a mixture of nine diastereomers and one regioisomer (six-membered glycerol ring in a ketal group), which was used without separation. Spirodiols **tT** and **tB** formed a 1:1 mixture of *cis/trans* diastereomers, depending on the orientation of the terminal hydroxymethyl group, and were similarly used without separation. After obtaining the spirodiols, the terminal hydroxyl groups were converted to (meth)acrylates by chemical acylation using (meth)acryloyl chloride. Acylation reactions were performed in DCM or biobased 2-MeTHF and the corresponding (meth)acrylates were obtained in 60–81 or 41–77% yields, respectively. Detailed monomer preparation procedures and analytical data is presented in ESI of Paper III and in "4. Material, methods and experiments".

3.3.2 Thiol-(meth)acrylate polymerizations

Thiol-acrylate polymerizations (Scheme 11) were carried out using spiro-di(meth)acrylates (**tBa**, **gBa**, **tTa** and **tTma**) and three commercially available dithiols: **PDT** (1,3-propanedithiol), **HDT** (1,6-hexanedithiol) and **TBBT** (4,4'-thiobisbenzenethiol). The dithiols were selected based on availability and structural diversity. Polymerizations were carried out by using 10 mol% DBU as a basic catalyst in DCM or 2-MeTHF. After adding the dithiol and spirodiol to the solvent in a round bottom flask, the mixture was cooled to 0 °C by ice-bath and the DBU was added. The ice-bath was removed, and the polymerization mixtures were stirred for 24–48 hours at ambient temperature. After the polymerization, the crude polymer was precipitated in MeOH. In the final step, yellowish or brownish solid polymers were collected and dried.

The polymers were obtained with a wide range of M_n= 5–27 kg/mol (Table 5). The polydispersity ranged from 1.5 to 3.6 and seems to rise when M_n increased. Very low MW (M_n= 5 kg/mol) was observed for poly(**gBa-TBBT**) (entry 7). Attempts to increase the MW unfortunately failed. Such low MW of poly(**gBa-TBBT**) might be due to increased steric hindrance between thio-diphenyl and glycerol ketal rings. Moreover, poly(**tBa-PDT**) was polymerized in a biobased solvent 2-MeTHF, and the results obtained were comparable to polymerization in DCM (entries 2 and 1, respectively).[112] The isolated yields of polymers in this series were 23–78%. The isolated yields strongly depended on the stickiness and the particle sizes of the specific polymer during the precipitation and filtration sequence.

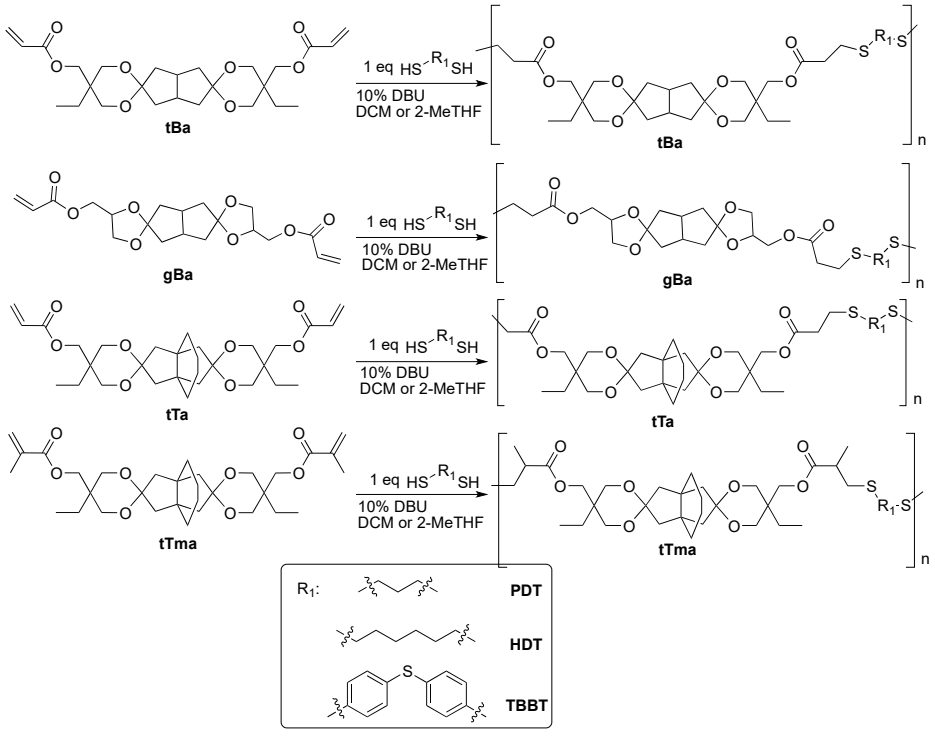

Scheme 11. Polymerization of thiol-(meth)acrylate polymers via Michael addition. Conditions: 1.0 eq of corresponding dithiol, 0.1 eq. DBU, solvent DCM or 2-MeTHF, 24–48h at RT.

Table 5. Selected spiro-(meth)acrylate polymerizations.

entry	polymer	[a]M_n (kg/mol)	$Đ$ (M_w/M_n)	isol. yield (%)	[b]T_g (°C)	[c]$T_{d,\,95\%}$ (°C)
1	poly(**tBa-PDT**)	26	1.8	77	15	320
2	poly(**tBa-PDT**)[d]	14	1.5	74	n.d	n.d.
3	poly(**tBa-HDT**)	18	2.1	67	7	321
4	poly(**tBa-TBBT**)	19	3.5	67	55	311
5	poly(**gBa-PDT**)	15	1.9	70	–7	322
6	poly(**gBa-HDT**)	15	2.3	23	–16	324
7	poly(**gBa-TBBT**)	5	1.4	n.d	n.d	n.d.
8	poly(**tTa-PDT**)	18	3.6	78	24	323
9	poly(**tTma-PDT**)	14	2.6	68	32	315
10	poly(**tTa-HDT**)	27	3.6	70	27	320
11	poly(**tTma-HDT**)	11	1.5	46	25	314
12	poly(**tTa-TBBT**)	22	1.8	77	40	317
13	poly(**tTma-TBBT**)	12	2.4	46	46	282

[a]Measured by SEC using $CHCl_3$ as eluent and PEO/PEG standards for mass determination. [b]Determined by DSC by heating up to 100 °C. [c]Measured by TGA, determined temperature at a 5% polymer mass loss. [d]Polymerization performed in 2-MeTHF

3.3.3 Structural influence on the thermal properties of the thiol-(meth)acrylate polymers

To evaluate the influence of the polymer structure on the thermal properties, the T_g was determined by DSC and $T_{d,\,95\%}$ by TGA at a 5% weight loss. DSC analysis was carried out by heating up to only 100 °C as it was observed that heating up to 200 °C most likely caused crosslinking via unreacted acrylate end groups that increased polymer T_g during the measuring process.

As expected, tricyclic spiro-acrylate polymers with TMP ketal showed higher T_g values than the bicyclic analogs, 24–27 vs. 7–15 °C (Table 5, entries 8, 10 and 1,3, respectively). This is probably caused by the additional ring in the tTa core, which increases the rigidity. As an exception, poly(**tTa-TBBT**) showed lower T_g than its bicyclic analog poly(**tBa-TBBT**), 40 and 55 °C (entries 12 and 4), respectively.

Polymers with glycerol ketal groups exhibited lower T_g values compared to polymers with TMP ketal groups, which hints at greater flexibility of the glycerol-derived copolymers, –16, –7, 7 and 15 °C, respectively (entries 5, 6 and 1, 3). Unfortunately, the tricyclic analogue with glycerol fragment is excluded because the ketalization of **T** with glycerol failed.

As expected, the elongation of the dithiol (from propyl to hexyl) decreased the T_g in all cases due to the additional flexibility of the polymer chain. Also, TBBT containing rigid aromatic rings showed higher T_g-s than polymers with aliphatic dithiols.

The choice of acrylate or methacrylate does not influence T_g significantly, as the values vary only slightly (see Table 5, entries 8–9; 10–11, 12–13). All polymers showed relatively similar thermal stability and the $T_{d,\,95\%}$ values were around 320 °C, except poly(**tTma-TBBT**) (Table 5, entry 13).

3.3.4 Thiol-(meth)acrylate polymer end group processing

During some of the polymerizations, the excess of the (meth)acrylates was observed by ^{1}H NMR in the crude polymer mixture. Unreacted (meth)acrylates can react at elevated temperatures and change the properties of corresponding polymers. Additionally, (meth)acrylates are potentially toxic to various organisms. Thus, to prevent these possible adverse effects, some thiol-(meth)acrylate copolymers were treated with monofunctional 1-decanethiol to block the (meth)acrylate polymer ends. As a result, the MW of polymers surprisingly dropped significantly during the monothiol processing. In the worst cases, the polymer lost up to 91% of its MW. Most likely, 1-decanethiol caused polymer chain cleavage by nucleophilic attack at the carbonyl group, or by nucleophilic substitution of the present dithiol in a copolymer.

Also, a slight dithiol excess was tested to avoid (meth)acrylate polymer chain ends. If there is still (meth)acrylate left at the polymer chain ends, a minimal amount of additional dithiol (approximately an extra 0.01 eq.) reacts with (meth)acrylate end groups and most likely increases the MW of the final polymers by 10–20%.

3.3.5 Hydrolytic degradation of thiol-(meth)acrylate copolymers

Considering that these polymers contain acid sensitive ketal groups, the chemical stability of the polymers was evaluated.[113] First, polymers were immersed in water solution at different pH values (0, 3, 8 and 14) for 14 days at 37 °C. As a result, the high stability of polymers in water was confirmed by SEC analysis, where MW-s of corresponding polymers remained unchanged. Most likely, the surface tension of water is too high to let acidic or basic solution into the samples and the possible degradation is prevented.

Next, the water solution was replaced by an HCl aqueous solution in acetone and the experiment was monitored by the NMR. Acetone has much lower surface tension and probably dissolves possible decomposition products, simplifying the overall procedure. First, polymers were immersed into 0.1 M HCl solution in water, mixed with acetone (1:9 volume, HCl solution:acetone) at kept at 50 °C. Solid polymer pieces disappeared within 5–8 hours, except poly(**tTa-TBBT**), which had several undissolved pieces left after 8 hours. After 72 hours, the solvents were evaporated and polymer residues were analyzed by NMR spectroscopy and SEC. SEC analysis showed M_n-s lower than 1.5 kg/mol in every case, which confirms an almost complete polymer degradation. NMR data showed the formation of diketones **B** and **T**, 20 and 10 mol%, respectively. The lower hydrolysis rate for **T** is most likely due to its somewhat lower solubility in acetone. However, the polymer degradation in 0.1 M solution was quite slow and the HCl solution concentration was increased to 1 M.

Further experiments were performed in an NMR tube, using 1 M HCl solution in water and acetone-d_6 (1:9 by volume, HCl solution: acetone-d_6). The samples were kept at 50 °C and NMR measurements were taken regularly.

After increasing the HCl concentration to 1 M, the hydrolysis rate of the ketal group increased significantly. The sample was visually fully dissolved within 1.5 hours. After 4 hours, the ketal groups were completely hydrolyzed (Figure 14) and the formation of diketone **B** was confirmed by the ^{1}H NMR data. In summary, these spiro-polymers are fully degradable under acidic conditions, and resultant diketones could be recovered. Moreover, the spiro-polymers were fully stable in the pH range 0–14 at slightly elevated temperatures (37 °C) in aqueous solutions. These conditions are inherent to bio-organisms and the materials could thereby be suitable for bio-related applications.

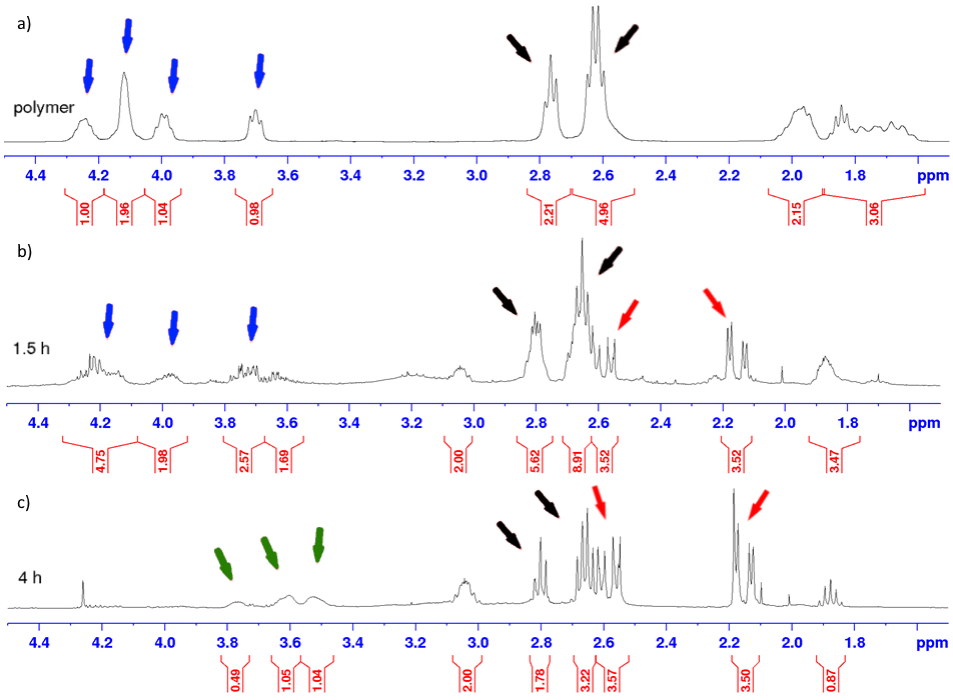

Figure 14. **Poly(gBa-PDT)** degradation in 1M HCl in acetone-d_6. Blue arrows show initial polymer signals (glycerol ring); black arrows – **PDT** fragment in polymer; green arrows – glycerol fragment after degradation; red arrows – the appearance of diketone **B**.

3.4 Isosorbide dilevulinate copolymers with dihydrazides

In this chapter, unpublished results on isosorbide dilevulinate hydrazone copolymers are discussed. In addition to isosorbide, these polymers also contain levulinate fragments, which can be derived from lignocellulosic biomass.[114]

3.4.1 Preparation of isosorbide dilevulinate

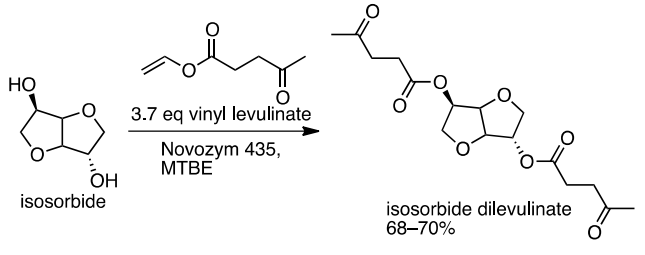

Scheme 12. Preparation of isosorbide dilevulinate.

Isosorbide dilevulinate was prepared via an esterification reaction between isosorbide and vinyl levulinate using enzymatic catalysis by Novozym 435 (Scheme 12). The purification of the dilevulinate was performed by a simple filtration and short silica-flash chromatography. The pure product was isolated in 68–70% yield. Alternatively, isosorbide dilevulinate can be prepared using levulinic acid chloride. However, the product synthesized via the acid chloride path contained acetalized levulinate side product which was difficult to remove by chromatography.

3.4.2 Isosorbide dilevulinate copolymerization with dihydrazides

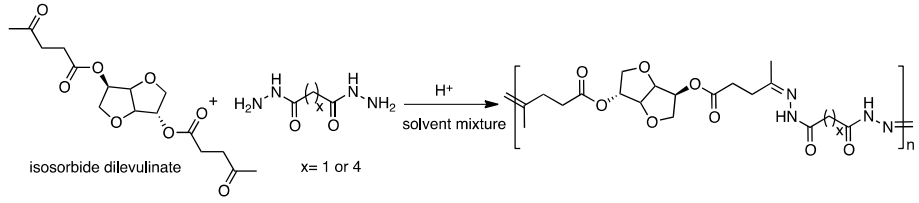

Scheme 13. Isosorbide dilevulinate copolymerization with adipic and malonic acid dihydrazides.

The polymerizations were performed in a smaller test scale (approximately 100–300 mg) to study the polymerizations and products (Scheme 13). The main goal was to find conditions, which would facilitate the formation of higher MW polymers. For this purpose, different solvent mixtures, levulinate-hydrazide ratios and temperatures were evaluated. Detailed results are presented in Table 6.

Prior to the polymerizations, isosorbide dilevulinate was dissolved in dioxane in a polymerization vial, followed by the addition of hydrazide dissolved in either H_2O, MeOH or AcOH. Based on the results (Table 6), the exact influence of the solvent mixtures on the molecular weights remains unclear. However, entries 1 and 5 show that the influence of methanol was marginal and it is primarily used to increase the solubility of dihydrazide. Entries 1–2 show that acetic acid is required in a bigger than catalytic amount, because otherwise the polymerization proceeds very poorly. Another strategy was to increase the amount of adipic acid dihydrazide relative to dilevulinate. However, M_n rose only marginally (from 1.8 to 2.6 kg/mol, entries 2–4). Polymerization was also evaluated at elevated temperatures (entries 5–7). SEC samples were taken from the same polymerization mixture after stirring at different temperatures to investigate possible influences on polymer MW-s. The SEC data showed a clear decrease of the M_n values after increasing the polymerization temperature until no polymer peak was detected after heating at 90 °C.

Table 6. Results of isosorbide dilevulinate copolymerizations with dihydrazides.

entry	monomer 1	monomer 2 (dihydra-zide)	dioxane (ml)	H_2O (ml)	AcOH (ml)	MeOH (ml)	T (°C)	time (h)	M_n (kg/mol)	$Đ$ (M_w/M_n)
1	isos.dilev.	adipic	3	2	1.3	2	rt	24	4.7	1.34
2	isos.dilev.	adipic	9	6	few drops	–	rt	24	1.8	1.22
3	added extra 10 mg of adipic acid dihydrazide						rt	24	2.3	1.39
4	added more 25 mg of adipic acid dihydrazide						rt	24	2.6	1.15
5	isos.dilev.	adipic	3	3	2	–	rt	24	3.9	1.28
6	additional heating						40	24	3.5	1.23
7	additional heating						90	polymer breakdown		
8	isos.dilev	malonic	2	1	0.5	0.5	rt	72	8.5	1.24
9	hexane-2,5-dione	adipic	3	1	1.3	1	rt	72	7.9	1.07
10	hexane-2,5-dione	malonic	3.5	3.5	0.2	0.2	rt	72	6.4	1.16

SEC was measured using DMF as an eluent (0.5 mL/min). For entries 1–7 PEG/PEO standards (with RID detector) and for entries 8–10 PS standards (with UV-detector) were used.

For a comparison, isosorbide dilevulinate was copolymerized with malonic acid dihydrazide (entry 8). However, due to RID detector artefacts, in this case the SEC data was obtained by using PS standards with UV-detector (instead of PEG/PEO standards with RID detector). Also, based on personal experience, PS standards typically show molecular weights twice as high for polymers compared to PEG/PEO standards. Thus, it is difficult to directly compare the MW-s, but we assume they are in the similar range. Additionally, a shorter hexane-2,5-dione monomer was used for comparison to assess the effect of long isosorbide dilevulinate molecule on copolymerizations. As a result, adipic and malonic acid dihydrazides afforded polymers with similar M_n as with isosorbide dilevulinate (entries 8–10). The poor solubility of these polymers might have limited the MW increase because the polymers typically precipitated out during the reaction. Similarly, the preparation of isosorbide dilevulinate copolymer with terephthalic acid dihydrazide failed due to poor solubility of the dihydrazide.

In addition to molecular weights, the isosorbide dilevulinate copolymer with adipic acid hydrazide (Table 6, entry 1) was characterized by DCS and TGA. The measured T_g and $T_{d,95\%}$ values were 73 and 209 °C, respectively (Figure 15).

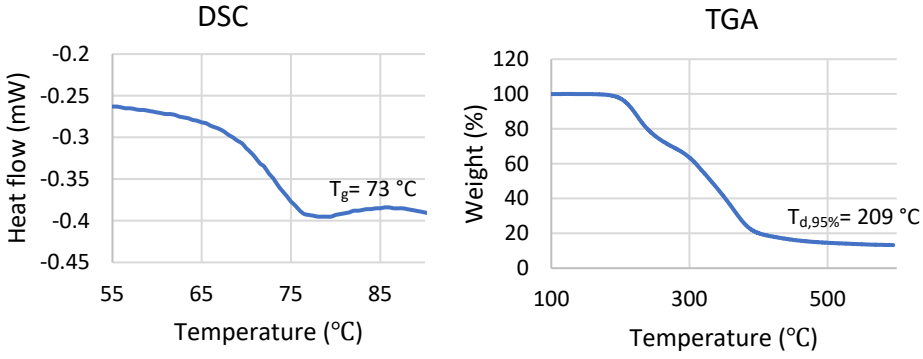

Figure 15. DSC and TGA curves for an isosorbide dilevulinate copolymer with adipic acid dihydrazide.

4. MATERIALS, METHODS, AND EXPERIMENTAL DETAILS

The reagents and solvents were obtained from commercial sources if not stated otherwise. 2-**IMA** was prepared by following our previously described regioselective enzymatic esterification.[66]

The monomers and polymers were characterized by NMR in a chloroform-*d* solutions using a Bruker Avanche II 400 MHz NMR spectrometer. ^{1}H and ^{13}C NMR spectra were recorded at 400.1 and 100.6 MHz, respectively. The chemical shifts are given in ppm and residual solvent signals were used for calibration (for ^{1}H, $CDCl_3$: $\delta = 7.26$ ppm, for ^{13}C, $CDCl_3$: $\delta = 77.0$ ppm).

Polymer formation in **Paper I** and **II** was determined by the decrease of the double bond signals ($C\underline{H_2}$=CH–) in the ^{1}H spectra. Monomer conversions were measured by comparing the broad non-overlapping isosorbide polymer signal in the range of 4.20–5.50 ppm with the remaining monomer double bond signal (*trans*-H) at 6.15–6.17 ppm. The degradation rate of the thiol-acrylate polymers (**Paper III**) was determined by ^{1}H NMR analysis in 1 M DCl solution 1:9 acetone-d_6 by observing the disappearing polymer signals and increasing diketone signals at 2.15 and 2.55 ppm. HRMS measurements were performed on Thermo Electron LTQ Orbitrap XL analyzer or on a hybrid instrument consisting of Varian 910 FT-ICR-MS and Varian J-320 3Q mass spectrometers with horizontal 7T superconductive magnet and nanoESI source. Varian Omega 9.1.21 software was used for FT-ICR-MS experimental setup and data acquisition. The molecular weights of the polymers were determined by size-exclusion chromatography (SEC) with THF and $CHCl_3$ as the solvent. A Shimadzu Prominence system equipped with three Shodex columns (KF-805, –804, and –802.5, coupled in series), and a refractive index detector (RID-20A) were used. Samples were run at 40 °C with an elution rate of 1 mL min^{-1}. Poly(ethylene oxide) standards (M_n = 3 860, 12 600, 49 640, and 96 100 g/mol) were used for calibration and the results were analyzed using Shimadzu LabSolution software.

4.1 Reactions procedures

4.1.1 Regioselective preparation of 5-IMA

Before the reaction, isosorbide was dried by azeotropic distillation using ACN (200 mL for 15 g of starting material) and Lipozyme RM IM was vacuumed several hours at RT to remove moisture. Dry isosorbide (13.48 g, 92.2 mmol) and Lipozyme RM IM (1.6 g) were weighed into the 250 mL round-bottomed flask. After that, MTBE (205 mL) as a solvent was added; the flask was flushed with Ar and closed with a rubber septum. The reaction mixture was shaken at 60 Hz for 72 hours until all the isosorbide was dissolved. The completion of the reaction was confirmed by ^{1}H NMR. After the reaction, the enzyme was filtrated using a small layer of neutral aluminum oxide on the glass filter. The crude mixture was

concentrated by rotary evaporator (water bath temperature: max 37 °C) and dissolved in 200 ml of EtOAc. The organic layer was extracted two times with sat. $NaHCO_3$ aqueous solution (2 × 30 mL), then two times with brine (2 × 30 mL). The combined water layer was also extracted twice with EtOAc (2 × 30 ml). The organic layer was collected, dried over $MgSO_4$ and filtrated. The product was obtained as a viscous transparent liquid (17.76 g, yield: 89.9%) and stored in EtOAc in the presence of a minimal amount (less than 1 mg) of HQ at 2–8 °C.

^{1}H NMR (400 MHz, $CDCl_3$) δ: 6.11 (d, $^2J_{HH}$=1.5 Hz, CH, 1H), 5.57 (d, $^2J_{HH}$=1.5 Hz, CH, 1H), 5.15 (ddd, $^3J_{HH}$= 5.8 Hz, $^3J_{HH}$= 5.7 Hz, $^3J_{HH}$= 5.0 Hz, CH, 1H), 4.85 (dd, $^3J_{HH}$= 5.7 Hz, $^3J_{HH}$= 4.7 Hz, CH, 1H), 4.35 (d, $^3J_{HH}$= 4.7 Hz, CH, 1H), 4.26 (d, $^3J_{HH}$= 3.3 Hz, CH, 1H), 3.88-3.76 (CH_2, 4H), 3.13 (bs, OH, 1H), 1.91 (s, CH_3, 3H). ^{13}C NMR (100.6 MHz, $CDCl_3$) δ: 166.71 (CO), 135.52 (C), 126.25 (CH_2), 88.18 (CH), 80.37 (CH), 75.84 (CH), 75.29 (CH_2), 74.18 (CH), 70.47 (CH_2), 18.16 (CH_3).

4.1.2 General procedure for conversion of carboxylic acids to acid chlorides

The side groups for isosorbide monomethacrylate monomers (**Paper I** and **II**) were introduced by the conventional chemical acylation using acyl chloride unless the enzymatic pathway was used. A typical chlorination of carboxylic acid was carried out as follows.

A corresponding carboxylic acid was weighed into the flask and dissolved partially in dry DCM (typical conc. 50 mL/g). Next, the flask was equipped with a rubber septum and flushed with argon gas. A catalytic amount of DMF (few drops) and oxalyl chloride (1.1–1.3 eq) were added dropwise. A rubber septum was equipped with a syringe needle to let out resultant gases from the flask. The reaction was let to stir at RT until the bubbling was not observed and all the starting material was dissolved (typically up to 5 h). The product was carefully concentrated by a rotary evaporator, and the argon gas was used to repressurize the flask. The resultant acyl chlorides were used immediately in the following reaction without characterization.

4.1.3 General procedure for conventional acylation of 5-IMA or 2-IMA

Some of the isosorbide monomethacrylate monomers in **Paper I** were prepared by the previously described enzymatic esterification of regioselectively pure isosorbide monomethacrylate (see detailed information in **Paper I**).[108] The other isosorbide monomethacrylates in **Paper I** and **II** were prepared by conventional acylation using corresponding acyl chlorides (see 4.1.2 General chlorination). A typical acylation reaction was performed as follows:

Regioselectively pure isosorbide monomer was dissolved in dry DCM, ACN or 2-MeTHF (typical conc. 100 mg/ml). After that, the reaction flask was equipped

with a rubber septum and flushed with argon gas to remove air. Next, freshly made corresponding acyl chloride (1.0–1.2 eq) and Et_3N (1.1–1.3 eq) were added simultaneously dropwise to the reaction mixture. After that, the reaction mixture was left to stir overnight at RT. The crude mixture was extracted with saturated $NaHCO_3$ aqueous solution (25 mL for 1 g of starting material) and the water layer was extracted two times with DCM (3 × 50 mL). The organic layers were collected, dried over $MgSO_4$ and concentrated by rotary evaporator. The products were purified by silica-flash chromatography using 8–40% EtOAc solution in petroleum ether as eluent. The products were typically stored in an EtOAc solution at 2–8 °C.

4.1.4 The monomer MC18 preparation

5-IMA (0.75 g, 3.49 mmol) was concentrated and weighed into the round-bottomed flask. After that, dry DCM (10 ml) was added as a solvent. Then, the flask was flushed with argon gas and equipped with a rubber septum. Freshly made 4-stearoyl-3-methoxybenzoyl chloride in DCM solution (1.46 g, 3.23 mmol, 0.92 eq in 5 mL of DCM) and Et_3N (0.52 ml, 3.77 mmol, 1.08 eq.) were injected simultaneously dropwise to the reaction mixture. After that, the reaction was let to stir at RT for 18 hours. The crude mixture was extracted with sat. $NaHCO_3$ aqueous solution (50 mL) and the water layer was washed two times with DCM (2 × 50 mL). The organic layers were collected, dried over anhydrous $MgSO_4$ and concentrated. The product (1.74 g, yield: 88%) as white solids was collected and stored in an EtOAc solution at 2–8 °C.

^{1}H NMR (400 MHz, $CDCl_3$) δ: 7.62 (dd, $^3J_{HH}$=8.3 Hz, $^4J_{HH}$=1.8 Hz, $CH_{(B6)}$, 1H), 7.60 (d, $^4J_{HH}$=1.8 Hz, $CH_{(B2)}$, 1H), 7.07 (d, $^3J_{HH}$=8.3 Hz, $CH_{(B5)}$, 1H), 6.17 (d, $^2J_{HH}$=1.5 Hz, $CH_{(10E)}$, 1H), 5.63 (d, $^2J_{HH}$=1.5 Hz, $CH_{(10Z)}$, 1H), 5.45 (dd, $^3J_{HH}$= 3.3 Hz, $CH_{(2)}$, 1H), 5.23 (ddd, $^3J_{HH}$= 5.8 Hz, $^3J_{HH}$= 5.7 Hz, $^3J_{HH}$= 5.0 Hz, $CH_{(5)}$, 1H), 4.97 (dd, $^3J_{HH}$= 5.7 Hz, $^3J_{HH}$= 4.7 Hz, $CH_{(4)}$, 1H), 4.61 (dd, $^3J_{HH}$= 4.7 Hz, $^3J_{HH}$= 2.0 Hz, $CH_{(5)}$, 1H), 4.09 (d, $^2J_{HH}$= 10.8 Hz, $CH_{2(1n)}$, 1H), 4.08 (dd, $^2J_{HH}$= 10.8 Hz, $^3J_{HH}$= 3.3 Hz, $CH_{2(1x)}$, 1H), 3.98 (dd, $^2J_{HH}$= 10.0 Hz, $^3J_{HH}$= 5.8 Hz, $CH_{2(6n)}$, 1H), 3.93 (dd, $^2J_{HH}$= 10.0 Hz, $^3J_{HH}$= 5.0 Hz, $CH_{2(6x)}$, 1H), 3.85 (s, $CH_3O_{(12)}$, 3H), 2.57 (t, $^3J_{HH}$= 7.5 Hz, $CH_{2(A2)}$, 2H), 1.97 (s, $CH_{3(9)}$, 3H), 1.74 (tt, $^3J_{HH}$= 7.5 Hz, $^3J_{HH}$= 7.5 Hz, $CH_{2(A3)}$, 2H), 1.35–1.22 (m, $CH_{2(A4–A17)}$, 28H), 0.86 (t, $^3J_{HH}$= 7.0 Hz, $CH_{3(A18)}$, 3H). ^{13}C NMR (100.6 MHz, $CDCl_3$) δ: 171.22 ($CO_{(A1)}$), 166.65 ($CO_{(7)}$), 164.88 ($CO_{(11)}$), 151.15 ($C_{(B3)}$), 144.15 ($C_{(B4)}$), 135.61 ($C_{(8)}$), 127.89 ($C_{(B1)}$), 126.31 ($CH_{2(10)}$), 122.85 ($C_{(B5)}$), 122.78 ($C_{(B6)}$), 113.37 ($C_{(B2)}$), 86.02 ($C_{(3)}$), 80.94 ($C_{(4)}$), 78.59 ($C_{(2)}$), 74.14 ($C_{(5)}$), 73.27 ($C_{(1)}$), 70.64 ($C_{(6)}$), 56.01 ($CH_3O_{(B3)}$), 33.94 ($CH_{2(A2)}$), 31.15 ($CH_{2(A3)}$), 29.63–28.97 ($CH_{2(A4–A15)}$), 24.89 ($CH_{2(A16)}$), 22.63 ($CH_{2(A17)}$), 18.24 ($CH_{3(9)}$), 14.05 ($CH_{3(A18)}$).

4.1.5 General procedure for free-radical polymerizations

Isosorbide monomethacrylate monomers were concentrated (if stored in a solution) and weighted. After that, monomers were dissolved in a selected polymerization solvent (typical conc. 0.1 mg/mL) and transferred into the pressure tube. AIBN was added in a solution of corresponding polymerization solvent (0.5 mol%). Next, the polymerization mixture was sparged typically for 30–60 minutes with Ar gas to remove dissolved oxygen. The pressure tube was sealed and placed into the pre-heated oven at 63 °C for 24 hours. After the polymerization, the monomer conversion was determined by ^{1}H NMR. The crude polymer was precipitated in MeOH (conc. 250–500 mL for 1 g of polymer). The solids were filtrated, washed with a small amount of additional MeOH, collected and dried for three days under vacuum at 70 °C.

4.1.6 Spirodiol tB synthesis

Diketone **B** (2.30 g, 16.65 mmol), TMP (5.36 g, 39.95 mmol, 2.40 eq) and *p*-toluenesulfonic acid monohydrate (92 mg, 0.48 mmol, 0.029 eq) were weighted into the round-bottomed flask (100 mL). The flask was equipped with Dean-Stark apparatus and a condenser. Toluene as a solvent was filled from the top of the Dean-Stark apparatus to fill a water trap and reaction flask (80 ml for the reaction mixture). After that, the reaction mixture was heated to the reflux temperature and left to stir overnight. The crude mixture was allowed to cool and concentrated by the rotary evaporator. The product was purified by silica-flash chromatography using 5% MeOH in DCM as an eluent. A final product was isolated as white solid crystals (5.77 g, yield: 93.5%).

^{1}H NMR (400 MHz, $CDCl_3$) δ: 3.77 (bs, CH_2, 2H), 3.74 (bs, CH_2, 2H), 3.69 (dd, $^{2}J_{HH}$=11.8 Hz, $^{4}J_{HH}$=2.0 Hz, CH_2, 4H), 3.55 (dd, $^{2}J_{HH}$=11.6 Hz, $^{3}J_{HH}$=7.7 Hz, CH_2, 4H), 2.53 (m, CH, 2H), 2.29 (m, CH_2, 2H), 2.08 (m, CH_2, 2H), 1.71 (m, CH_2, 4H), 1.29 (q, $^{4}J_{HH}$=7.7 Hz, CH_2, 2H), 1.25 (q, $^{4}J_{HH}$=7.7 Hz, CH_2, 2H), 0.83 (t, $^{4}J_{HH}$=7.7 Hz, CH_3, 3H), 0.82 (t, $^{4}J_{HH}$=7.7 Hz CH_3, 3H). ^{13}C NMR (100.6 MHz, $CDCl_3$) δ: 110.3 (C), 67.1 (CH_2), 66.3 (CH_2), 63.0 (CH_2), 43.4 (CH_2), 42.9 (CH_2), 38.1 (CH), 36.9 (CH), 36.9 (C), 36.8 (C), 36.7 (CH_2), 36.1 (CH_2), 35.8 (CH), 23.8 (CH_2), 7.0 (CH_3).

4.1.7 Spirodiol gB synthesis

Diketone **B** (4.058 g, 29.3 mmol), glycerol (7.1 g, 78.8 mmol, 2.55 eq) and *p*-toluenesulfonic acid monohydrate (0.22 g, 0.04 eq) were weighted into the round-bottomed flask (100 mL). The flask was equipped with Dean-Stark apparatus and condenser. DMF (8 mL) and cyclohexane (100 mL) mixture was added as a solvent. After that, the reaction was started by heating reaction mixture to the reflux temperatures and left stirring for overnight. After the reaction, the crude mixture was allowed to cool and the mixture was concentrated by the rotary evaporator. The mixture was purified by silica-flash chromatography using 5%

MeOH solution in DCM as an eluent. A final product was isolated as viscous yellowish liquid (7.60 g, yield: 90.4%).

^{1}H NMR (400 MHz, $CDCl_3$) δ: 4.15 (CH, 2H, m), 3.94 (CH_2, 2H, m), 3.72 (CH_2, 2H, m), 3.68 (CH_2, 2H, m), 3.57 (CH_2, 2H, m), 2.59 (CH, 2H), 2.30 (OH, 2H), 1.98 (CH_2, 4H), 1.71 (CH_2, 4H). ^{13}C NMR (100.6 MHz, $CDCl_3$) δ: 119.3 (C), 76.3–75.5 (CH), 65.9–62.9 (CH_2), 42.2–41.1 (CH_2), 37.1–36.5 (CH).

4.1.8 Preparation of spiro-diacrylate tBa

tB (1.979 g, 5.34 mmol) was weighted into a round-bottomed flask and dissolved in a dry DCM (15 mL). The flask was flushed with Ar gas, closed with rubber septum and cooled down with an ice-bath. After that, Et_3N (2.0 mL) and acryloyl chloride (0.99 mL, 2.2) eq were added simultaneously dropwise. Shortly after addition, the ice-bath was removed and reaction was left stirring for overnight. The completion of the reaction was confirmed by TLC. After the reaction, the mixture was quenched with sat. $NaHCO_3$ aqueous solution (50 mL) and thereafter extracted three times with DCM (3 × 50 mL). The organic layers were collected, dried over $MgSO_4$ and filtered. The resultant mixture was concentrated and purified by silica-flash chromatography using 30% EtOAc solution in petroleum ether as an eluent. A pure product was obtained as a visqous transparent liquid (2.07 g, yield: 81%).

^{1}H NMR (400 MHz, $CDCl_3$) δ: 6.36 (dd, $^{3}J_{HH}$= 17.4 Hz, $^{2}J_{HH}$=1.2 Hz, CH_2, 2H), 6.09 (dd, $^{3}J_{HH}$= 17.5 Hz, $^{3}J_{HH}$=10.4 Hz, CH, 2H), 5.76 (dd, $^{3}J_{HH}$= 10.4 Hz, $^{2}J_{HH}$=1.2 Hz, CH_2, 2H), 4.29 (bs, CH_2, 2H), 4.24 (bs, CH_2, 2H), 3.68 (dd, $^{2}J_{HH}$=11.8 Hz, $^{4}J_{HH}$=1.3 Hz, CH_2, 4H), 3.55 (dd, $^{2}J_{HH}$=11.8 Hz, $^{3}J_{HH}$=6.0 Hz, CH_2, 4H), 2.51 (m, CH, 2H), 2.23 (m, CH_2, 2H), 2.06 (m, CH_2, 2H), 1.70 (m, CH_2, 4H), 1.32 (t, $^{3}J_{HH}$=7.6 Hz, CH_2, 2H), 1.27 (t, $^{3}J_{HH}$=7.6 Hz, CH_2, 2H), 0.79 (q, $^{3}J_{HH}$=7.6 Hz, CH_3, 3H), 0.78 (q, $^{3}J_{HH}$=7.6 Hz, CH_3, 3H). ^{13}C NMR (100.6 MHz, $CDCl_3$) δ: 166.0 (CO), 130.6 (CH_2), 128.2 (CH), 110.2 (C), 66.8 (CH_2), 66.1 (CH_2), 63.8 (CH_2), 43.0 (CH_2), 42.2 (CH_2), 37.8 (CH), 37.0 (CH_2), 36.8 (C), 36.2 (CH_2), 35.9 (CH), 35.8 (C), 23.8 (CH_2), 6.8 (CH_3).

4.1.9 Preparation of spiro-diacrylate gBa

gB (3.915 g, 13.67 mmol) was weighted into a round-bottomed flask and dissolved in a dry DCM (30 mL). The flask was flushed with Ar gas, closed with rubber septum and cooled down with an ice-bath. After that, Et_3N (4.7 mL) and acryloyl chloride (3.27 mL, 2.2 eq were added simultaneously dropwise. Shortly after addition, the ice-bath was removed and reaction was left stirring for overnight. The completion of the reaction was confirmed by TLC. After the reaction, the mixture was quenched with sat. $NaHCO_3$ aqueous solution (50 mL) and thereafter extracted three times with DCM (3 × 50 mL). The organic layers were collected, dried over MgSO4 and filtered. The resultant mixture was concentrated and purified by silica-flash chromatography using 30% EtOAc solution in

petroleum ether as an eluent. The pure product was obtained as a viscous transparent liquid (3.219 g, yield: 60 %).

^{1}H NMR (400 MHz, $CDCl_3$) δ: 6.39 (dd, $^{3}J_{HH}$= 17.2 Hz, $^{2}J_{HH}$=1.3 Hz, CH_2, 2H), 6.10 (dd, $^{3}J_{HH}$= 17.2 Hz, $^{3}J_{HH}$=10.4 Hz, CH, 2H), 5.82 (dd, $^{3}J_{HH}$= 10.4 Hz, ^{2}JHH=1.3 Hz, CH_2, 2H), 3.36–4.20 (CH_X, 10H), 2.56 (CH, 2H), 1.94 (CH_2, 4H), 1.68 (CH_2, 4H). ^{13}C NMR (100.6 MHz, $CDCl_3$) δ: 165.7 (CO), 131.31 (CH_2), 127.8 (CH), 119.6 (C), 73.4 (CH), 72.8 (CH), 66.5 (CH_2), 66.4 (CH_2), 65.8 (CH_2), 66.7 (CH_2), 64.5 (CH_2), 42.2–41.1 (CH_2), 37.0–36.6 (CH).

4.1.10 General procedure for thiol-acrylate polymerizations

Diacrylates was concentrated under vacuum, the content of solvent residues (typically DCM or EtOAc) were estimated by ^{1}H NMR and taken into account in the calculations. After that, the di(meth)acrylates were dissolved in $CHCl_3$ or 2-MeTHF (conc. 100 mg/ml). The selected dithiol (1.0 eq) was added to the solution. Next, the flask was flushed with Ar gas and cooled in ice-bath. The reaction was initiated by adding DBU (0.1 eq) solution in a corresponding polymerization solvent (DCM or 2-MeTHF). The ice-bath was removed shortly after DBU addition, and the mixture was let to stir for 24–48 hours at RT. The progress of polymerizations was monitored by ^{1}H NMR by comparing meth(acrylate)-group signals with forming polymer signals. After the polymerization, the crude polymer was precipitated in MeOH or Et_2O (100–250 mL) and left stirring for overnight. The sticky polymer residues were isolated by decanting MeOH or Et_2O solution and washing with a small amount of additional precipitation solvent. The final polymer was dried under vacuum at 80 °C and characterized by NMR, SEC, DSC and TGA.

4.1.11 Preparation of isosorbide dilevulinate

Into the flask were weighted pre-dried isosorbide (1.02 g, 6.96 mmol), Novozym 435 (0.475 g, 10 w%) and vinyl levulinate (3.74 g, 25.7 mmol, 3.7 eq). MTBE (13 mL) as solvent was added and reaction mixture was shaked for 48 hours at RT (30–32 °C). After the reaction, the crude product mixture was filtrated through the small amount of aluminium oxide and washed with EtOAc (15 mL). Next, the crude mixture was purified by the short silica-flash chromatography using 20% EtOAc solution in petroleum ether as an eluent. The final product was obtained as a transparent viscous liquid (1.60 g, 67% yield) and was stored at 2–8 °C in EtOAc solution.

^{1}H NMR (400 MHz, $CDCl_3$) δ: 5.17 (m, 1H), 5.12 (m, 1H), 4.79 (m, 1H), 4.45 (m, 1H), 3.95 (m, 2H), 3.91 (m, 1H), 3.78 (m, 1H), 2.83–2.52 (m, 8H), 2.17 (s, 3H), 2.16 (s, 3H). ^{13}C NMR (100.6 MHz, $CDCl_3$) δ: 206.31, 172.09, 171.17, 85.78, 80.69, 78.10, 74.09, 73.18, 70.27, 37.79, 37.74, 29.75, 29.71, 27.85, 27.61.

4.1.12 General procedure for isosorbide dilevulinate copolymerization with dihydrazides

Isosorbide dilevulinate (1.0 eq) was dissolved in dioxane (conc. 15 mL/g). After that, dihydrazide (1.0 eq) was dissolved in different water and methanol (if used) mixtures (approximate conc. 40 mL/g). Solutions were mixed into the reaction flask, and acetic acid was added as a catalyst. The mixture was stirred for 1–3 days at a given temperature (20 to 90 °C). After the reaction, the polymer was precipitated in 1:5 *i*-PrOH/Et_2O solution (1.25 L for a gram of theoretical amount of product). Solid product was filtrated, washed with a small amount of precipitation solution and dried under vacuum. Molecular weights of copolymers were determined by SEC using DMF as eluent (0.5 mL/min) and PEO/PEG or PS standards.

SUMMARY

The world population is rising rapidly and there is an extremely high demand for energy and materials. Exploiting conventional fossil-based fuel is not sustainable because it consumes non-renewable resources and causes significant adverse effects on the environment. The world has started moving towards the use of renewable and carbon free energy resources. Plastics are one of the fields where biobased feedstocks could provide a replacement to the fossil-based counterparts. In the present thesis, isosorbide and citric acid derived building blocks were investigated as an alternative in novel biobased plastics.

Isosorbide is a biobased diol derived from glucose, and has been extensively studied in many applications, including drugs, solvents, and as a precursor for different chemicals and polymers. In the context of biobased polymers, isosorbide is a versatile building block having a rigid bicyclic structure, which is rather rare. Isosorbide has been mainly investigated as a difunctional polymer building block in polymer main chains. Recently, a regioselective acylation was developed for both *exo* and *endo* hydroxyl group of isosorbide, which allows the investigation of isosorbide as a monofunctional polymer building block as a single regioisomer.

The first approach of the present thesis was to investigate regioselectively pure isosorbide-5-methacrylates and their regioisomers. Regioselectively pure isosorbide-5-methacrylate was first prepared and the remaining free OH group was acylated with linear saturated carboxylic acids with the length from acetate (C2) to icosanoate (C20). These monomers were polymerized by conventional free-radical polymerization. M_n values were ranged from 32 to 81 kg/mol and $Đ$ values 1.8–3.0. Depending on the length of pendant linear side chain, the polymers exhibited amorphous (C2–C12) or semicrystalline (C13–C20) behavior. Amorphous polymer with acetate sidegroup showed the highest T_g of 107 °C. When the chain length exceeded 14 carbons (C14), both melting and isotropization transitions were recorded, which indicated the presence of liquid crystal mesophase.

The second goal of the thesis was to investigate isosorbide-5-polymethacrylates with lignin-related side groups attached to *exo* position of the isosorbide as esters. These substituents involved the following aromatics: non-, mono-, di-, trisubstituted *m*/*p*-methoxybenzoates; *p*-cyanobenzoate with strongly polar cyano group; vanillic acid esters with acetate, caproate and stearate at *p*-OH. In some cases, the monomers were purified by simple crystallization, thus avoiding chromatography. The polymerizations were evaluated in different solvents (EtOAc, toluene, GVL, chloroform, 2-MeTHF and DMSO) to find the most suitable for these monomers. As a result, DMSO was selected as main solvent for larger-scale polymerizations due to higher MW (M_n= 38–90 kg/mol), conversions (88–94%) and good solubility in general.

The thermal properties of the polymers were assessed by DSC and TGA. DSC experiments showed that these polymers showed T_g-s over 100 °C in most cases, which is quite competitive in the context of biobased polymers. In addition, the

polymer with polar cyano groups showed the highest T_g of 168 °C among these isosorbide monomethacrylate polymers. The polymer PC18 with long aliphatic stearoyl ester also showed a liquid crystallinity, as analogous PAIMA18 without vanillic acid fragment, having both melting and isotropization transitions (18 and 132 °C, respectively), but with wider liquid crystalline temperature range than PAIMA18.

The third part of the thesis involved an investigation of thiol-(meth)acrylate copolymers, which were derived from biobased building blocks, such as citric acid, glycerol and trimethylolpropane (TMP). The monomers were synthesized from the bi- and tricyclic diketones **B** and **T**, which were ketalized with glycerol or TMP in high yields (up to 93%) to obtain different spiro-diols. The diols were converted to the corresponding di(meth)acrylate esters, and were copolymerized with dithiols (1,3-PDT, 1,6-HDT and TBBT) via the Michael addition reaction. The copolymers were obtained with M_n= 5–27 kg/mol. The thermal properties of polymers were investigated by DSC and TGA. DSC showed T_g in the range –7–55 °C. As expected, copolymers with longer dithiols showed lower T_g-s as longer alkyl side chains gave more flexibility to the polymer chains. On the other hand, rigid TBBT-based copolymers exhibited higher T_g-s in every polymer structural combination. It was also found that polymers with TMP ketal group have higher T_g-s than polymers with the glycerol-based ketal group.

Moreover, as the ketal bonds are acid-sensitive, the hydrolytic degradation of thiol-acrylate polymers was demonstrated, which potentially could be reused in the chemical recycling of such polymers.

Additionally, isosorbide dilevulinate copolymers with different hydrazides were investigated to develop new polymers from biobased isosorbide and levulinic acid. The copolymers were prepared in different solvent mixtures at different temperatures, using different dihydrazides. As a result, the polymers showed relatively low molecular weights (M_n < 10 kg/mol) and poor solubility in typical solvents. However, the isosorbide dilevulinate copolymer with adipic acid dihydrazide showed T_g = 73 °C and $T_{d,\,95\%}$ = 209 °C at low molecular weights, which may be competitive in the biobased plastics field.

In summary, by having a very broad spectrum of properties, these novel biobased polymers might have potential to replace fossil-based counterparts in certain fields, especially in thermally demanding applications as thermoplastics. In the future, research on the efficient synthesis of biobased building blocks from raw materials should be continued to help these (and similar) polymers compete with fossil-based polymers.

SUMMARY IN ESTONIAN

Uudsed polümeerid lignotselluloosilisest toormest

Maailma rahvaarvu suurenemise ja inimeste elatustaseme kiire tõusuga on kasvanud nõudlus energiale ja materjalidele, mis mõlemad vajavad samuti rohkelt ressurssi. Siiani on selleks kasutatud mittetaastuvaid fossiilseid tooraineid, kuid paraku on nende intensiivne kasutamine juba avaldanud äärmiselt kahjulikku mõju meie keskkonnale. Seetõttu on tänapäeva maailmas võetud kurss taastuvate ressursside kasutamise suunas, näiteks mitmete biobaseeruvate toorainete kasutamine erinevate materjalide tootmisel. Plastikute tootmisel on üheks alternatiivseks ehitusplokiks isosorbiid, millest tehtud polümeerid võiksid pakkuda konkurentsi fossiilsetele polümeeridele.

Isosorbiid on glükoosist toodetav diool, mida kasutatakse näiteks farmaatsiatööstuses, aga seda on uuritud ka polümeerikeemia kontekstis. Polümeeride vallas pakub isosorbiid huvi eelkõige oma jäiga bitsüklilise struktuuri tõttu, mis on biomassist saadavate ühendite hulgas pigem harv omadus. Jäik struktuur on üheks eelduseks, et saadaval polümeeril võiksid olla keskmisest kõrgemad termilised näitajad, näiteks klaasistumistemperatuur (T_g), millest allpool on polümeer pigem jäik ning millest ülevalpool pehme ja vormitav. Lisaks on tänu kahele hüdroksüülrühmale võimalik isosorbiidi funktsionaliseerida väga erinevatel viisidel, kasutades teda nii mono- kui difunktsionaalse monomeerina. Peale selle võimaldab regioselektiivne ensümaatiline atsüleerimine isosorbiidi *ekso* ja *endo* hüdroksüülrühmi selektiivselt modifitseerida.

Selle doktoritöö esimene osa hõlmab isosorbiid-5-metakrülaatide ja sellest saadud polümeeride uurimist. Töö käigus esterdati isosorbiid-5-metakrülaadi vaba *ekso* hüdroksüülrühm kasutades erinevaid lineaarseid küllastunud karboksüülhappeid, pikkusega alates atsetaadist (C2) kuni ikosonaadini (C20). Saadud monomeerid polümeriseeriti kasutades vabaradikaalpolümerisatsiooni. Polümerisatsioonis saadud polümeeride molekulmass varieerus vahemikus M_n= 32–81 kg/mol ja polüdisperssus $Đ$= 1.8–3.0. Sõltuvalt lineaarse kõrvalahela pikkusest jagunesid polümeerid amorfseteks (C2–C12) ja semikristallseteks (C13–C20). Amorfsetest polümeeridest näitas kõrgeimat klaasistumistemperatuuri atsetaat (C2) kõrvalahelaga polümeer (T_g= 107 °C). Polümeerid, mille kõrvalahela pikkus on 14 ja rohkem süsinikku (s.t. alates C14) omavad nii sulamis- kui isotropisatiooniüleminekut, mis omakorda viitab vedelkristallilistele omadustele ehk näitab koordineeritud mesofaasi olemasolu vedelas faasis.

Selle doktoritöö teises osas uuriti isosorbiid-5-polümetakrülaate, kus isosorbiidi *ekso* hüdroksüülrühm oli esterdatud erinevate potentsiaalselt ligniinist saadavate aromaatsete hapetega. Kõrvalahelatena olid esindatud bensoaat, mono-, di-, trimetoksübensoaadid; *p*-tsüanobensoaat jäiga ja polaarse tsüanorühmaga; vaniljehappe estrid atsetaadiga (C2), kaproaadiga (C6) ja stearaadiga (C18). Lisaks demonstreeriti tahkete monomeeride puhastamist ümberkristallimise meetodi abil, vältimaks kallimat kromatograafia meetodit.

Järgnevalt testiti monomeeride polümerisatsiooni erinevates lahustites (EtOAc, tolueen, GVL, kloroform, 2-MeTHF and DMSO), et leida sobivaim sedatüüpi

monomeeridele. Testimise tulemusena valiti polümerisatsiooni solvendiks DMSO, sest see andis keskmisest kõrgemaid molekulmasse (M_n= 38–90 kg/mol) ja konversioone (88–94%) ning tagas üldjuhul hea monomeeride ja polümeeride lahustumise. Peale tingimuste optimeerimist polümeerisiti monomeerid DMSO-s suuremas gramm-skaalas ning mõõdeti polümeeride termilisi omadusi kasutades kalorimeetrilisi (DSC) ja termogravimeetrilisi (TGA) meetodeid. DSC mõõtmiste käigus leiti, et saadud polümeeride T_g-d ületasid enamasti 100 °C, mis on konkurentsivõimeline tulemus võrreldes teiste biobaseeruvate polümeeridega. Sellest seeriast kõrgeimat T_g-d (168 °C) näitas polaarse tsüanogrupiga polümeer, mis on ühtlasi ka kõrgeim tulemus taoliste isosorbiid polümetakrülaatide hulgas. Lisaks näitas pika C18 kõrvalahelaga polümeer vedelkristalsetele polümeeridele omaseid sulamis- ja isotropisatsiooniüleminekuid.

Selle töö kolmas osa hõlmas tiool-akrülaatide kopolümeeride sünteesi ja uuringuid. Need ühendid valmistati kommertsiaalsetest biotoormest toodetavatest kemikaalidest nagu sidrunhape, glütserool ja trimetüloolpropaan (TMP). Täpsemalt sünteesiti monomeerid sidrunhappest saadud bi- ja trisüklilistest diketoonidest, mis ketaliseeriti kõrge saagisega (kuni 93%) glütserooli või TMP-ga erinevateks dioolideks. Dioolid konverteeriti di(met)akrülaatideks, mis edasi kopolümeriseeriti erinevate ditioolidega (1,3-PDT, 1,6-HDT ja TBBT-ga) kasutades Michael'i liitumisreaktsiooni. Saadud polümeerid näitasid molekulmasse vahemikus M_n= 5–27 kg/mol. Kopolümeeride termilisi omadusi uuriti DSC ja TGA-ga. DSC-s näitasid kopolümeerid T_g-d vahemikus –7–55 °C. Ootuspäraselt näitasid pikemate ja painduvamate alifaatsete ditioolidega kopolümeerid madalamaid T_g-sid ning jäikade aromaatsete TBBT ahelatega polümeerid kõrgemaid T_g-sid. Samuti leiti, et TMP ketaalrühmaga kopolümeeride T_g-d on kõrgemad võrreldes glütserooli fragmenti sisaldavate analoogidega. Lõpuks demonstreeriti polümeeride hüdrolüütilist lagunemist diketooniks, mis avab võimaluse polümeeride keemiliseks taaskasutamiseks.

Töö viimases osas uuriti isosorbiid dilevulinaadi-dihüdrasiidide kopolümerisatsioone. Antud uurimuse eesmärk oli leida uusi biobaseeruvaid polümeere isosorbiidi ja levuliinhappe baasil. Kopolümeere sünteesiti erinevatel temperatuuridel ja solvendisegudes, et leida sobivamaid tingimusi. Kahjuks näitasid kopolümeerid pigem madalaid molekulaarmasse (M_n < 10 kg/mol) ja tagasihoidlikku lahustuvust. Küll aga isosorbiid dilevulinaadi kopolümeer adipaathappe dihüdrasiidiga näitas eeskujulikke termilisi omadusi ka madalate masside korral (T_g = 73 and $T_{d,95\%}$ = 209 °C).

Kokkuvõtteks sünteesiti ja uuriti antud töös uut tüüp biobaseeruvaid polümeere, millel on lai spekter omadusi, mis tulenevad erinevatest asendusrühmadest. Uuritud polümeerid võiksid osaliselt asendada fossiilpäritolu plastikuid mitmetes termiliselt nõudlikkes rakendustes, näiteks termoplastikutena. Seeläbi suudaksid sellised taastuvast toormest saadavad ühendid säästa loodust. Antud töö kontekstis tasub tulevikus edasi arendada biopõhiste ehitusplokkide efektiivsemat ja jätkusuutlikumat sünteesiteed, mis aitaksid töös valmistatud (ja sarnastel) polümeeridel veelgi paremini konkureerida fossiilpäritolu polümeeridega.

REFERENCES

(1) Brydson, J. A. *Plastics Materials*, 7th edition.; London, 1999.

(2) Shanmugam, V.; Das, O.; Neisiany, R. E.; Babu, K.; Singh, S. Polymer Recycling in Additive Manufacturing: An Opportunity for the Circular Economy. **2020**. https://doi.org/10.1007/s42824-020-00012-0.

(3) *Global plastic waste set to almost triple by 2060, says OECD*. https://www.oecd.org/environment/global-plastic-waste-set-to-almost-triple-by-2060.htm (accessed 2023-09-27).

(4) *Plastic leakage and greenhouse gas emissions are increasing – OECD*. https://www.oecd.org/environment/plastics/increased-plastic-leakage-and-greenhouse-gas-emissions.htm (accessed 2023-09-27).

(5) Rainieri, S.; Barranco, A. Trends in Food Science & Technology Microplastics, a Food Safety Issue? *Trends Food Sci Technol* **2019**, *84*, 55–57. https://doi.org/10.1016/j.tifs.2018.12.009.

(6) Thushari, G. G. N.; Senevirathna, J. D. M. Heliyon Plastic Pollution in the Marine Environment. *Heliyon* **2020**, *6* (8). https://doi.org/10.1016/j.heliyon.2020.e04709.

(7) Sun, X.; Xie, M.; Mai, L.; Zeng, E. Y. Biobased Plastic: A Plausible Solution toward Carbon Neutrality in Plastic Industry? *J Hazard Mater* **2022**, *435*, 129037. https://doi.org/10.1016/j.jhazmat.2022.129037.

(8) Moshood, T. D.; Nawanir, G.; Ghani, A. A.; Mahmud, F.; Mohamad, F.; Ahmad, M. H. Expanding Policy for Biodegradable Plastic Products and Market Dynamics of Bio-Based Plastics: Challenges and Opportunities. *Sustainability* **2021**, *13*, 6170–6170. https://doi.org/10.3390/su13116170.

(9) Holmberg, A. L.; Reno, K. H.; Wool, P.; Epps, T. H. Soft Matter Biobased Building Blocks for the Rational Design of Renewable Block Polymers. *Soft Matter* **2014**, *10*, 7405–7424. https://doi.org/10.1039/c4sm01220h.

(10) Rajvanshi, J.; Sogani, M.; Kumar, A.; Arora, S.; Syed, Z.; Sonu, K. Science of the Total Environment Perceiving Biobased Plastics as an Alternative and Innovative Solution to Combat Plastic Pollution for a Circular Economy. *Science of the Total Environment* **2023**, *874*, 162441. https://doi.org/10.1016/j.scitotenv.2023.162441.

(11) *Plastic pollution is growing relentlessly as waste management and recycling fall short, says OECD*. https://www.oecd.org/newsroom/plastic-pollution-is-growing-relentlessly-as-waste-management-and-recycling-fall-short.htm (accessed 2023-09-27).

(12) Rahimi, A.; García, J. M. Chemical Recycling of Waste Plastics for New Materials Production. *Nat Rev Chem* **2017**, *1* (0046). https://doi.org/10.1038/s41570-017-0046.

(13) Fenouillot, F.; Rousseau, A.; Colomines, G.; Saint-Loup, R.; Pascault, J. P. Polymers from Renewable 1,4:3,6-Dianhydrohexitols (Isosorbide, Isomannide and Isoidide): A Review. *Progress in Polymer Science (Oxford)* **2010**, *35* (5), 578–622. https://doi.org/10.1016/j.progpolymsci.2009.10.001.

(14) Pirzadi, Z.; Meshkani, F. From Glycerol Production to Its Value-Added Uses: A Critical Review. *Fuel* **2022**, *329*, 125044. https://doi.org/10.1016/j.fuel.2022.125044.

(15) Ghasemlou, M.; Daver, F.; Ivanova, E. P.; Adhikari, B. Bio-Based Routes to Synthesize Cyclic Carbonates and Polyamines Precursors of Non-Isocyanate Polyurethanes: A Review. *Eur Polym J* **2019**, *118*, 668–684. https://doi.org/10.1016/j.eurpolymj.2019.06.032.

(16) Chen, Y.; Nielsen, J. Biobased Organic Acids Production by Metabolically Engineered Microorganisms. *Curr Opin Biotechnol* **2016**, *37*, 165–172. https://doi.org/10.1016/j.copbio.2015.11.004.
(17) Feldman, D. Polymer History. *Des Monomers Polym* **2008**, *11*, 1–15. https://doi.org/10.1163/156855508X292383.
(18) Andrady, A. L.; Rajapakse, N. Additives and Chemicals in Plastics. **2016**. https://doi.org/10.1007/698.
(19) Geyer, R.; Jambeck, J. R.; Law, K. L. Production, Use, and Fate of All Plastics Ever Made. *Sci Adv* **2017**, *3* (7). https://doi.org/10.1126/sciadv.1700782.
(20) Brydson, J. A. *Plastics Materials*, 7th edition.; Butterworth-Heinemann, Oxford: London, 1999.
(21) Pathak, P.; Sharma, S.; Ramakrishna, S. Circular Transformation in Plastic Management Lessens the Carbon Footprint of the Plastic Industry. *Materials Today Sustainability* **2023**, *22*, 100365. https://doi.org/10.1016/j.mtsust.2023.100365.
(22) Diggle, A.; Walker, T. R. Environmental and Economic Impacts of Mismanaged Plastics and Measures for Mitigation. *Environments* **2022**, *9* (15). https://doi.org/10.3390/environments9020015.
(23) Jiang, J.; Shi, K.; Zhang, X.; Yu, K.; Zhang, H.; He, J. From Plastic Waste to Wealth Using Chemical Recycling: A Review. *J Environ Chem Eng* **2022**, *10*, 106867. https://doi.org/10.1016/j.jece.2021.106867.
(24) Thiounn, T.; Smith, R. C. Advances and Approaches for Chemical Recycling of Plastic Waste. *Journal of Polymer Science* **2020**, *58*, 1347–1364. https://doi.org/10.1002/pol.20190261.
(25) Morici, E.; Carroccio, S. C.; Bruno, E.; Scarfato, P.; Filippone, G.; Dintcheva, N. T. Recycled (Bio)Plastics and (Bio)Plastic Composites: A Trade Opportunity in a Green Future. *Polymers (Basel)* **2022**, *14* (2038). https://doi.org/10.3390/ polym14102038.
(26) Liu, T.; Zhao, B.; Zhang, J. Recent Development of Repairable, Malleable and Recyclable Thermosetting Polymers through Dynamic Transesterification. *Polymer (Guildf)* **2020**, *194*, 122392. https://doi.org/10.1016/j.polymer.2020.122392.
(27) Huang, J.; Veksha, A.; Ping, W.; Giannis, A.; Lisak, G. Chemical Recycling of Plastic Waste for Sustainable Material Management: A Prospective Review on Catalysts and Processes. *Renewable and Sustainable Energy Reviews* **2022**, *154*, 111866. https://doi.org/10.1016/j.rser.2021.111866.
(28) Yamamoto, M.; Kinnaman, T. C. Is Incineration Repressing Recycling? *J Environ Econ Manage* **2022**, *111*, 102593. https://doi.org/10.1016/j.jeem.2021.102593.
(29) Lerici, L. C.; Renzini, M. S.; Pierella, L. B. Chemical Catalyzed Recycling of Polymers: Catalytic Conversion of PE, PP and PS into Fuels and Chemicals over H-Y. *Procedia Materials Science* **2015**, *8*, 297–303. https://doi.org/10.1016/j.mspro.2015.04.076.
(30) Feghali, E.; Tauk, L.; Ortiz, P.; Vanbroekhoven, K. Catalytic Chemical Recycling of Biodegradable Polyesters. *Polym Degrad Stab* **2020**, *179*, 109241. https://doi.org/10.1016/j.polymdegradstab.2020.109241.
(31) Chen, X.; Yan, N. A Brief Overview of Renewable Plastics. *Materials Today Sustainability* **2020**, *7–8*, 100031. https://doi.org/10.1016/j.mtsust.2019.100031.
(32) *Market – European Bioplastics e.V.* https://www.european-bioplastics.org/market/ (accessed 2023-09-28).

(33) Coppola, G.; Gaudio, M. T.; Lopresto, C. G.; Calabro, V.; Curcio, S.; Chakraborty, S. Bioplastic from Renewable Biomass: A Facile Solution for a Greener Environment. *Earth Systems and Environment* **2021**, *5* (2), 231–251. https://doi.org/10.1007/S41748-021-00208-7.

(34) Stegmann, P.; Daioglou, V.; Londo, M.; Vuuren, D. P. Van. Plastic Futures and Their CO2 Emissions. *Nature* **2022**, *612*, 272. https://doi.org/10.1038/s41586-022-05422-5.

(35) Sousa, A. F.; Silvestre, A. J. D. Plastics from Renewable Sources as Green and Sustainable Alternatives. *Curr Opin Green Sustain Chem* **2022**, *33*, 100557. https://doi.org/10.1016/j.cogsc.2021.100557.

(36) Storz, H.; Vorlop, K. D. Bio-Based Plastics: Status, Challenges and Trends. *Applied Agricultural and Forestry Research* **2013**, *4*, 321–332. https://doi.org/10.3220/LBF_2013_321-332.

(37) Wellenreuther, C.; Zander, N. Cost Competitiveness of Sustainable Bioplastic Feedstocks – A Monte Carlo Analysis for Polylactic Acid. *Clean Eng Technol* **2022**, *6*, 100411. https://doi.org/10.1016/j.clet.2022.100411.

(38) Albuquerque, T. L.; Marques Júnior, J. E.; Queiroz, L. P.; Ricardo, A. D. S.; Rocha, M. V. P. Polylactic Acid Production from Biotechnological Routes: A Review. *Int J Biol Macromol* **2021**, *186*, 933–951. https://doi.org/10.1016/j.ijbiomac.2021.07.074.

(39) Sudesh, K.; Iwata, T. Sustainability of Biobased and Biodegradable Plastics. *Clean (Weinh)* **2008**, *36* (5–6), 433–442. https://doi.org/10.1002/clen.200700183.

(40) Rameshkumar, S.; Shaiju, P.; Connor, K. E. O.; P, R. B. Bio-Based and Biodegradable Polymers – State-of-the-Art, Challenges and Emerging Trends. *Curr Opin Green Sustain Chem* **2020**, *21*, 75–81. https://doi.org/10.1016/j.cogsc.2019.12.005.

(41) Weinland, D. H.; Putten, R. Van; Gruter, G. M. Reviewing the Synthetic Challenges in Step Growth Polymerization. *Eur Polym J* **2022**, *164*, 110964. https://doi.org/10.1016/j.eurpolymj.2021.110964.

(42) Battegazzore, D.; Bocchini, S.; Nicola, G.; Martini, E.; Frache, A. Isosorbide, a Green Plasticizer for Thermoplastic Starch That Does Not Retrogradate. *Carbohydr Polym* **2015**, *119*, 78–84. https://doi.org/10.1016/j.carbpol.2014.11.030.

(43) Rose, M.; Palkovits, R. Isosorbide as a Renewable Platform Chemical for Versatile Applications-Quo Vadis? *ChemSusChem* **2012**, *5* (1), 167–176. https://doi.org/10.1002/cssc.201100580.

(44) Li, G.; Liu, W.; Ye, C.; Li, X.; Si, C. Chemocatalytic Conversion of Cellulose into Key Platform Chemicals. *Int J Polym Sci* **2018**, *2018*. https://doi.org/10.1155/2018/4723573.

(45) Almeida, R. M. De; Li, J.; Nederlof, C.; Connor, P. O.; Makkee, M. Cellulose Conversion to Isosorbide in Molten Salt Hydrate Media. *ChemSusChem* **2010**, *3*, 325–328. https://doi.org/10.1002/cssc.200900260.

(46) Bonnin, I.; Mereau, R.; Tassaing, T.; De Oliveira Vigier, K. One-Pot Synthesis of Isosorbide from Cellulose or Lignocellulosic Biomass: A Challenge? *Beilstein Journal of Organic Chemistry* **2020**, *16*, 1713–1721. https://doi.org/10.3762/bjoc.16.143.

(47) Delbecq, F.; Khodadadi, M. R.; Padron, D. R.; Varma, R.; Len, C.; Supérieure, E.; Organique, D. C.; Buckmaster, R. J.; Compiègne, F. Isosorbide: Recent Advances in Catalytic Production. *Molecular Catalysis* **2020**, *482*, 110648. https://doi.org/10.1016/j.mcat.2019.110648.

(48) Zou, J.; Cao, D.; Tao, W.; Zhang, S.; Cui, L.; Zeng, F.; Cai, W. Sorbitol Dehydration into Isosorbide over a Cellulose-Derived Solid Acid Catalyst. *The Royal Society of Chemistry* **2016**, *6*, 49528–49536. https://doi.org/10.1039/c6ra05214b.

(49) Belluati, M.; Tabasso, S.; Bucciol, F.; Tabanelli, T.; Cavani, F.; Cravotto, G.; Manzoli, M. Sustainable Isosorbide Production by a Neat One-Pot MW-Assisted Catalytic Glucose Conversion. *Catal Today* **2023**, *418*, 114086. https://doi.org/10.1016/j.cattod.2023.114086.

(50) Naves, A. F.; Fernandes, H. T. C.; Immich, A. P. S.; Catalani, L. H. Enzymatic Syntheses of Unsaturated Polyesters Based on Isosorbide and Isomannide. *Journal of Polymer Science* **2013**, *51*, 3881–3891. https://doi.org/10.1002/pola.26789.

(51) Flèche, G.; Huchette, M. Isosorbide. Preparation, Properties and Chemistry. *Starch – Stärke* **1986**, *38* (1), 26–30. https://doi.org/10.1002/star.19860380107.

(52) Hockett, B. R. C.; Fletcher, H. G.; Sheffield, E. L.; Goepp, R. M.; Sheffield, E. L. Hexitol Anhydrides. The Structure of Isosorbide, a Crystalline Dianhydrosorbitol. *Journal of American Chemical Society* **1946**, *68* (6), 927–930. https://doi.org/10.1021/ja01210a003.

(53) Ben, M.; Azizi, N.; Ba, A.; Chevalier, Y.; Majdoub, M. Industrial Crops & Products New Microcapsules Based on Isosorbide for Cosmetotextile: Preparation and Characterization. *Ind Crops Prod* **2018**, *123*, 591–599. https://doi.org/10.1016/j.indcrop.2018.07.020.

(54) Aricò, F. Isosorbide as Biobased Platform Chemical: Recent Advances. *Curr Opin Green Sustain Chem* **2020**, *21*, 82–88. https://doi.org/10.1016/j.cogsc.2020.02.002.

(55) Lee, J.; Lee, S.; Yoon, D.; Yoon, W. J.; Im, S. S.; Moon, B.; Oh, H. Bin. Tandem Mass Spectrometric Analysis of Isosorbide-1,4-Cyclohexane-Dicarboxylic Acid Polyester Oligomer Cations Using Ion-Trap Mass Spectrometry. *Rapid Communications in Mass Spectrometry* **2013**, *27*, 1913–1918. https://doi.org/10.1002/rcm.6645.

(56) Saska, J.; Dutta, S.; Kindler, A.; Zuend, S. J.; Mascal, M. Efficient and Scalable Production of Isoidide from Isosorbide. *ACS Sustain Chem Eng* **2021**, *9*, 11565–11570. https://doi.org/10.1021/acssuschemeng.1c04141.

(57) Aricò, F. Isosorbide as Biobased Platform Chemical: Recent Advances. *Curr Opin Green Sustain Chem* **2020**, *21*, 82–88. https://doi.org/10.1016/j.cogsc.2020.02.002.

(58) Silber, S. Nitrates: Why and How Should They Be Used Today? *Eur J Clin Pharmacol* **1990**, *38*, 35–51. https://doi.org/10.1007/BF01417564.

(59) Durand, M.; Zhu, Y.; Aubry, J. Solubilizing and Hydrotropic Properties of Isosorbide Monoalkyl- and Dimethyl-Ethers. *J Surfact Deterg* **2009**, *12*, 371–378. https://doi.org/10.1007/s11743-009-1128-4.

(60) Yang, Y.; Huang, J.; Zhang, R.; Zhu, J. Designing Bio-Based Plasticizers: Effect of Alkyl Chain Length on Plasticization Properties of Isosorbide Diesters in PVC Blends. *Mater Des* **2017**, *126*, 29–36. https://doi.org/10.1016/j.matdes.2017.04.005.

(61) Han, Y.; Zhang, C.; Yang, Y.; Weng, Y.; Ma, P.; Xu, P. Epoxidized Isosorbide-Based Esters with Long Alkyl Chains as Efficient and Enhanced Thermal Stability and Migration Resistance PVC Plasticizers. *Polym Test* **2023**, *123*, 108048. https://doi.org/10.1016/j.polymertesting.2023.108048.

(62) Nonque, F.; Sahut, A.; Jacquel, N.; Saint-Loup, R.; Woisel, P.; Potier, J. Isosorbide Monoacrylate: A Sustainable Monomer for the Production of Fully Bio-Based Polyacrylates and Thermosets. *Polym Chem* **2020**, *11* (43), 6903–6909. https://doi.org/10.1039/d0py00957a.

(63) Moon, N. G.; Mazzini, F.; Pekkanen, A. M.; Wilts, E. M.; Long, T. E. Sugar-Derived Poly(β-Thioester)s as a Biomedical Scaffold. *Macromol Chem Phys* **2018**, *219* (16), 1–9. https://doi.org/10.1002/macp.201800177.

(64) Gallagher, J. J.; Hillmyer, M. A.; Reineke, T. M. Isosorbide-Based Polymethacrylates. *ACS Sustain Chem Eng* **2015**, *3* (4), 662–667. https://doi.org/10.1021/sc5008362.

(65) Juais, D.; Naves, A. F.; Li, C.; Gross, R. A.; Catalani, L. H. Isosorbide Polyesters from Enzymatic Catalysis. *Macromolecules* **2010**, *43*, 10315–10319. https://doi.org/10.1021/ma1013176.

(66) Matt, L.; Parve, J.; Parve, O.; Pehk, T.; Pham, T. H.; Liblikas, I.; Vares, L.; Jannasch, P. Enzymatic Synthesis and Polymerization of Isosorbide-Based Monomethacrylates for High-Tg Plastics. *ACS Sustain Chem Eng* **2018**, *6* (12), 17382–17390. https://doi.org/10.1021/acssuschemeng.8b05074.

(67) Caretto, A.; Passoni, V.; Brenna, N.; Sitta, M.; Ogliosi, L.; Catel, G.; Turri, S.; Gri, G. Fully Biobased Polyesters Based on an Isosorbide Monomer for Coil Coating Applications. *ACS Sustainable Chem. Eng.* **2018**, *6*, 14125–15134. https://doi.org/10.1021/acssuschemeng.8b02659.

(68) Gómez-de-miranda-jiménez-de-aberasturi, O.; Centeno-pedrazo, A.; Fernández, S. P.; Alonso, R. R.; Medel, S.; Cuevas, M.; Monsegue, L. G.; Wildeman, S. De; Benedetti, E.; Klein, D.; Henneken, H.; Ochoa-gómez, J. R.; Fernández, S. P.; Alonso, R. R.; Medel, S.; Cuevas, J. M.; Monsegue, G.; Wildeman, S. De; Benedetti, E.; Klein, D.; Henneken, H. The Future of Isosorbide as a Fundamental Constituent for Polycarbonates and Polyurethanes. *Green Chemistry Letters and Reviews* **2021**, *14* (3), 534–544. https://doi.org/10.1080/17518253.2021.1965223.

(69) Matt, L.; Liblikas, I.; Bonjour, O.; Jannasch, P.; Vares, L. Synthesis and Anionic Polymerization of Isosorbide Mono-Epoxides for Linear Biobased Polyethers. *Polym Chem* **2021**, *12*, 5937–5941. https://doi.org/10.1039/d1py00687h.

(70) *Thermal Transitions of Homopolymers: Glass Transition & Melting Point*. https://www.sigmaaldrich.com/EE/en/technical-documents/technical-article/materials-science-and-engineering/polymer-synthesis/thermal-transitions-of-homopolymers (accessed 2023-11-08).

(71) Yan, J.; Oyedeji, O.; Leal, J. H.; Donohoe, B. S.; Semelsberger, T. A.; Li, C.; Hoover, A. N.; Webb, E.; Bose, E. A.; Zeng, Y.; Williams, C. L.; Schaller, K. D.; Sun, N.; Ray, A. E.; Tanjore, D. Characterizing Variability in Lignocellulosic Biomass: A Review. *ACS Sustain Chem Eng* **2020**, *8* (22), 8059–8085. https://doi.org/10.1021/acssuschemeng.9b06263.

(72) Bass, G. F.; Epps, T. H. Recent Developments towards Performance-Enhancing Lignin-Based Polymers. *Polym Chem* **2021**, *12*, 4130–4158. https://doi.org/10.1039/d1py00694k.

(73) Messman, J. M.; Baker, F. S.; Naskar, A. K. Turning Renewable Resources into Value-Added Polymer: Development of Lignin-Based Thermoplastic. *Green Chemistry* **2012**, *14*, 3295–3303. https://doi.org/10.1039/c2gc35933b.

(74) Li, X.; Zheng, Y. Biotransformation of Lignin: Mechanisms, Applications and Future Work. *Biotechnol Prog* **2019**, *e2922*, 1–21. https://doi.org/10.1002/btpr.2922.

(75) Grossman, A.; Vermerris, W. Lignin-Based Polymers and Nanomaterials. *Curr Opin Biotechnol* **2019**, *56*, 112–120. https://doi.org/10.1016/j.copbio.2018.10.009.
(76) Kun, D.; Pukánszky, B. Polymer/Lignin Blends: Interactions, Properties, Applications. *Eur Polym J* **2020**, *93*, 618–641. https://doi.org/10.1016/j.eurpolymj.2017.04.035.
(77) Shi, K.; Liu, G.; Sun, H. Polylactic Acid/Lignin Composites: A Review. *Polymers (Basel)* **2023**, *15*, 2807.
(78) Wang, C.; Kelley, S. S.; Venditti, R. A. Lignin-Based Thermoplastic Materials. *ChemSusChem* **2016**, *9*, 770–783. https://doi.org/10.1002/cssc.201501531.
(79) Börcsök, Z.; Pásztory, Z. The Role of Lignin in Wood Working Processes Using Elevated Temperatures: An Abbreviated Literature Survey. *European Journal of Wood and Wood Products* **2021**, *79* (3), 511–526. https://doi.org/10.1007/s00107-020-01637-3.
(80) Doherty, W. O. S.; Mousavioun, P.; Fellows, C. M. Value-Adding to Cellulosic Ethanol: Lignin Polymers. *Ind Crops Prod* **2011**, *33* (2), 259–276. https://doi.org/10.1016/j.indcrop.2010.10.022.
(81) Karunarathna, M. S.; Smith, R. C. Valorization of Lignin as a Sustainable Component of Structural Materials and Composites: Advances from 2011 to 2019. *Sustainability* **2020**, *12*, 734. https://doi.org/10.3390/su12020734.
(82) Jia, Z.; Lu, C.; Wang, L. Preparation and Characterization of High Boiling Solvent Lignin-Based Polyurethane Film with Lignin as the Only Hydroxyl Group Provider. *The Royal Society of Chemistry* **2015**, *5*, 53949–53955. https://doi.org/10.1039/c5ra09477a.
(83) Wang, Y.; Meng, X.; Pu, Y.; Ragauskas, A. J. Recent Advances in the Application of Functionalized in Value-Added Polymeric Materials. *Polymers (Basel)* **2020**, *12*, 2277. https://doi.org/10.3390/polym12102277.
(84) Vila, C.; Santos, V.; Saake, B.; Parajó, J. C. Manufacture, Characterization, and Properties of Poly-(Lactic Acid) and Its Blends with Esterified Pine Lignin. *Bioresources* **2016**, *11* (2), 5322–5332.
(85) Antunes, F.; Mota, I. F.; Burgal, S.; Pintado, M.; Costa, P. S. A Review on the Valorization of Lignin from Sugarcane By-Products: From Extraction to Application. *Biomass and Bioenergy* **2022**, *166*, 106603. https://doi.org/10.1016/j.biombioe.2022.106603.
(86) Martinkova, L.; Grulich, M.; Miroslav, P.; Kristkova, B.; Winkler, M. Bio-Based Valorization of Lignin-Derived Phenolic Compounds: A Review. *Biomolecules* **2023**, *13*, 717. https://doi.org/10.3390/ biom13050717.
(87) Holmberg, A. L.; Reno, K. H.; Nguyen, N. A.; Wool, R. P.; Epps, T. H. Syringyl Methacrylate, a Hardwood Lignin-Based Monomer for High-Tg Polymeric Materials. *ACS Macro Lett* **2016**, *5*, 574–578. https://doi.org/10.1021/acsmacrolett.6b00270.
(88) Bonjour, O.; Nederstedt, H.; Arcos-Hernandez, M. V.; Laanesoo, S.; Vares, L.; Jannasch, P. Lignin-Inspired Polymers with High Glass Transition Temperature and Solvent Resistance from 4-Hydroxybenzonitrile, Vanillonitrile, and Syringonitrile Methacrylates. *ACS Sustain Chem Eng* **2021**, *9* (50), 16874–16880. https://doi.org/10.1021/acssuschemeng.1c07048.
(89) Yamago, S.; Nakamura, Y. Recent Progress in the Use of Photoirradiation in Living Radical Polymerization. *Polymer (Guildf)* **2013**, *54* (3), 981–994. https://doi.org/10.1016/j.polymer.2012.11.046.

(90) Szekeli, A.; Klussmann, M. Molecular Radical Chain Initiators for Ambient- to Low-Temperature Applications. *Chem. Asian J.* **2019**, *14*, 105–115. https://doi.org/10.1002/asia.201801636.
(91) Gridnev, A. A.; Ittel, S. D. Catalytic Chain Transfer in Free-Radical Polymerizations. *Chem. Rev.* **2001**, *101*, 3611–3659. https://doi.org/10.1021/cr9901236.
(92) Moad, G.; Solomon, D. H. *The Chemistry of Radical Polymerization*, 2nd Edition.; Elsevier: Oxford, 2006.
(93) Moad, G.; Rizzardo, E.; Thang, S. H. RAFT Polymerization and Some of Its Applications. *Chem. Asian J.* **2013**, *8*, 1634–1644. https://doi.org/10.1002/asia.201300262.
(94) Nicolas, J.; Guillaneuf, Y.; Lefay, C.; Bertin, D.; Gigmes, D.; Charleux, B. Progress in Polymer Science. *Prog Polym Sci* **2013**, *38* (1), 63–235. https://doi.org/10.1016/j.progpolymsci.2012.06.002.
(95) Matyjaszewski, K. Atom Transfer Radical Polymerization: From Mechanisms to Applications. *Isr. J. Chem.* **2012**, *52*, 206–220. https://doi.org/10.1002/ijch.201100101.
(96) Corrigan, N.; Jung, K.; Moad, G.; Hawker, C. J.; Matyjaszewski, K.; Boyer, C. Reversible-Deactivation Radical Polymerization (Controlled/Living Radical Polymerization): From Discovery to Materials Design and Applications. *Progress in Polymer Science* **2020**, *111*, 101311. https://doi.org/10.1016/j.progpolymsci.2020.101311.
(97) Parkatzidis, K.; Wang, H. S.; Truong, N. P.; Anastasaki, A. Perspective Recent Developments and Future Challenges in Controlled Radical Polymerization: A 2020 Update. *Chem* **2020**, *6* (7), 1575–1588. https://doi.org/10.1016/j.chempr.2020.06.014.
(98) Sahin, M.; Ayalur-Karunakaran, S.; Manhart, J.; Wolfahrt, M.; Kern, W.; Schlögl, S. Thiol-Ene versus Binary Thiol–Acrylate Chemistry: Material Properties and Network Characteristics of Photopolymers. *Adv Eng Mater* **2017**, *19* (4), 1–10. https://doi.org/10.1002/adem.201600620.
(99) Vandenbergh, J.; Ranieri, K.; Junkers, T. Synthesis of (Bio)-Degradable Poly(β-Thioester)s via Amine Catalyzed Thiol–Ene Click Polymerization. *Macromol. Chem. Phys.* **2012**, *213* (24), 2611–2617. https://doi.org/10.1002/macp.201200470.
(100) Hebner, T. S.; Fowler, H. E.; Herbert, K. M.; Skillin, N. P.; Bowman, C. N.; White, T. J. Polymer Network Structure, Properties, and Formation of Liquid Crystalline Elastomers Prepared via Thiol – Acrylate Chain Transfer Reactions. *Macromolecules* **2021**, *54*, 11074–11082. https://doi.org/10.1021/acs.macromol.1c01919.
(101) Moon, N. G.; Mazzini, F.; Pekkanen, A. M.; Wilts, E. M.; Long, T. E. Sugar-Derived Poly(β-Thioester)s as a Biomedical Scaffold. *Macromol. Chem. Phys.* **2018**, 1800177. https://doi.org/10.1002/macp.201800177.
(102) Drzeżdżon, J.; Jacewicz, D.; Sielicka, A.; Chmurzyński, L. Characterization of Polymers Based on Differential Scanning Calorimetry Based Techniques. *TrAC Trends in Analytical Chemistry* **2019**, *110*, 51–56. https://doi.org/10.1016/j.trac.2018.10.037.

(103) Saadatkhah, N.; Carillo Garcia, A.; Ackermann, S.; Leclerc, P.; Latifi, M.; Samih, S.; Patience, G. S.; Chaouki, J. Experimental Methods in Chemical Engineering: Thermogravimetric Analysis—TGA. *Can J Chem Eng* **2020**, *98* (1), 34–43. https://doi.org/10.1002/cjce.23673.
(104) Patra, S.; Ajayan, P. M.; Narayanan, T. N. Dynamic Mechanical Analysis in Materials Science: The Novice's Tale. *Oxford Open Materials Science* **2020**, *1* (1). https://doi.org/10.1093/oxfmat/itaa001.
(105) Barth, H. G.; Jackson, Christian.; Boyes, B. E. Size Exclusion Chromatography. *Anal Chem* **1994**, *66* (12), 595–620. https://doi.org/10.1021/ac00084a022.
(106) Dong, Y.; Dong, L.; Gu, X.; Wang, Y.; Liao, Y.; Luque, R.; Chen, Z. Sustainable Production of Active Pharmaceutical Ingredients from Lignin-Based Benzoic Acid Derivatives *via* "Demand Orientation." *Green Chemistry* **2023**, *25* (10), 3791–3815. https://doi.org/10.1039/D3GC00241A.
(107) Gomes, E. D.; Rodrigues, A. E. Lignin Biorefinery: Separation of Vanillin, Vanillic Acid and Acetovanillone by Adsorption. *Sep Purif Technol* **2019**, *216*, 92–101. https://doi.org/10.1016/j.seppur.2019.01.071.
(108) Laanesoo, S.; Bonjour, O.; Parve, J.; Parve, O.; Matt, L.; Vares, L.; Jannasch, P. Poly(Alkanoyl Isosorbide Methacrylate)s: From Amorphous to Semicrystalline and Liquid Crystalline Biobased Materials. *Biomacromolecules* **2021**, *22* (2), 640–648. https://doi.org/10.1021/acs.biomac.0c01474.
(109) Nonque, F.; Benlahoues, A.; Audourenc, J.; Sahut, A.; Saint-Loup, R.; Woisel, P.; Potier, J. Study on Polymerization of Bio-Based Isosorbide Monomethacrylate for the Formation of Low-T and High-T Sustainable Polymers. *Eur Polym J* **2021**, *160*, 110799. https://doi.org/10.1016/j.eurpolymj.2021.110799.
(110) Wang, S.; Shuai, L.; Saha, B.; Vlachos, D. G.; Epps, T. H. From Tree to Tape: Direct Synthesis of Pressure Sensitive Adhesives from Depolymerized Raw Lignocellulosic Biomass. *ACS Cent Sci* **2018**, *4* (6), 701–708. https://doi.org/10.1021/acscentsci.8b00140.
(111) Bonjour, O.; Nederstedt, H.; Arcos-hernandez, M. V; Laanesoo, S.; Vares, L.; Jannasch, P. Lignin-Inspired Polymers with High Glass Transition Temperature and Solvent Resistance from 4 – Hydroxybenzonitrile, Vanillonitrile, and Syringonitrile Methacrylates. **2021**. https://doi.org/10.1021/acssuschemeng.1c07048.
(112) Dannecker, P.; Biermann, U.; Sink, A.; Bloesser, F. R.; Metzger, J. O.; Meier, M. A. R. Fatty Acid–Derived Aliphatic Long Chain Polyethers by a Combination of Catalytic Ester Reduction and ADMET or Thiol-Ene Polymerization. *Macromol Chem Phys* **2019**, *220* (4). https://doi.org/10.1002/macp.201800440.
(113) Cordes, E. H.; Bull, H. G. Mechanism and Catalysis for Hydrolysis of Acetals, Ketals, and Ortho Esters. *Chem Rev* **1974**, *74* (5), 581–603. https://doi.org/10.1021/cr60291a004.
(114) Isikgor, F. H.; Becer, C. R. Lignocellulosic Biomass: A Sustainable Platform for the Production of Bio-Based Chemicals and Polymers. *Polym Chem* **2015**, *6* (25), 4497–4559. https://doi.org/10.1039/C5PY00263J.

APPENDIX

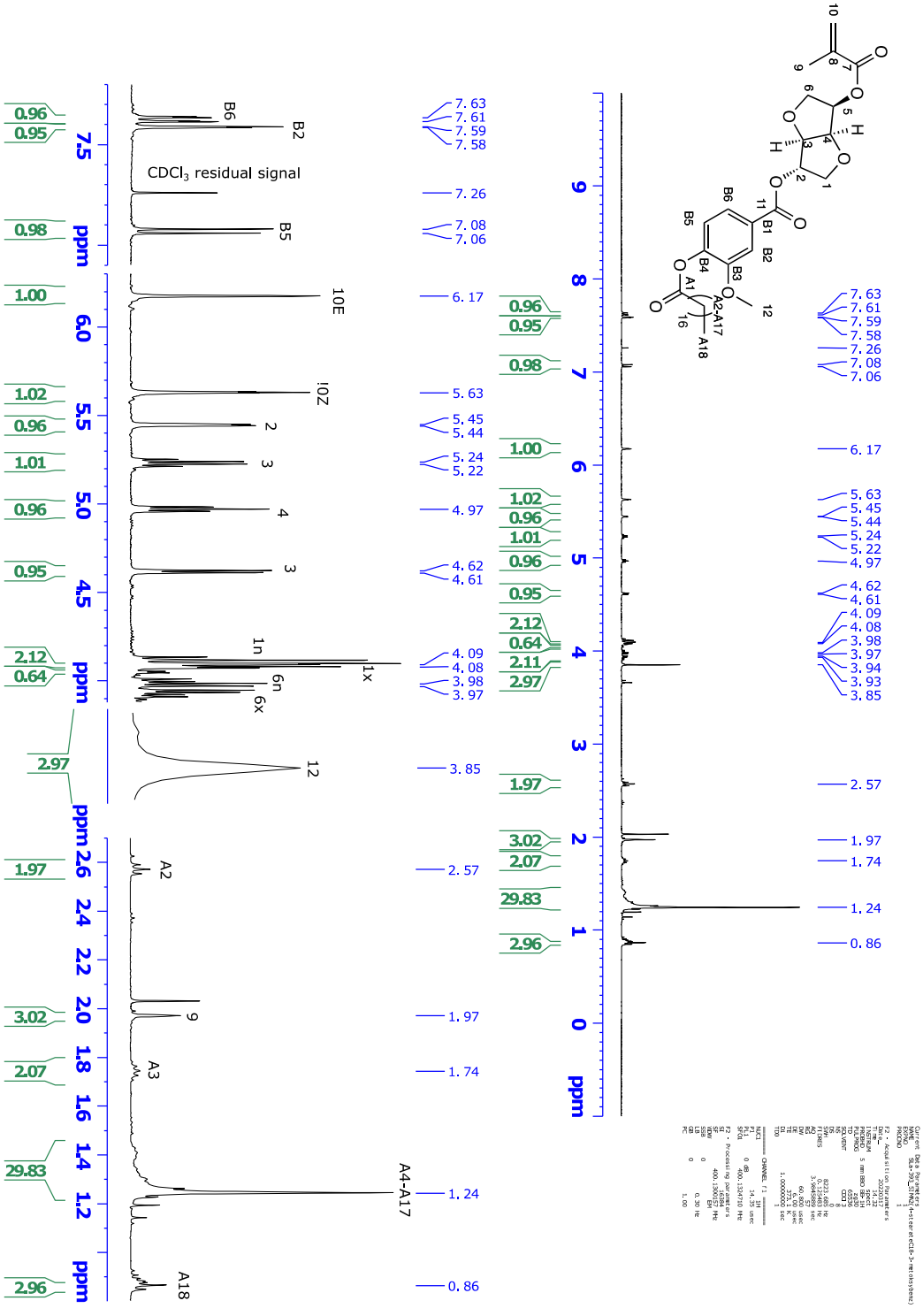

Figure A1. ^{1}H NMR spectrum of **MC18**.

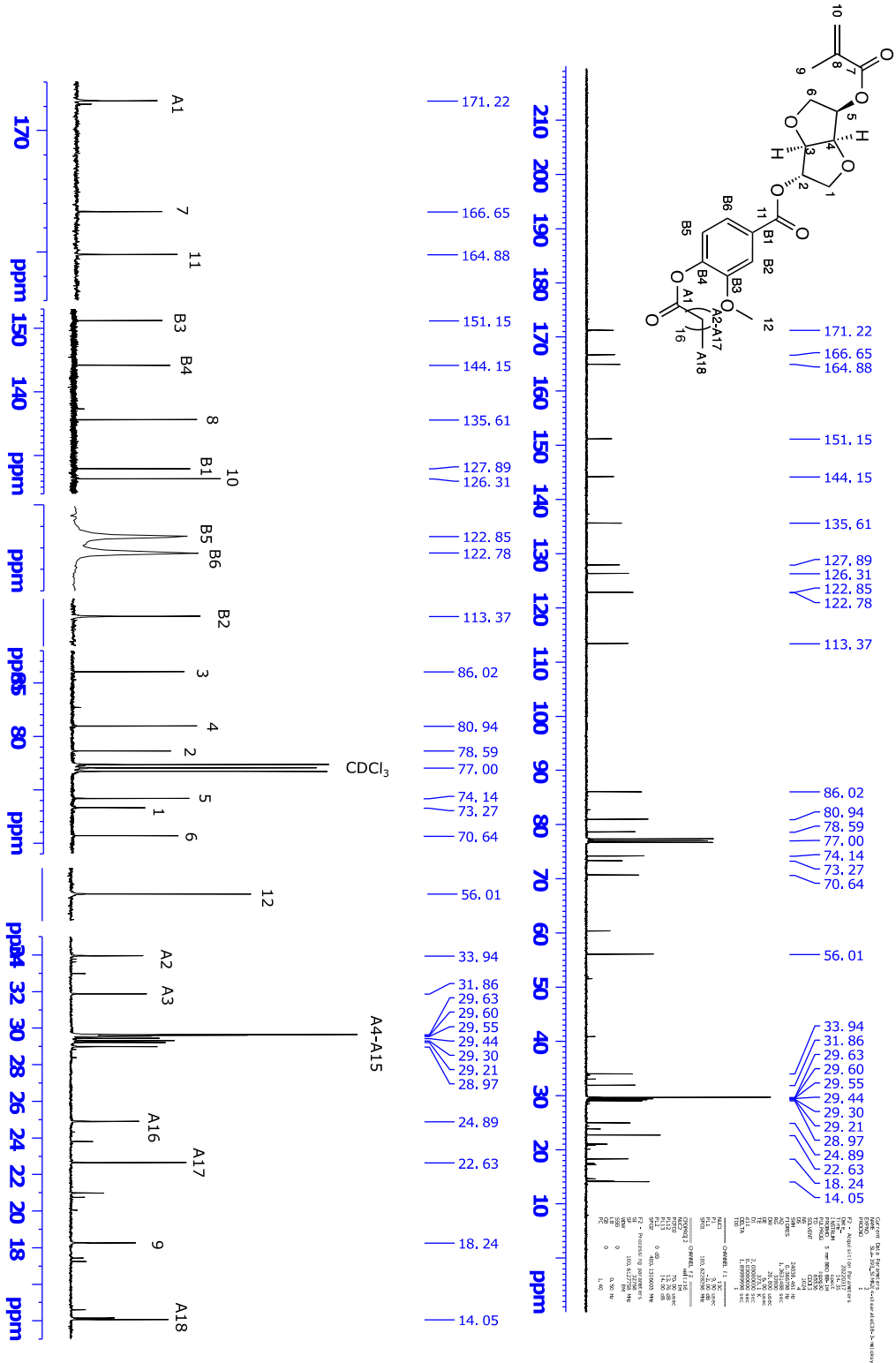

Figure A2. ^{13}C NMR spectrum of **MC18**.

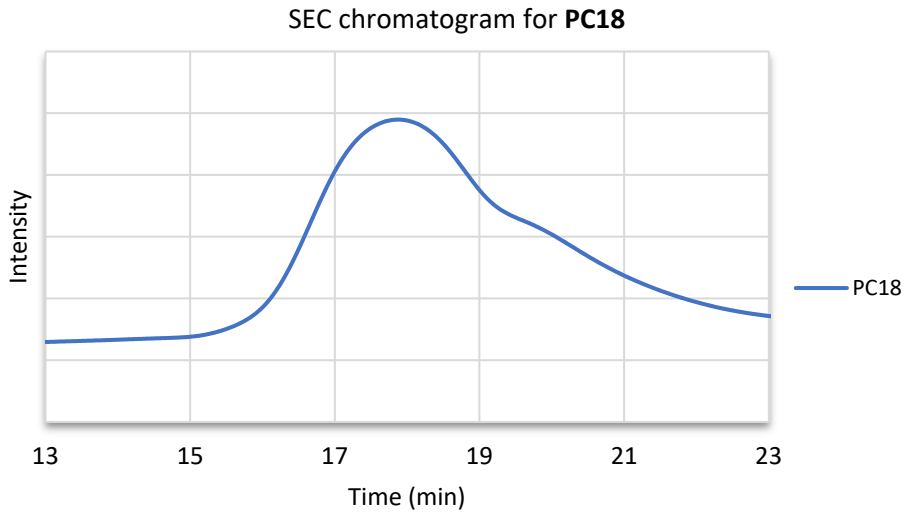

Figure A3. SEC chromatogram for **PC18**. Eluated in THF (1 ml/min).

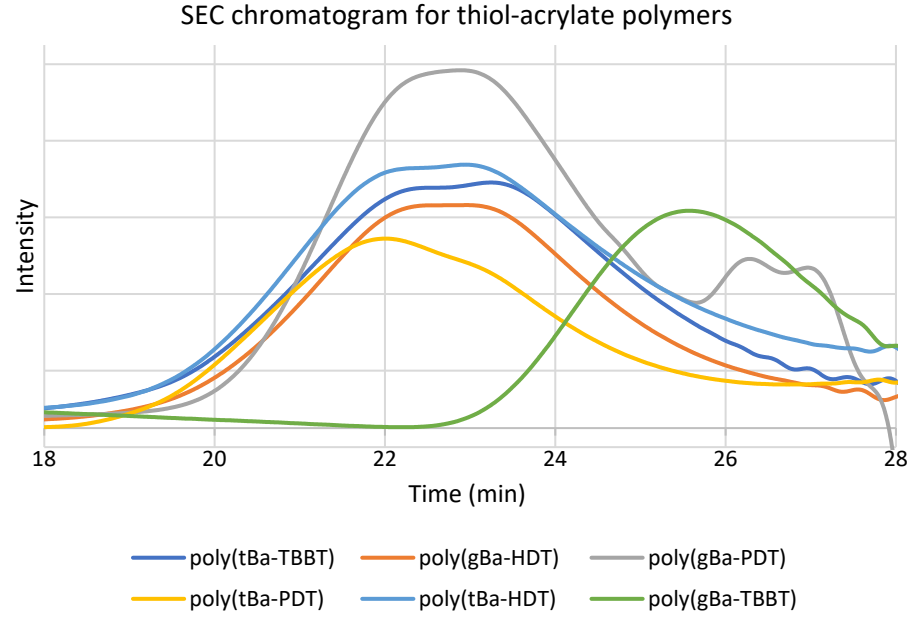

Figure A4. SEC chromatogram for thiol-acrylate polymers containing diketone **B**. Eluated in chloroform (1 ml/min).

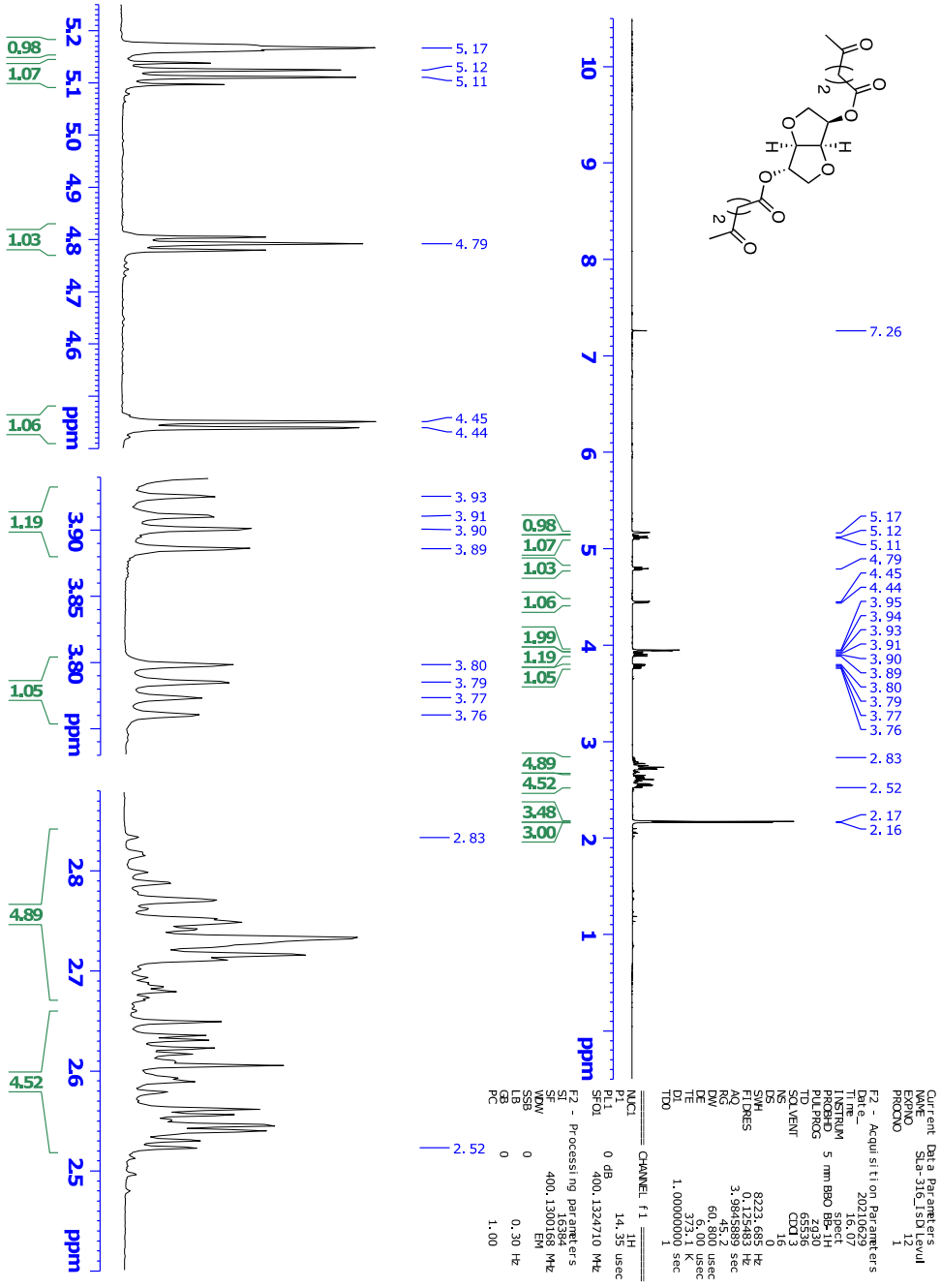

Figure A5. ^{1}H NMR spectrum of **isorbide dilevulinate**.

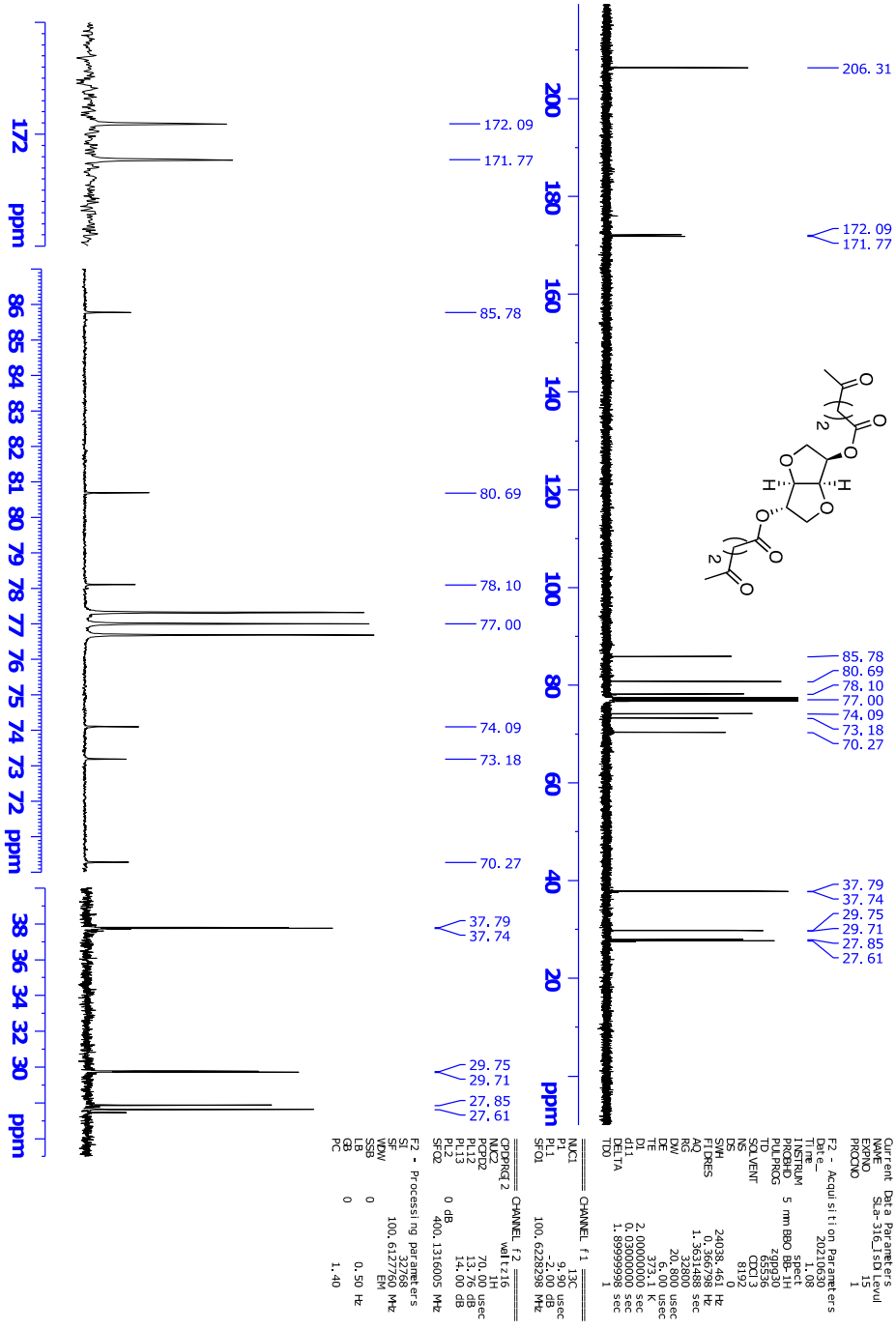

Figure A6. ^{13}C NMR spectrum of **isosorbide dilevulinate**.

ACKNOWLEDGEMENTS

I would like to thank supervisors Lauri Vares and Patric Jannasch for the opportunity to go through the not easiest journey of PhD and for a lot of experience on different levels. It was not only about how to collect interesting data, analyze and to form it into a publication. This period taught me many different skills, for example how to struggle with different stressful situations as the science is not like a regular chemical analysis according to some ISO standard. Moreover, I had opportunity to work with high-tech laboratory techniques and obtain useful knowledge. I feel that PhD journey improved my essential skills and will be useful both in further professional career and personal life.

My very warm appreciation to my lab mates Rauno, Livia and Alina for collaboration. Our different individual strong sides helped us to move forward faster for mutual goals. Very special thanks to Olivier Bonjour from Lund University, who continuously performed thermal analysis to our endless number of samples and never said that it is enough now!

Also, I would like to thank my previous supervisor Lauri Toom during the Master studies, who gave me broad knowledge about NMR and the other interesting lab techniques, which was a very good basis to walk through the PhD.

Так же хочу поблагодарить свою жену, которая помогала мне проходить докторантуру. Ты всегда слушала мои проблемы. Приготовила еду на каждый день, чтобы я не проголодался в лабе. Даже сама помогала мне пару раз посуду мыть в лабе, когда я торопился, помнишь?

Also, would like to thank my friends and family. It has been a very long time (since 2012) to work in Institute of Technology and it is time to move forward. Thank you for all!

PUBLICATIONS

CURRICULUM VITAE

Name: Siim Laanesoo
Date of birth: January 30, 1991
Citizenship: Estonian
Contact: Institute of Technology, University of Tartu
Nooruse 1, 50411, Tartu, Estonia
E-mail: siim.laanesoo@ut.ee

Education:

2018–…	University of Tartu, PhD studies in engineering and technology
2015–2017	University of Tartu, MSc in chemistry
2010–2015	University of Tartu, BSc in chemistry
1998–2010	Lähte Gymnasium, Secondary education

Language skills:

Estonian	native language
Russian	good in speech and writing
English	good in speech and writing

Professional employment:

2018–2023	University of Tartu, Institute of Technology, Junior Researcher Fellow
05.2018–11.2018	University of Tartu, Institute of Technology, Chemist
09.2017–02.2018	TBD-Biodiscovery, Organic Chemist
04.2015–12.2015	University of Tartu, Institute of Technology, Chemist
06.2012–08.2012	Saybolt Eesti, Summer internship, Analytical Chemist

Scientific publications:

Laanesoo, S.; Bonjour, O.; Parve, J.; Parve, O.; Matt, L.; Vares, L.; Jannasch, P. Poly(Alkanoyl Isosorbide Methacrylate)s: From Amorphous to Semi-crystalline and Liquid Crystalline Biobased Materials. Biomacromolecules 2021, 22 (2), 640–648. doi.org/ 10.1021/acs.biomac.0c01474

Bonjour, O.; Nederstedt, H.; Arcos-Hernandez, M. V.; **Laanesoo**, **S**.; Vares, L.; Jannasch, P. Lignin-Inspired Polymers with High Glass Transition Temperature and Solvent Resistance from 4-Hydroxybenzonitrile, Vanillonitrile, and Syringonitrile Methacrylates. ACS Sustain. Chem. Eng. 2021, 9 (50), 16874–16880. doi.org/10.1021/acssuschemeng.1c07048

Sedrik, R.; Bonjour, O.; **Laanesoo, S**.; Liblikas, I.; Pehk, T.; Jannasch, P.; Vares, L. Chemically Recyclable Poly(β-Thioether Ester)s Based on Rigid Spirocyclic Ketal Diols Derived from Citric Acid. Biomacromolecules 2022, 23 (2), 2685–2696. doi.org/ 10.1021/acs.biomac.2c00452

Laanesoo, S.; Bonjour, O.; Sedrik, R.; Tamsalu, I.; Jannasch, P.; Vares, L. Combining Isosorbide and Lignin-Related Benzoic Acids for High-Tg Polymethacrylates. European Polymer Journal **2024**, *202*, 112595. https://doi.org/10.1016/j.eurpolymj.2023.112595.

ELULOOKIRJELDUS

Nimi: Siim Laanesoo
Sünniaeg: 30. jaanuar 1991
Kodakondsus: Eesti
Kontakt: Tehnoloogiainstituut, Tartu Ülikool
Nooruse 1, 50411, Tartu, Eesti
E-mail: siim.laanesoo@ut.ee

Haridus:

2018–…	Tartu Ülikool, doktorantuur (tehnika ja tehnoloogia)
2015–2017	Tartu Ülikool, magistriõpe (keemia)
2010–2015	Tartu Ülikool, bakalaureuseõpe (keemia)
1998–2010	Lähte Ühisgümnaasium, keskharidus

Keeleoskus:

eesti keel	emakeel
vene keel	hea kõnes ja kirjas
inglise keel	hea kõnes ja kirjas

Teenistuskäik:

2018–2023	Tartu Ülikool, Tehnoloogiainstituut, nooremteadur
05.2018–11.2018	Tartu Ülikool, Tehnoloogiainstituut, keemik
09.2017–02.2018	OÜ TBD-Biodiscovery, keemik
04.2015–12.2015	Tartu Ülikool, Tehnoloogiainstituut, keemik
06.2012–08.2012	Saybolt Eesti AS, suvepraktika, analüüsikeemik

Teaduspublikatsioonid ja patendiavaldused:

Laanesoo, S.; Bonjour, O.; Parve, J.; Parve, O.; Matt, L.; Vares, L.; Jannasch, P. Poly(Alkanoyl Isosorbide Methacrylate)s: From Amorphous to Semi-crystalline and Liquid Crystalline Biobased Materials. Biomacromolecules 2021, 22 (2), 640–648. doi.org/ 10.1021/acs.biomac.0c01474.

Bonjour, O.; Nederstedt, H.; Arcos-Hernandez, M. V.; **Laanesoo**, **S**.; Vares, L.; Jannasch, P. Lignin-Inspired Polymers with High Glass Transition Temperature and Solvent Resistance from 4-Hydroxybenzonitrile, Vanillonitrile, and Syringonitrile Methacrylates. ACS Sustain. Chem. Eng. 2021, 9 (50), 16874–16880. doi.org/10.1021/acssuschemeng.1c07048.

Sedrik, R.; Bonjour, O.; **Laanesoo, S**.; Liblikas, I.; Pehk, T.; Jannasch, P.; Vares, L. Chemically Recyclable Poly(β-Thioether Ester)s Based on Rigid Spirocyclic Ketal Diols Derived from Citric Acid. Biomacromolecules 2022, 23 (2), 2685–2696. doi.org/ 10.1021/acs.biomac.2c00452.

Laanesoo, S.; Bonjour, O.; Sedrik, R.; Tamsalu, I.; Jannasch, P.; Vares, L. Combining Isosorbide and Lignin-Related Benzoic Acids for High-Tg Polymethacrylates. European Polymer Journal **2024**, *202*, 112595. https://doi.org/10.1016/j.eurpolymj.2023.112595.

DISSERTATIONES TECHNOLOGIAE UNIVERSITATIS TARTUENSIS

1. **Imre Mäger**. Characterization of cell-penetrating peptides: Assessment of cellular internalization kinetics, mechanisms and bioactivity. Tartu 2011, 132 p.
2. **Taavi Lehto**. Delivery of nucleic acids by cell-penetrating peptides: application in modulation of gene expression. Tartu 2011, 155 p.
3. **Hannes Luidalepp**. Studies on the antibiotic susceptibility of *Escherichia coli*. Tartu 2012, 111 p.
4. **Vahur Zadin**. Modelling the 3D-microbattery. Tartu 2012, 149 p.
5. **Janno Torop**. Carbide-derived carbon-based electromechanical actuators. Tartu 2012, 113 p.
6. **Julia Suhorutšenko**. Cell-penetrating peptides: cytotoxicity, immunogenicity and application for tumor targeting. Tartu 2012, 139 p.
7. **Viktoryia Shyp**. G nucleotide regulation of translational GTPases and the stringent response factor RelA. Tartu 2012, 105 p.
8. **Mardo Kõivomägi**. Studies on the substrate specificity and multisite phosphorylation mechanisms of cyclin-dependent kinase Cdk1 in *Saccharomyces cerevisiae*. Tartu, 2013, 157 p.
9. **Liis Karo-Astover**. Studies on the Semliki Forest virus replicase protein nsP1. Tartu, 2013, 113 p.
10. **Piret Arukuusk**. NickFects–novel cell-penetrating peptides. Design and uptake mechanism. Tartu, 2013, 124 p.
11. **Piret Villo**. Synthesis of acetogenin analogues. Asymmetric transfer hydrogenation coupled with dynamic kinetic resolution of α-amido-β-keto esters. Tartu, 2013, 151 p.
12. **Villu Kasari**. Bacterial toxin-antitoxin systems: transcriptional cross-activation and characterization of a novel *mqsRA* system. Tartu, 2013, 108 p.
13. **Margus Varjak**. Functional analysis of viral and host components of alphavirus replicase complexes. Tartu, 2013, 151 p.
14. **Liane Viru**. Development and analysis of novel alphavirus-based multifunctional gene therapy and expression systems. Tartu, 2013, 113 p.
15. **Kent Langel**. Cell-penetrating peptide mechanism studies: from peptides to cargo delivery. Tartu, 2014, 115 p.
16. **Rauno Temmer**. Electrochemistry and novel applications of chemically synthesized conductive polymer electrodes. Tartu, 2014, 206 p.
17. **Indrek Must**. Ionic and capacitive electroactive laminates with carbonaceous electrodes as sensors and energy harvesters. Tartu, 2014, 133 p.
18. **Veiko Voolaid**. Aquatic environment: primary reservoir, link, or sink of antibiotic resistance? Tartu, 2014, 79 p.
19. **Kristiina Laanemets**. The role of SLAC1 anion channel and its upstream regulators in stomatal opening and closure of *Arabidopsis thaliana.* Tartu, 2015, 115 p.

20. **Kalle Pärn**. Studies on inducible alphavirus-based antitumour strategy mediated by site-specific delivery with activatable cell-penetrating peptides. Tartu, 2015, 139 p.
21. **Anastasia Selyutina**. When biologist meets chemist: a search for HIV-1 inhibitors. Tartu, 2015, 172 p.
22. **Sirle Saul**. Towards understanding the neurovirulence of Semliki Forest virus. Tartu, 2015, 136 p.
23. **Marit Orav**. Study of the initial amplification of the human papillomavirus genome. Tartu, 2015, 132 p.
24. **Tormi Reinson**. Studies on the Genome Replication of Human Papillomaviruses. Tartu, 2016, 110 p.
25. **Mart Ustav Jr**. Molecular Studies of HPV-18 Genome Segregation and Stable Replication. Tartu, 2016, 152 p.
26. **Margit Mutso**. Different Approaches to Counteracting Hepatitis C Virus and Chikungunya Virus Infections. Tartu, 2016, 184 p.
27. **Jelizaveta Geimanen**. Study of the Papillomavirus Genome Replication and Segregation. Tartu, 2016, 168 p.
28. **Mart Toots**. Novel Means to Target Human Papillomavirus Infection. Tartu, 2016, 173 p.
29. **Kadi-Liis Veiman**. Development of cell-penetrating peptides for gene delivery: from transfection in cell cultures to induction of gene expression *in vivo*. Tartu, 2016, 136 p.
30. **Ly Pärnaste**. How, why, what and where: Mechanisms behind CPP/cargo nanocomplexes. Tartu, 2016, 147 p.
31. **Age Utt**. Role of alphavirus replicase in viral RNA synthesis, virus-induced cytotoxicity and recognition of viral infections in host cells. Tartu, 2016, 183 p.
32. **Veiko Vunder**. Modeling and characterization of back-relaxation of ionic electroactive polymer actuators. Tartu, 2016, 154 p.
33. **Piia Kivipõld**. Studies on the Role of Papillomavirus E2 Proteins in Virus DNA Replication. Tartu, 2016, 118 p.
34. **Liina Jakobson**. The roles of abscisic acid, CO_2, and the cuticle in the regulation of plant transpiration. Tartu, 2017, 162 p.
35. **Helen Isok-Paas**. Viral-host interactions in the life cycle of human papillomaviruses. Tartu, 2017, 158 p.
36. **Hanna Hõrak**. Identification of key regulators of stomatal CO_2 signalling via O_3-sensitivity. Tartu, 2017, 260 p.
37. **Jekaterina Jevtuševskaja**. Application of isothermal amplification methods for detection of *Chlamydia trachomatis* directly from biological samples. Tartu, 2017, 96 p.
38. **Ülar Allas**. Ribosome-targeting antibiotics and mechanisms of antibiotic resistance. Tartu, 2017, 152 p.
39. **Anton Paier**. Ribosome Degradation in Living Bacteria. Tartu, 2017, 108 p.
40. **Vallo Varik**. Stringent Response in Bacterial Growth and Survival. Tartu, 2017, 101 p.

41. **Pavel Kudrin**. In search for the inhibitors of *Escherichia coli* stringent response factor RelA. Tartu, 2017, 138 p.
42. **Liisi Henno**. Study of the human papillomavirus genome replication and oligomer generation. Tartu, 2017, 144 p.
43. **Katrin Krõlov**. Nucleic acid amplification from crude clinical samples exemplified by *Chlamydia trachomatis* detection in urine. Tartu, 2018, 118 p.
44. **Eve Sankovski**. Studies on papillomavirus transcription and regulatory protein E2. Tartu, 2018, 113 p.
45. **Morteza Daneshmand**. Realistic 3D Virtual Fitting Room. Tartu, 2018, 233 p.
46. **Fatemeh Noroozi**. Multimodal Emotion Recognition Based Human-Robot Interaction Enhancement. Tartu, 2018, 113 p.
47. **Krista Freimann**. Design of peptide-based vector for nucleic acid delivery in vivo. Tartu, 2018, 103 p.
48. **Rainis Venta**. Studies on signal processing by multisite phosphorylation pathways of the *S. cerevisiae* cyclin-dependent kinase inhibitor Sic1. Tartu, 2018, 155 p.
49. **Inga Põldsalu**. Soft actuators with ink-jet printed electrodes. Tartu, 2018, 85 p.
50. **Kadri Künnapuu**. Modification of the cell-penetrating peptide PepFect14 for targeted tumor gene delivery and reduced toxicity. Tartu, 2018, 114 p.
51. **Toomas Mets**. RNA fragmentation by MazF and MqsR toxins of *Escherichia coli.* Tartu, 2019, 119 p.
52. **Kadri Tõldsepp**. The role of mitogen-activated protein kinases MPK4 and MPK12 in CO_2-induced stomatal movements. Tartu, 2019, 259 p.
53. **Pirko Jalakas**. Unravelling signalling pathways contributing to stomatal conductance and responsiveness. Tartu, 2019, 120 p.
54. **S. Sunjai Nakshatharan**. Electromechanical modelling and control of ionic electroactive polymer actuators. Tartu, 2019, 165 p.
55. **Eva-Maria Tombak**. Molecular studies of the initial amplification of the oncogenic human papillomavirus and closely related nonhuman primate papillomavirus genomes. Tartu, 2019, 150 p.
56. **Meeri Visnapuu**. Design and physico-chemical characterization of metal-containing nanoparticles for antimicrobial coatings. Tartu, 2019, 138 p.
57. **Jelena Beljantseva**. Small fine-tuners of the bacterial stringent response – a glimpse into the working principles of Small Alarmone Synthetases. Tartu, 2020, 104 p.
58. **Egon Urgard**. Potential therapeutic approaches for modulation of inflammatory response pathways. Tartu, 2020, 120 p.
59. **Sofia Raquel Alves Oliveira**. HPLC analysis of bacterial alarmone nucleotide (p)ppGpp and its toxic analogue ppApp. Tartu, 2020, 122 p.
60. **Mihkel Örd**. Ordering the phosphorylation of cyclin-dependent kinase Cdk1 substrates in the cell cycle. Tartu, 2021, 228 p.
61. **Fred Elhi**. Biocompatible ionic electromechanically active polymer actuator based on biopolymers and non-toxic ionic liquids. Tartu, 2021, 140 p.

62. **Liisi Talas**. Reconstructing paleo-diversity, dynamics and response of eukaryotes to environmental change over the Late-Glacial and Holocene period in lake Lielais Svētiņu using sedaDNA. Tartu, 2021, 118 p.
63. **Livia Matt**. Novel isosorbide-based polymers. Tartu, 2021, 118 p.
64. **Koit Aasumets**. The dynamics of human mitochondrial nucleoids within the mitochondrial network. Tartu, 2021, 104 p.
65. **Faiza Summer**. Development and optimization of flow electrode capacitor technology. Tartu, 2022, 109 p.
66. **Olavi Reinsalu**. Cancer-testis antigen MAGE-A4 is incorporated into extracellular vesiclesand is exposed to the surface. Tartu, 2022, 130 p.
67. **Tetiana Brodiazhenko**. RelA-SpoT Homolog enzymes as effectors of Toxin-Antitoxin systems. Tartu, 2022, 132 p.
68. **Georg-Marten Lanno**. Development of novel antibacterial drug delivery systems as wound scaffolds using electrospinning technology. Tartu, 2022, 175 p.
69. **Liubov Cherkashchenko**. New insights into alphaviral nsP2 functions. Tartu, 2023, 171 p.
70. **Kristina Kiisholts**. Peptide-based drug carriers and preclinical nanomedicine applications for endometriosis treatment. Tartu, 2023, 138 p.
71. **Kai Rausalu**. Alphaviral nsP2 protease: From requirements for functionality to inhibition. Tartu, 2023, 175 p.
72. **Laura Sandra Lello**. Unraveling the intricate nature of the alphavirus RNA replicase. Tartu, 2023, 219 p.
73. **Houman Masnavi**. Visibility Aware Navigation. Tartu, 2023, 180 p.
74. **Kadir Aktas**. Cosmic Ray Tomography based Object Reconstruction and Recognition. Tartu, 2023, 104 p.
75. **Egils Avots**. Brain abnormality detection using statistical analysis of individual structural connectivity networks and EEG signals. Tartu, 2023, 223 p.
76. **Sainan Wang**. Structure-guided insights into the functions of CHIKV nsP2. Tartu, 2024, 154 p.
77. **Anneli Samel**. Unveiling the characteristics of cancer-testis antigen MAGEA10. Tartu, 2024, 136 p.
78. **Ikechukwu Ofodile**. Fault tolerant attitude control for nanosatellites: ESTCube-2 case. Tartu, 2024, 130 p.
79. **Olena Zamora**. Impacts of plant hormones on controlling stomatal conductance. Tartu, 2024, 166 p.
80. **Mariliis Hinnu**. *In vitro* methods for studying the mechanisms of ribosome-targeting antibiotics. Tartu, 2024, 143 p.
81. **Chung-Yueh Yeh**. Characterization of MPK and HT1 kinases in CO_2-induced stomatal movements. Tartu, 2024, 118 p.
82. **Iman Dadras**. Low power neural network-based control and actuation solutions for insect-scale robots. Tartu, 2024, 149 p.
83. **Fatemeh Rastgar**. Towards reliable real-time trajectory optimization. Tartu, 2024, 158 p.

84. **Maria Maloverjan**. Optimizing cell-penetrating peptide-based nanoparticles for delivery of nucleic acid therapeutics. Tartu, 2024, 172 p.
85. **Joonas Merisalu.** Resistive switching in memristor structures with multilayer dielectrics. Tartu, 2024, 149 p.